1-1-2005

Field testing of railroad flatcar bridges

Kristine Suzanne Palmer
Iowa State University

Field testing of railroad flatcar bridges

by

Kristine Suzanne Palmer

A thesis submitted to the graduate faculty

in partial fulfillment of the requirements for the degree of

MASTER OF SCIENCE

Major: Civil Engineering (Structural Engineering)

Program of Study Committee:
F. Wayne Klaiber, Co-major Professor
Terry J. Wipf, Co-major Professor
Loren W. Zachary

Iowa State University

Ames, Iowa

2005

Graduate College
Iowa State University

This is to certify that the master's thesis of

Kristine Suzanne Palmer

has met the thesis requirements of Iowa State University

Signatures have been redacted for privacy

TABLE OF CONTENTS

LIST OF FIGURES

LIST OF TABLES

ABSTRACT

In a research project conducted by the Bridge Engineering Center at Iowa State University (ISU), the behavior of low-volume bridges composed of two railroad flatcars (RRFCs) was investigated. The feasibility of using railroad flatcars as the superstructure for bridges on low-volume roads has been investigated in two previous research projects at ISU. The results of these projects verified that bridges composed of three RRFCs are efficient and economical alternatives for low-volume road bridges. To verify the adequacy of bridges composed of two RRFCs, two bridges were tested: one in Buchanan County, Iowa, and one in Delaware County, Iowa.

The Buchanan County Bridge 2 (BCB2), the second Buchanan County RRFC bridge to be tested by ISU, is composed of two 56-ft V-deck RRFCs and spans 54 ft – 0 in. The RRFCs are simply-supported with concrete abutments. A reinforced concrete beam acts as the longitudinal flatcar connection (LFC) and distributes live loads between the RRFCs. The BCB2 has a gravel driving surface and a guardrail system.

The Delaware County Bridge (DCB) spans 66 ft – 4 in. and is composed of two 89-ft RRFCs which were each symmetrically cut to 67 ft – 6 in. The RRFCs are supported at their bolsters by a built-up cap beam which is supported by HP piles. The LFC consists of a steel plate welded to the adjacent RRFCs along the length of the connection. The DCB also has a gravel driving surface and a guardrail system.

Through the load tests, it was found that bridges designed like the BCB2 have total stresses below the allowable stress of the steel and deflections below the AASHTO bridge design specification limits. In bridges designed like the DCB, the thickness of the gravel driving surface must be limited for the total stresses and deflections to be below the allowable stress of the steel and the AASHTO bridge design specification limits. To assist bridge inspectors, live load distribution factors were developed for use with the AASHTO rating method. Based on the results of this research, it has been determined that with the proper driving surface, bridges composed of two RRFCs are an effective option for low-volume road bridges.

1. INTRODUCTION

1.1 Background

Because the Mississippi River forms the eastern border of Iowa and the Missouri River forms the western border of Iowa, the state has a large number of tributary streams. Iowa has approximately 25,000 bridges that cross these tributary streams, as well as rivers and in some cases, roads. Approximately 80 percent of these bridges are on county roads and thus must be maintained by the counties [1]. According to a 2004 National Bridge Inventory report, Iowa has 5,260 structurally deficient bridges and 1,699 functionally obsolete bridges [1]. However, Iowa ranks 30th in the United States in terms of population [2]. This lower tax base limits the funds that are available for Iowa counties to repair or replace deficient and obsolete bridges. Because of this, the Bridge Engineering Center (BEC) at Iowa State University (ISU) has researched low-cost bridge alternatives for use on low-volume roads (LVR). One such alternative is the use of decommissioned railroad flatcars (RRFCs) for the superstructure in bridges.

The viability of using RRFCs as an economical alternative for LVR bridges was investigated in two previous research projects conducted by the ISU BEC: a 1999 feasibility study [3] and a 2003 demonstration project, TR-444 [4].

The feasibility study noted that RRFCs were decommissioned due to age, damage caused by derailments, and economics. Since derailments typically cause significant structural damage to the RRFCs, it was determined that RRFCs involved in derailments were not suitable for use in bridges. It was also recommended that the RRFCs selected for use in LVR bridges have a redundant cross-section. That is, several girders contribute to the structural strength of the RRFC. Non-redundant cross-sections, those with only the interior girder capable of supporting traffic loads, are acceptable only if an efficient longitudinal flatcar connection is present to transfer loads from one flatcar to the other [3].

As part of the feasibility study, a Tama County Bridge (TCB) was field tested to determine the structural adequacy of RRFC bridges. The TCB consists of two RRFCs for a combined width of 18 ft – 8 in. and spans 42 ft – 0 in. Timber decking was used to transfer the loads transversely. To simulate the theoretical behavior of the TCB under equivalent loading, a computer model was generated and analyzed with ANSYS. Results from both the field test and the analytical model showed that the maximum strains in the girders of the RRFCs were well below the yield strength of the steel, and that the deflections were relatively small. Thus, the feasibility study determined that RRFC bridges were effective and potentially economic alternatives for LVR bridges [3].

In the demonstration project that followed the feasibility study, a process for selecting RRFCs was developed, a laboratory specimen of a longitudinal flatcar connection (LFC) was constructed and tested in the laboratory, and two RRFC demonstration bridges were designed, constructed, and field tested. In addition to field testing, computer models of the two bridges were developed to obtain theoretical results which were then compared to the experimental results [4].

After the inspection of numerous RRFCs, it was determined that although the size and position of the elements may be different, the basic configuration is the same in most RRFCs. The elements can be classified into four categories: decking, girders, secondary members, and transverse members. Of these, the girders are the largest members, and thus, carry most of the loads. To assist in the selection off adequate RRFCs for use in bridges, selection criteria were developed. The five criteria for RRFC selection are:

1. Structural Element Sizes, Load Distributing Capabilities, and Support Locations: The RRFC should have a redundant cross-section or exterior girders with the ability to form a proper LFC and adequate strength and stability at bearing locations.

2. Member Straightness/Damage: Damaged or deformed members will not adequately carry or distribute loads. Visual inspection and string lines should be used to determine member straightness.

3. Structural Element Connections: Choose welds over rivets since rivets lose strength over time. Welds must be checked for fatigue cracks.

4. Uniform Matching Cambers: For the transverse connection, the cambers of the two adjacent RRFCs must be within a tolerance of ± 1 in.

5. RRFC Availability: Use easily accessible RRFCs so more bridges can be built without additional design work [4].

The two bridges that were constructed and tested for the demonstration project are located in Buchanan and Winnebago Counties in Iowa. The Buchanan County Bridge (BCB) is a single-span bridge that consists of three RRFCs and has a 56 ft – 0 in. span, a 29 ft – 1 1/2 in. width, and asphalt millings for the driving surface. The LFC between the RRFCs are two reinforced concrete (R/C) beams. It was this LFC that was constructed and tested in the laboratory; the specimen was tested in torsion and flexure to confirm its structural adequacy and behavior. The specimen maintained its shape and structural integrity throughout the tests and was thus deemed adequate for use. The Winnebago County Bridge (WCB) is a three-span bridge that also consists of three RRFCs and has a total length of 89 ft – 0 in., a 26 ft – 9 1/2 in. width, and a gravel driving surface. The center span is 66 ft – 0 in., and each end span is 11 ft – 6 in. The LFC between the RRFCs are two small R/C beams, intermittent steel plates welded to the two adjacent RRFCs, and transverse timber planking [4].

Through field testing, the strains and deflections due to a live load were determined. Based on the results of the field testing and theoretical analyses, design recommendations for the maximum live load moments in the interior and exterior girders were developed. The theoretical analyses consisted of grillage models of the two bridges that were subjected to the same loading that was used in the field tests. The grillage model analyses verified the experimental results, which indicated that the maximum strains in the RRFCs were well below the yield strength of the steel, and that the deflections were relatively small when

compared to AASHTO suggested allowable limits. Thus, the demonstration project concluded that RRFC bridges are effective, economical alternatives for LVR bridges [4].

Based upon the results from the demonstration project, it was proposed that further study of RRFC bridges be undertaken to investigate different span lengths for use with existing abutments and bridges consisting of only two RRFCs. With the data from the additional testing, the design recommendations [4] could be improved, and a rating methodology for RRFC bridges for use by county engineers and consultants could be developed.

The county engineers that participated in the demonstration project were questioned regarding their decision to continue using RRFC bridges and the benefits associated with RRFC bridges. Both Jim Witt, County Engineer for Winnebago County, and Brian Keierleber, County Engineer for Buchanan County, cited cost as the main factor for choosing to install more RRFC bridges in their counties. The RRFC bridges built in Winnebago County and Buchanan County cost approximately $27 per square foot and $35 per square foot, respectively. Both of these values are well below the typical Iowa Department of Transportation (Iowa DOT) standard slab bridge costs, which are approximately $70 per square foot. In addition to cost, Witt also explained that county forces can be used to install RRFC bridges, which saves time and money.

1.2 Objective and Scope of Project

Based on the recommendations for further study in the 2003 ISU RRFC demonstration project [4], a research project to continue investigating the behavior of various RRFC bridges was initiated. The primary objectives of the research were to (1) obtain data on the structural behavior of different RRFC bridges, (2) refine the design methodology presented in the demonstration project, TR-444, and (3) develop a load rating process for RRFC bridges. The following tasks were completed to achieve the objectives:

- Inspection and selection of RRFCs for use in LVR bridge superstructures.
- Field testing of two previously constructed RRFC bridges, each consisting of two flatcars: a 56 ft – 0 in. span and a 66 ft – 4 in. span.

1.3 Selected RRFC Bridge Sites

Buchanan County participated in previous RRFC research projects and was interested in developing the concept further. Delaware County also expressed interest in constructing a RRFC bridge. Thus, the two bridges tested are located in these counties. The following sections describe the sites and bridges analyzed for this project.

1.3.1 Buchanan County Bridge 2

The bridge in Buchanan County crosses the Dry Creek about five miles southeast of Quasqueton, Iowa, on 290th Street. Because this bridge is the second RRFC bridge tested in Buchanan County, this bridge will be referred to as BCB2. Presented in Figure 1.1a is a map of a portion of Buchanan County showing the major highways in that portion of the county. The general location of the bridge is identified with a dashed rectangle and labeled Detail A, which is presented as Figure 1.1b. The actual location of the bridge has been identified with a dashed circle. Details on the design and construction of BCB2 are presented in Section 2.1.

1.3.2 Delaware County Bridge

The bridge Delaware County, referred to as DCB, crosses the Elk Creek approximately three miles northeast of Greeley, Iowa, at the intersection of 270th Avenue and Rainbow Road. Presented in Figure 1.2a is a map of a portion of Delaware County showing the major highways in that portion of the county. The general location of the bridge is identified with a dashed rectangle and labeled Detail A, which is presented as Figure 1.2b. The approximate location of the bridge is identified with a dashed circle. Details on the design and construction of DCB are presented in Section 2.2.

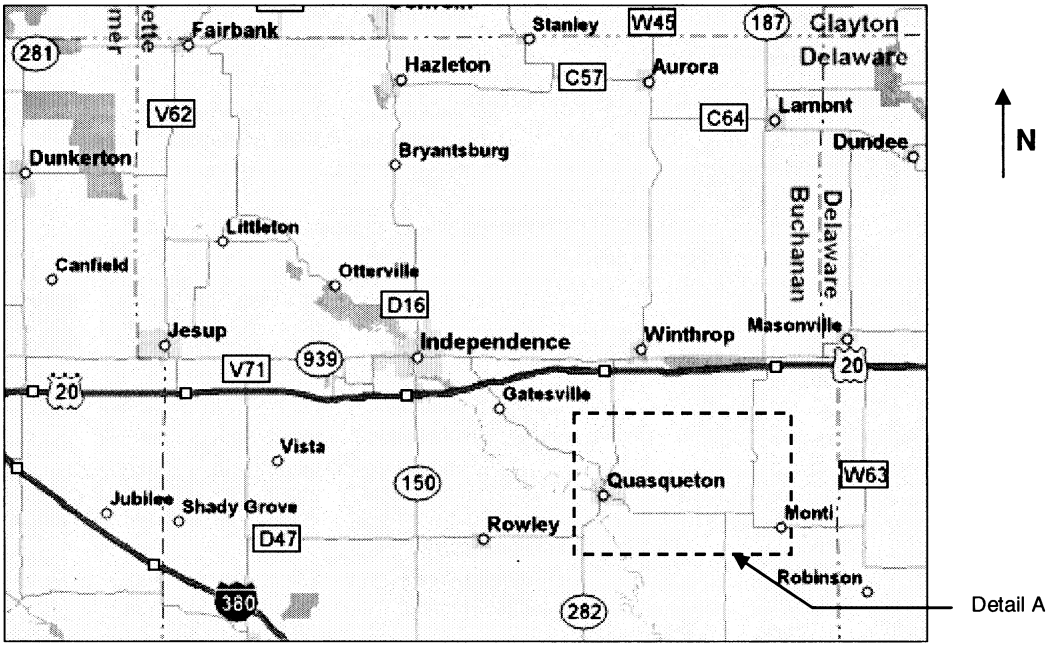

a. Map of a Portion of Buchanan County [5]

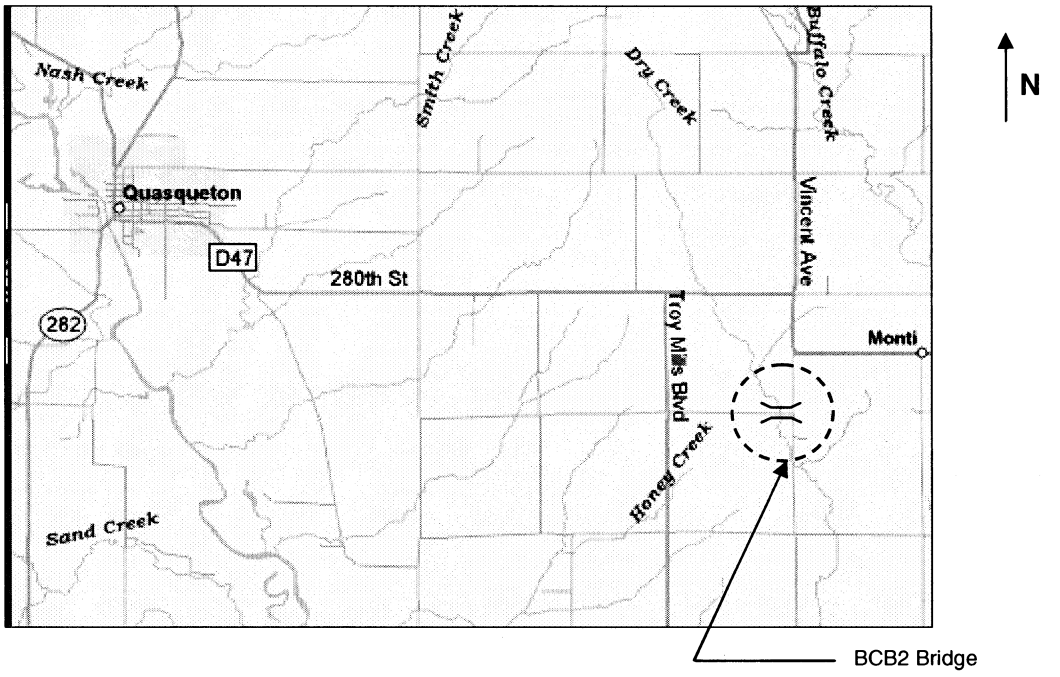

b. Detail A [5]

Figure 1.1. Location of the BCB2 site.

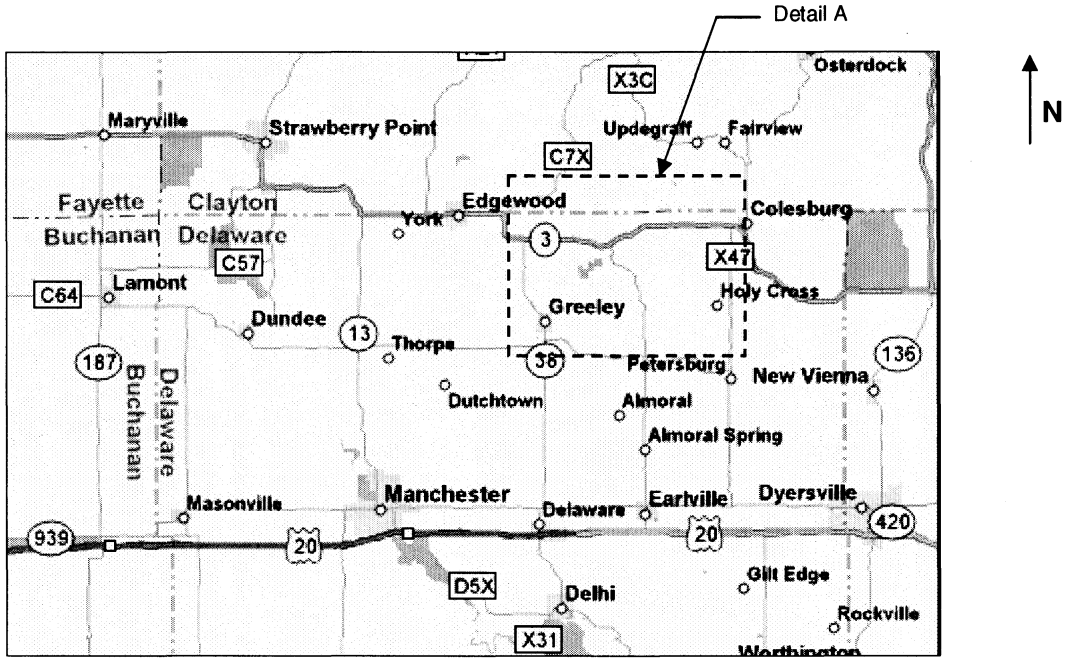

a. Map of a Portion of Delaware County [5]

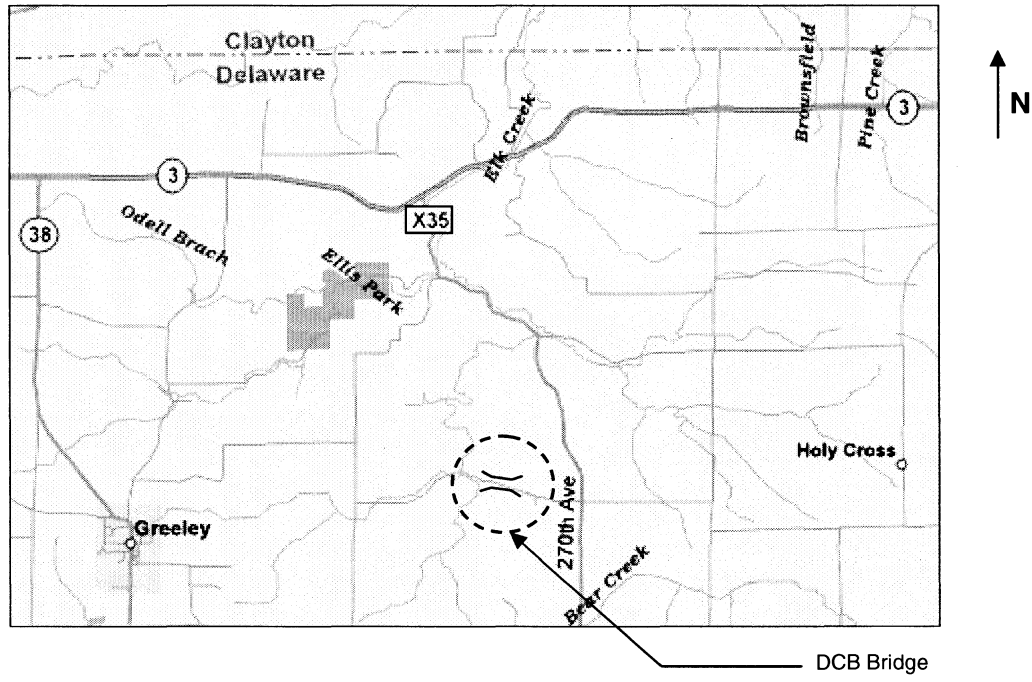

b. Detail A [5]

Figure 1.2. Location of the DCB site.

2. DESIGN AND CONSTRUCTION OF THE RRFC BRIDGES

2.1 BCB2 Design and Construction

2.1.1 BCB2 Design

The BCB2, which was designed by the Buchanan County Engineering Department, is based on the BCB. The BCB was designed, constructed, and tested for the demonstration project, TR-444 [4]. Table 2.1 compares design characteristics of the BCB and BCB2. Although both bridges use 56-ft V-deck RRFCs and have a 54 ft – 0 in. span, the BCB consists of three RRFCs while the BCB2 consists of two. In both bridges, the LFC, which will be discussed later, is a R/C beam; however, the BCB2 LFC is wider than the BCB LFC. These changes in the design caused the width of the bridge to decrease from 29 ft – 1 1/2 in. (BCB) to 20 ft – 7 in. (BCB2).

As may be seen in Figure 2.1a, the 56-ft RRFCs have three main girders, two exterior and one interior, and six small secondary girders, all of which are W-shaped. The main girders are connected with C-shaped transverse members. The deck has a V shape, shown in Figure 2.1d, because the elevation of the top flange of the interior girder is 8 in. lower than that of the exterior girders. Although the elevation of the top flange of the interior girder is constant along the length of the RRFC, the depth of the interior girder varies along the length of the RRFC; these dimensions are shown in Figure 2.2. Unlike the interior

Table 2.1. BCB design vs. BCB2 design.

	BCB	BCB2
Type of RRFCs	56-ft V-deck	56-ft V-deck
Number of RRFCs	3	2
Span (center-to-center of abutments)	54 ft	54 ft
Bridge Width	29 ft – 1 1/2 in.	20 ft – 7 in.
LFC Width	14 1/2 in.	30 1/2 in.

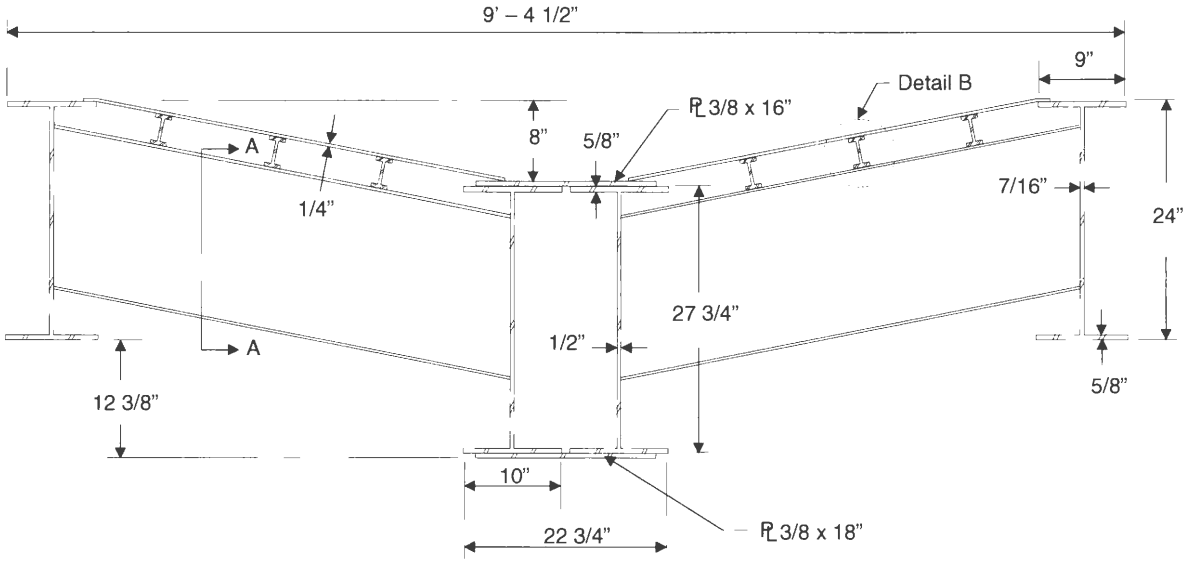

a. Cross-section at midspan

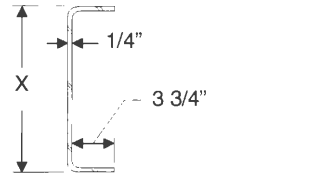

X = 12" for the Small Transverse Member.

X = 16 3/8" for the Large Transverse Member.

b. Section A - A

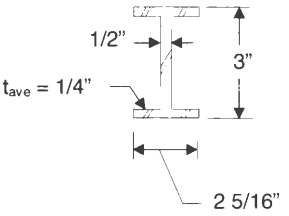

c. Detail B

d. The V-deck

Figure 2.1. Details of the 56-ft V-deck RRFCs used in the BCB2 [4].

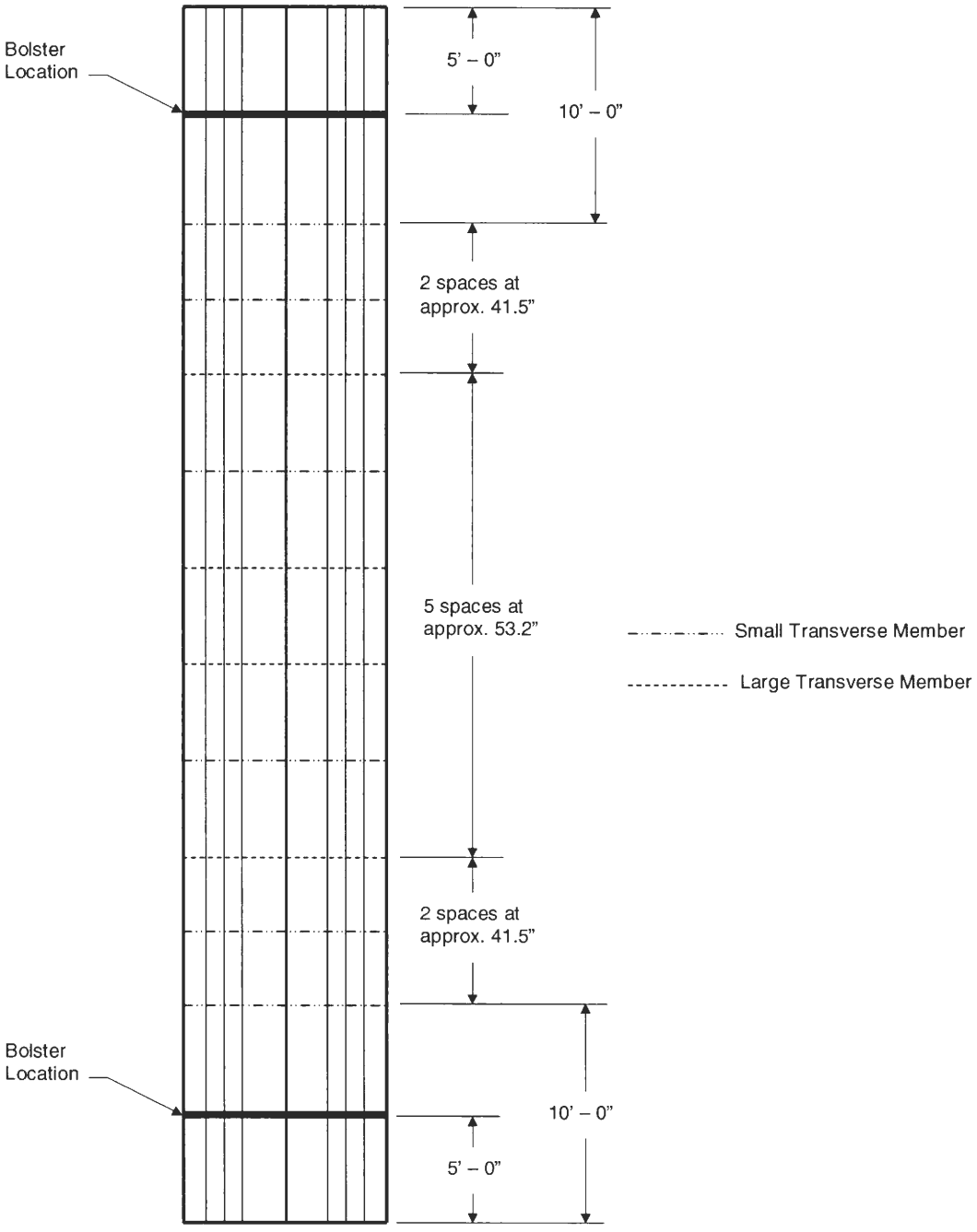

e. Locations of small and large transverse members

Figure 2.1. Continued.

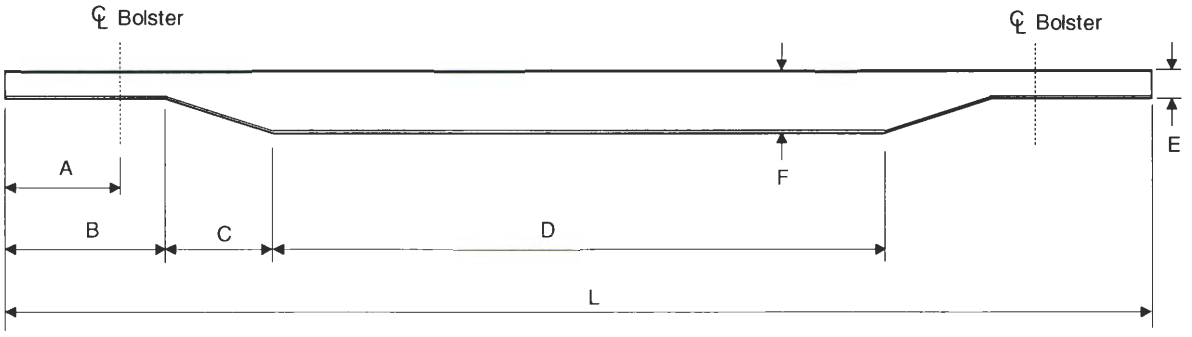

A = Distance from end to bolster
B = Minor Cross-Section Region
C = Transition Region
D = Major Cross-Section Region
L = Length of RRFC

Bridge	Dimensions						
	A	B	C	D	E	F	L
BCB2	5' - 0"	7' - 2"	8' - 9"	24' - 2"	1' - 1 1/4"	2' - 3 3/4"	56' - 0"
DCB	0' - 9"	1' - 9"	8' - 4"	47' - 4"	1' - 1 3/4"	2' - 6 1/4"	67' - 6"

Figure 2.2. Dimensions of the interior girders in the RRFCs used in BCB2 and DCB.

girder, the depth of the exterior girders is constant along the length of the RRFC. Thus, as previously shown in the cross-sectional view of the RRFC at midspan in Figure 2.1a, the depth of the exterior girder is 24 in. along the entire length of the RRFC.

The BCB2 abutments are nearly identical to the BCB abutments, which were designed for the demonstration project, TR-444 [4]. The concrete abutments are composed of a 3-ft by 3-ft cap beam with a 1-ft deep, 2-ft high backwall and are reinforced as shown in Figure 2.3a. Each concrete abutment is supported by three HP10x42 piles spaced on 9 ft – 10 1/2 in. centers. The RRFCs are positioned on the abutments as shown in Figure 2.3b, and a photograph of the side view of an abutment is shown in Figure 2.3c. One difference between the BCB abutments and the BCB2 abutments is the type of joint at the abutments. Both BCB2 abutments have expansion joints while the BCB has one integral abutment and

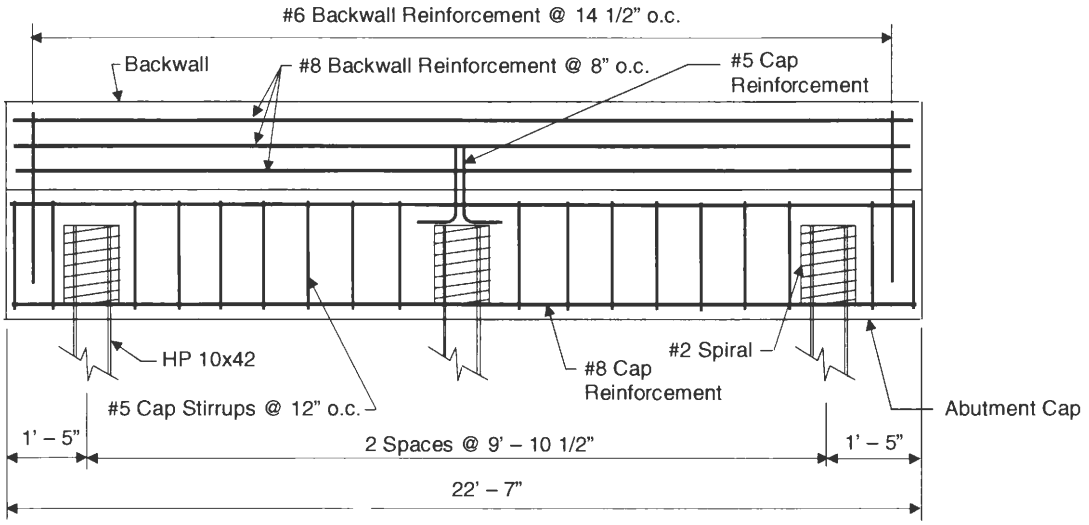

a. End view showing reinforcement in abutments [4]

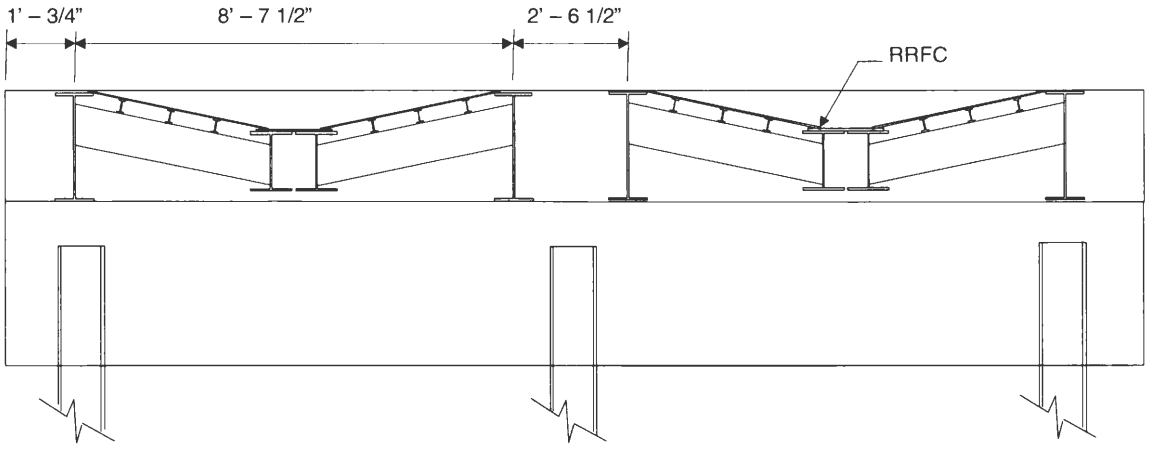

b. Location of RRFCs on abutment [4]

Figure 2.3. Details of BCB2 reinforced concrete abutments.

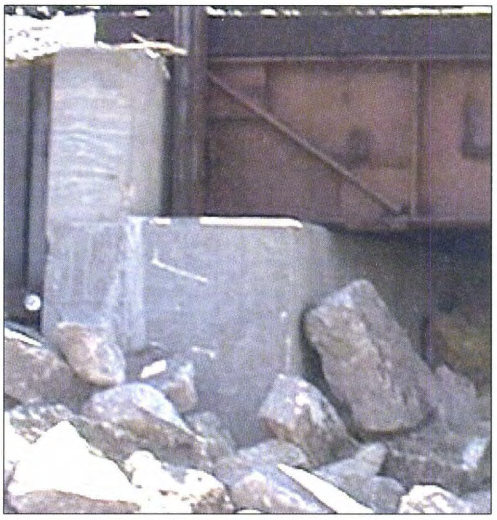

c. Side view of concrete abutment

Figure 2.3. Continued.

one abutment with an expansion joint. As may be seen in Figure 2.4a, the expansion joint consists of a 3/4-in. gap between the RRFC girders and the backwall. In order to prevent gravel and debris from falling into the expansion joint, a 8-in. by 1/2-in. plate was used to cover the gap.

Another difference between the abutments of the two bridges is the interior girder support at the abutments. As shown in Figure 2.4a, both the interior and exterior girders rest on bearing plates; however, at the abutments, the elevation of the bottom flanges of the interior girders is 1 1/2 in. higher than that of the bottom flanges of the exterior girders. Based on a recommendation in the demonstration project, TR-444, additional 1-in. plates were placed beneath the interior girders at the BCB2 abutments as seen in the photograph in Figure 2.4b. At the BCB abutments, the interior girders rest on a concrete seat rather than additional bearing plates [4]. This detail was modified for ease of construction.

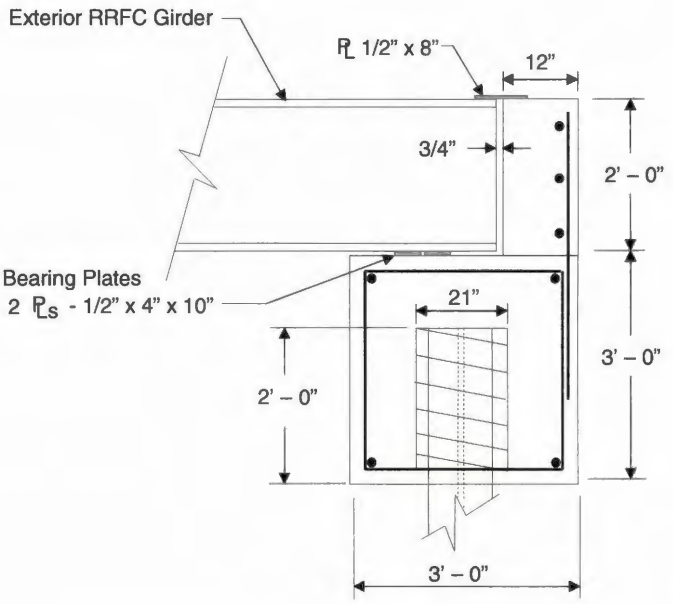

a. Side view of expansion joint (both abutments)

b. View of interior girder resting on abutment cap beam

Figure 2.4. Details of BCB2 abutment cap beam.

The LFC between the RRFCs in the BCB2 is a R/C beam which was based on the LFC in the BCB. The structural adequacy of the BCB LFC was verified with a laboratory specimen for the demonstration project, TR-444 [4]. Shown in Figure 2.5 is the cross-section of the BCB2 and the LFC between the two RRFCs. The beam has a width of 30 1/2 in. and a depth of 24 in. The reinforcement consists of two #11 bars for tension reinforcement and two #5 bars for compression reinforcement positioned as shown in Figure 2.5b. With this reinforcement, the concrete beam can support its own weight. As with the BCB, the adjacent RRFCs are also "tied" together with 3/4-in. threaded rods on 2-ft intervals along the length of the connection.

2.1.2. BCB2 Construction

The BCB2 was constructed by the Buchanan County construction crew, who followed the process for constructing a RRFC bridge developed in the demonstration project, TR-444 [4]. However, recommendations from TR-444 were incorporated into the construction of the BCB2 in order to aid construction. In addition to using additional bearing plates beneath the interior girders at the abutments rather than a concrete seat, the formwork for the LFC was left in place once the LFC was completed.

As shown in Figure 2.6a, the 56-ft V-deck RRFCs have protrusions above the deck; however, in order for the RRFCs to be used in a bridge, the protrusions must be removed. Therefore, before the RRFCs were shipped to Buchanan County for use in the BCB2, the protrusions were trimmed off. A photograph of a 56-ft V-deck RRFC without the protrusions is shown in Figure 2.6b.

As described in further detail in the final report for the demonstration project, the abutments were first constructed, and then the RRFCs were positioned on the abutments as described in Section 2.1.1. Once the RRFCs were in place, the LFC was constructed utilizing leave-in-place formwork. Shoring was not used for the construction of the R/C

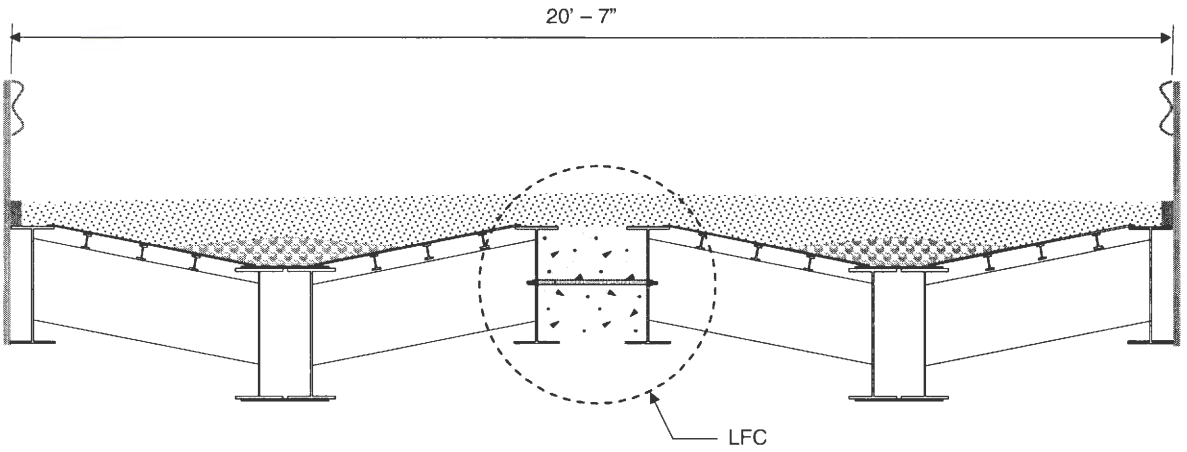

a. Cross-section of BCB2

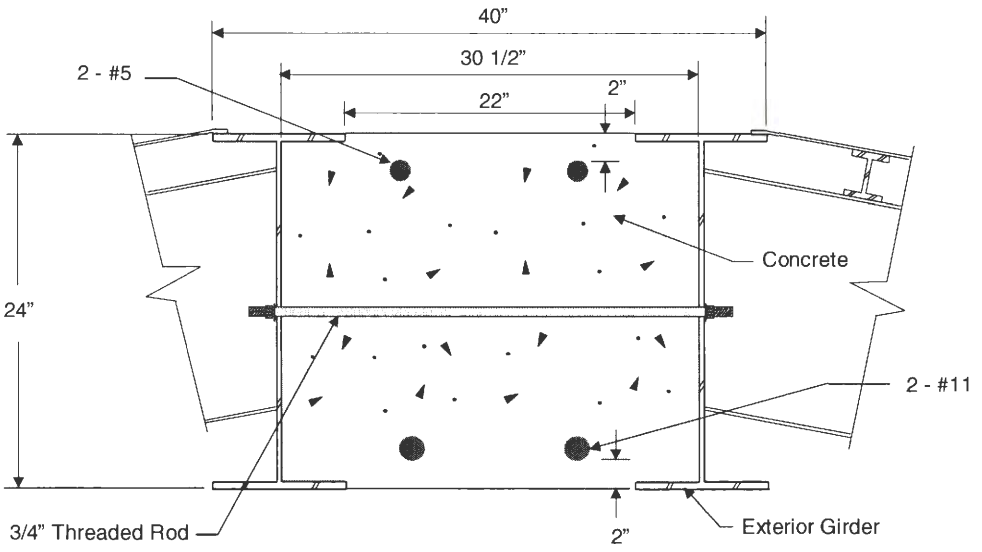

b. Details of LFC

Figure 2.5. Longitudinal RRFC connection used in BCB2.

a. The 56-ft V-deck RRFC prior to trimming

b. The 56-ft V-deck RRFC after trimming

Figure 2.6. Photographs of the 56-ft V-deck RRFC.

beam. After the LFC was completed, pea gravel was placed on the RRFC decks over the interior girders to aid drainage and to fill in the V-deck. A layer of gravel was placed over the remaining RRFC deck and the pea gravel for the driving surface. Finally, the guardrail system was installed. The BCB2 has a guardrail system that consists of guardrail posts on 6-ft intervals welded to the flanges of the exterior girders with a thrie beam attached to the guardrail posts. The completed BCB2 is shown in Figure 2.7.

2.2 DCB Design and Construction

2.2.1 DCB Design

The DCB, which was designed by the Delaware County Engineering Department, consists of two 89-ft RRFCs and has a width of 18 ft – 4 in. Because the DCB did not require an 89-ft span, only a 67 ft – 6 in. portion of each RRFC was used. In order to keep the RRFCs symmetric, 10 ft – 9 in. were removed from each end of both RRFCs. From center-to-center of the abutments, the DCB spans 66 ft – 4 in.

As may be seen in Figure 2.8a, the 89-ft flatcars have three primary girders, two exterior and one interior, which are W-shapes, and six small secondary girders, which are inverted T-shapes. Also shown in Figure 2.8 are the three different transverse members that connect the primary girders: S-shaped members (Cross-section D), L-shaped members (Cross-section E), and U-shaped members (Cross-section F). The depth of the interior girder varies along the length of the RRFC; these dimensions are shown previously in Figure 2.2. The depths of the exterior girders remain constant (d = 15 in.) along the entire length of the RRFC. On the DCB, the south RRFC has an additional 1-in. steel plate welded to the bottom flange of the interior girder.

Both of the abutments are composed of a built-up cap beam supported by seven HP10x42 piles which are positioned beneath the primary girders of the RRFCs as shown in Figure 2.9a. As may be seen in Figure 2.9b, each cap beam consists of two C12x30

a. Side view of BCB2

b. End view of BCB2

Figure 2.7. Completed BCB2.

c. Underneath BCB2

Figure 2.7. Continued.

channels with a 14-in. x 1-in. steel plate welded to the top of the channels. The cap beam channels are connected to the piles with 3/4-in. bolts. Each bolster of the RRFCs rests on the cap beam while pieces of HP8x36 piles are positioned between the exterior girders and the cap beam as shown in Figure 2.9a. The pieces of HP8x36 piles are required beneath the exterior girders because the elevation of the bottom flanges of the exterior girders is 8 in. higher than the elevation of the bottom of the bolsters at the interior girders. The backwall, seen in Figure 2.10a, and the wing walls, seen in Figure 2.10b, consist of 3-in. x 12-in. wood planks. The backwall is held in place by the HP8x36 piles while timber piles are used to support the wing walls.

Unlike the BCB2, a R/C beam was not used as the LFC in the DCB. Instead, as shown in Figure 2.11, the RRFCs were positioned with no space between the bottom

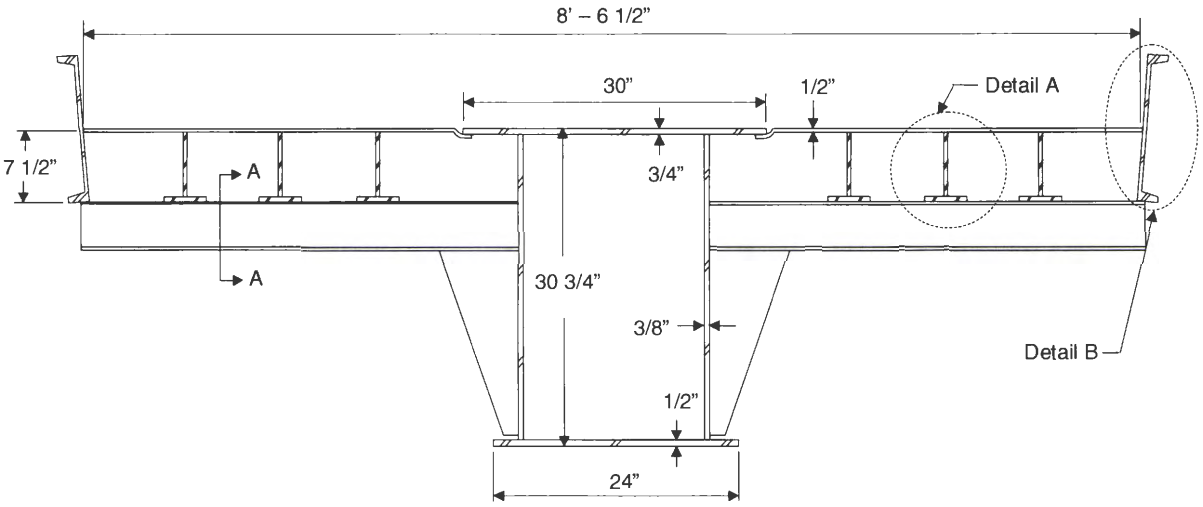

a. Cross-section with S-shape transverse member (Cross-section D)

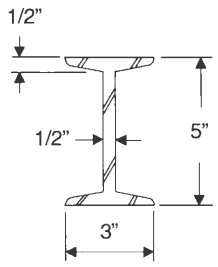

b. Section A – A (S-shape)

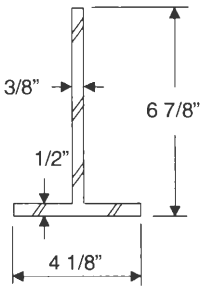

c. Detail A (Tee-shape)

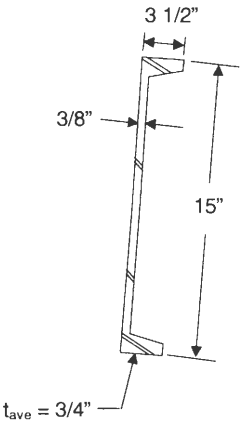

d. Detail B

Figure 2.8. Details of the 89 ft RRFCs used in the DCB [4].

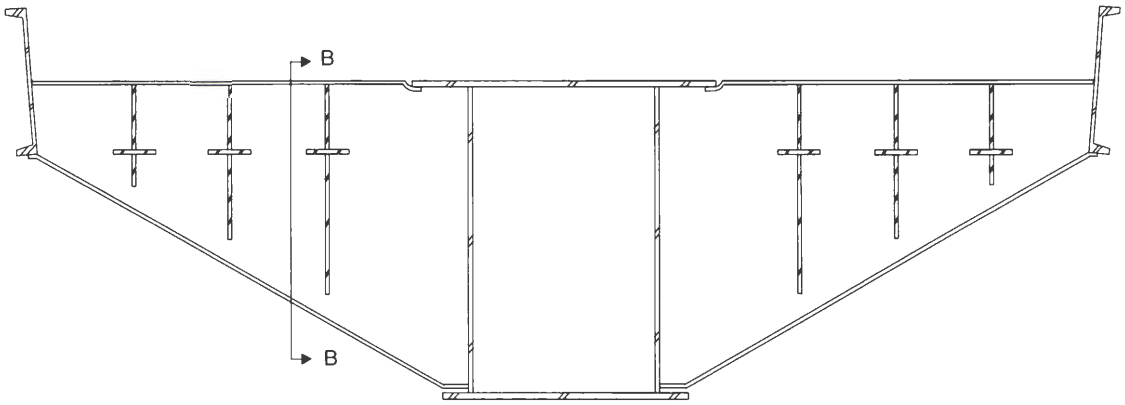

e. Cross-section with L-shaped transverse member (Cross-section E)

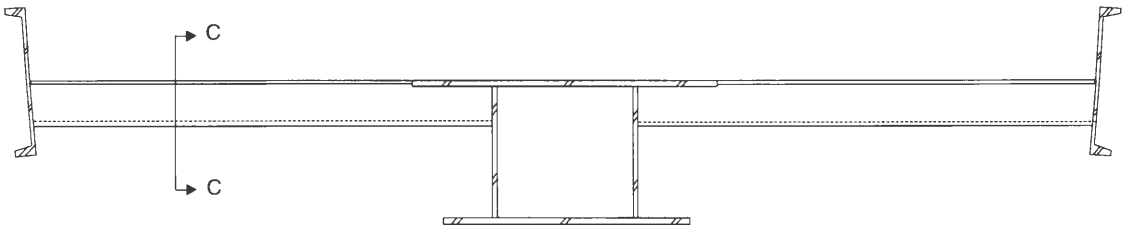

f. Cross-section with U-shaped transverse member (Cross-section F)

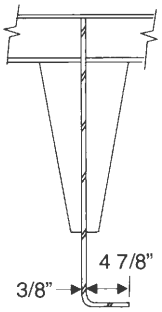

g. Section B – B (L-shape)

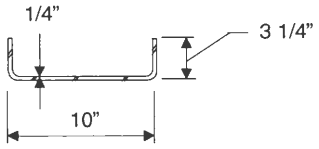

h. Section C – C (U-shape)

Figure 2.8. Continued.

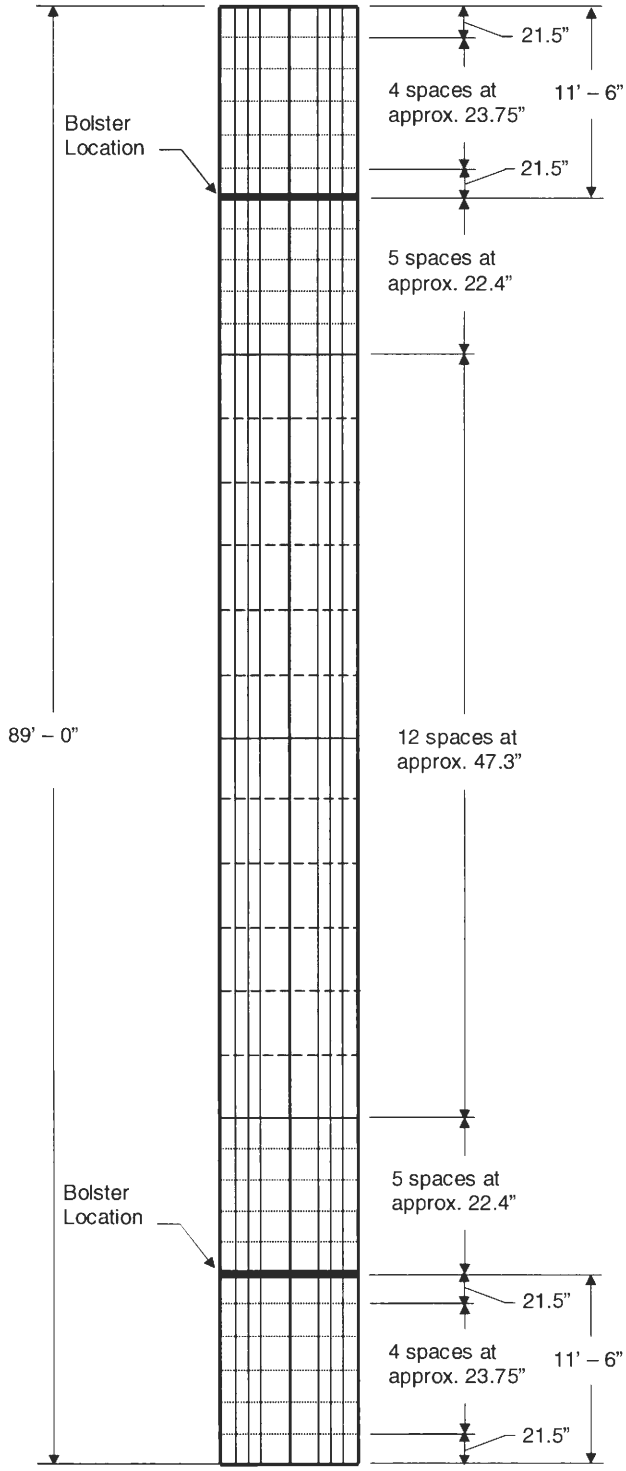

i. Transverse member locations

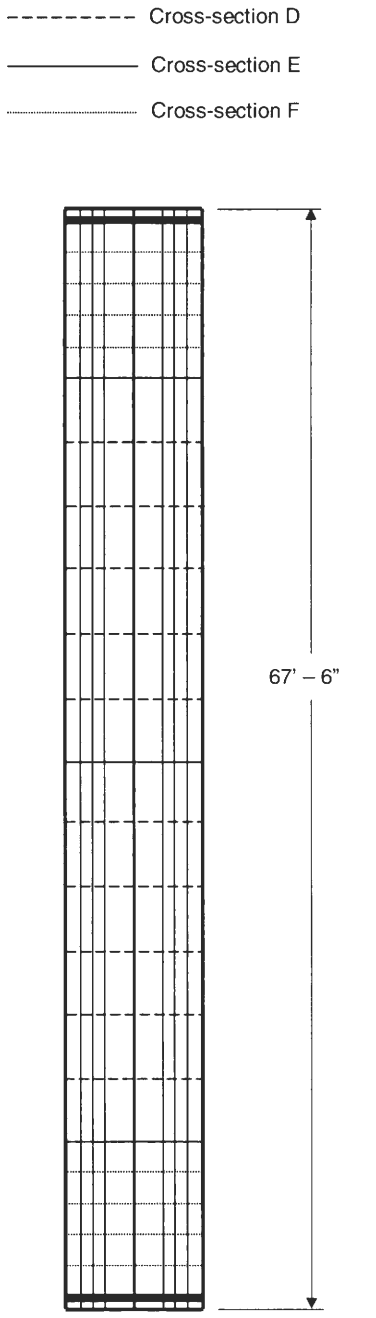

j. Portion of RRFC used in DCB

Figure 2.8. Continued.

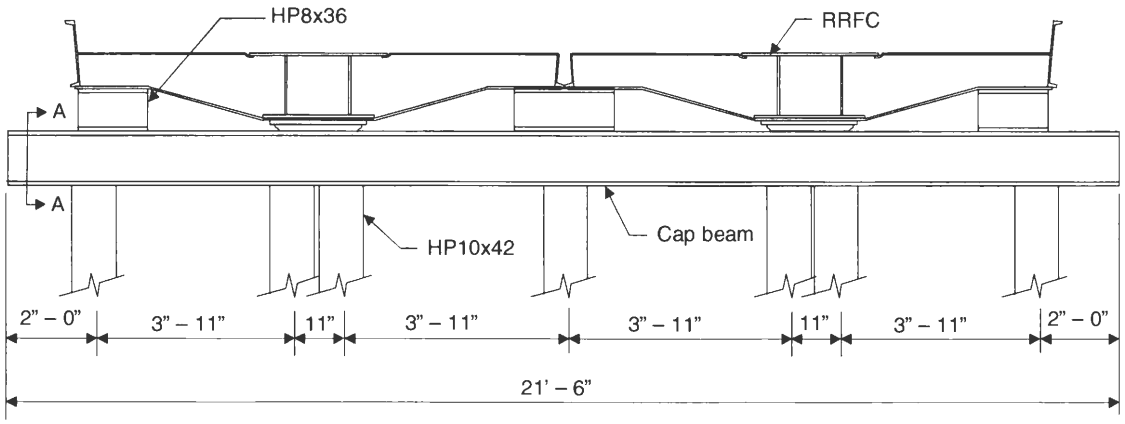

a. RRFC placement [4]

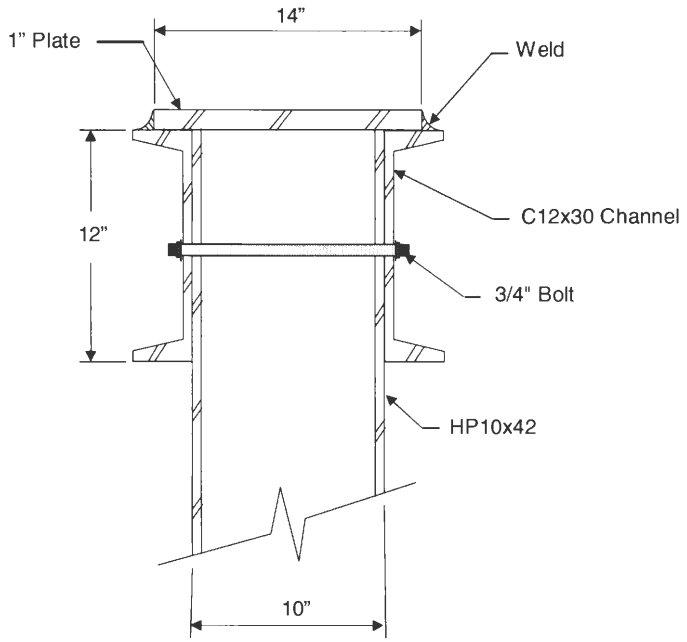

b. Section A-A

Figure 2.9. Details of DCB abutments.

b. Photograph of abutment and backwall

b. Photograph of wing wall and side view of cap beam

Figure 2.10. Photographs of DCB abutments.

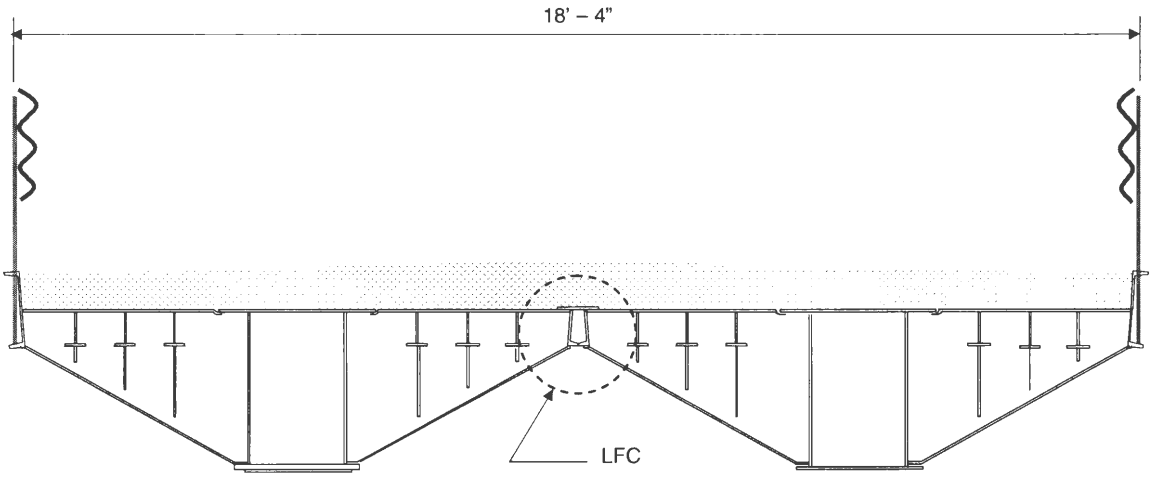

a. Cross-section of DCB

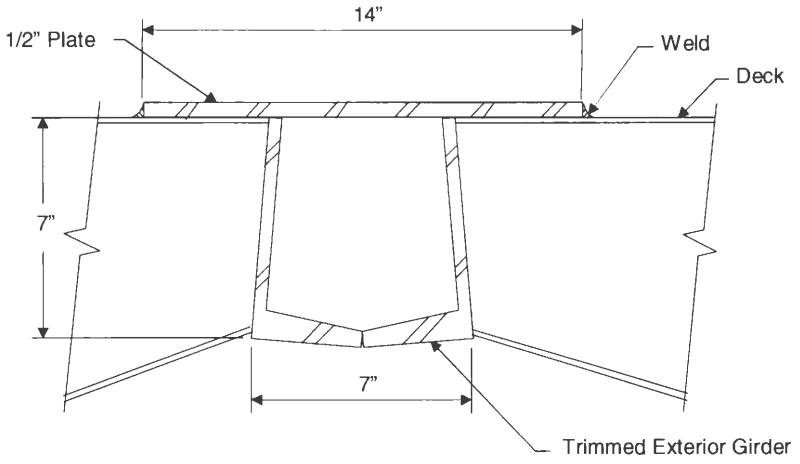

b. Details of LFC

Figure 2.11. Longitudinal RRFC connection used in the DCB.

flanges of the exterior girders. The two exterior girders that comprise the connection were trimmed so that the top of the girders were even with the top of the deck and thus not extending into the driving surface. Although no space was present between the bottom flanges of the exterior girders at the connection, the trimming of the top half of the exterior girders created a 7-in. gap between the two RRFCs. In order to connect the two RRFCs and to provide a flat deck, a 14-in. by 1/2-in. plate was positioned over the adjacent exterior girders. The plate was welded full length and extended the entire length of the RRFC. To complete the LFC, the transverse members, which are spaced approximately 4 ft apart, were welded together across the RRFCs.

2.2.2 DCB Construction

The DCB was constructed by a contractor hired by Delaware County. The construction process for the DCB differed from the process used for the BCB2 because the DCB LFC is not comprised of a R/C beam, and the type of RRFC used is different. The DCB more closely resembles the WCB, which was designed, constructed, and tested for the demonstration project, TR-444 and also consists of 89-ft RRFCs. However, the WCB LFC utilizes a small R/C beam in addition to steel plates welded at the connection [4]. Despite the difference in the LFC, the basic process for constructing the DCB followed the process developed in the demonstration project, TR-444, for the WCB [4].

As shown in Figure 2.12a, the 89-ft RRFCs have protrusions above the deck; however, in order for the RRFCs to be used in a bridge, the protrusions must be removed. Therefore, before the RRFCs were shipped to Delaware County for use in the DCB, the protrusions were trimmed off. The 89-ft RRFCs were also cut to the required 67 ft – 6 in. sections before being shipped to Delaware County. A photograph of a trimmed 89-ft RRFC without the protrusions is shown in Figure 2.12b.

a. The 89-ft RRFC prior to trimming

b. The trimmed 89-ft RRFC

Figure 2.12. Photographs of the 89-ft RRFC.

As described in further detail in the final report for the demonstration project, the abutments were first constructed, and then the RRFCs were positioned on the abutments as described in Section 2.2.1. Once the RRFCs were in place, the 14-in. by 1/2-in. plate was welded over the trimmed exterior girders to form the LFC. After the LFC was completed, a fabric liner was placed over the RRFC deck to prevent gravel from falling through small holes in the deck. A layer of gravel was then placed over the fabric liner for the driving surface. The layer of gravel has a 3-in. crown; the thickness of the gravel layer is 10 in. along the center of the bridge and 7 in. along the edges of the bridge. Finally, a guardrail system was installed. The DCB guardrail system consists of guardrail posts welded on 6-ft intervals to the flanges of the exterior girders with a thrie beam attached to the guardrail posts. The completed DCB is shown in Figure 2.13.

a. Side view of DCB

Figure 2.13. Completed DCB.

b. End view of DCB

c. Underneath DCB

Figure 2.13. Continued.

3. RRFC BRIDGE FIELD LOAD TESTING

The behavior of the RRFC bridges was determined by loading each bridge with a tandem-axle truck loaded with gravel. For both trucks, the width of the front tires was 15 in., the width of the individual tandem tires was 9 in., and the overall width of the rear tandem tires was 2 ft – 0 in. Truck dimensions and the axle weights of the trucks used in the tests are shown in Figure 3.1. The field load tests on BCB2 and DCB will be discussed in the following sections.

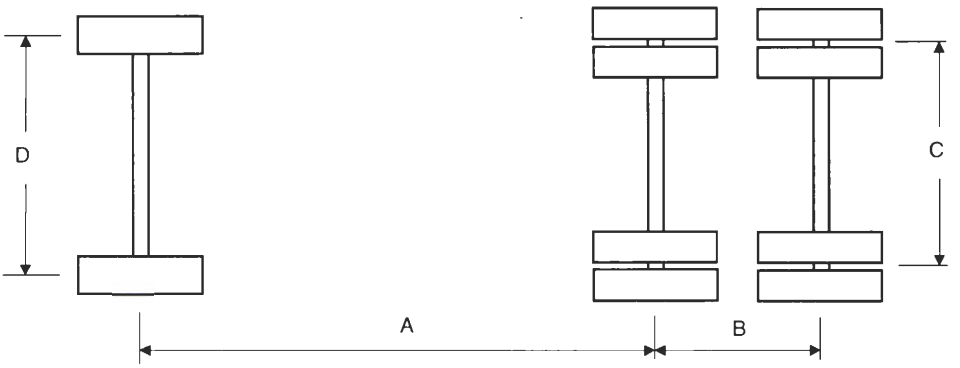

a. Top view

b. Side view

Bridge	Dimensions				Load (lbs)		
	A	B	C	D	F	T	Gross
BCB2	13' -11"	4' - 5"	6' - 0"	6' - 9 1/2"	15,200	34,320	49,520
DCB	15' - 11"	4' - 5"	6' - 0"	7' - 1"	19,480	33,160	52,640

Figure 3.1. Dimensions and weights of test trucks used in RRFC bridge field tests.

3.1 BCB2 Field Testing

3.1.1 BCB2 Instrumentation

In order to determine the structural strength and behavior of the bridge, girder strains in the BCB2 were measured and recorded during the field load tests using strain transducers and a data acquisition system, respectively. For additional bridge behavior data and to determine the load distribution to the primary girders, girder deflections were measured during the tests using deflection transducers. Throughout each test, deflections and strains were measured and recorded continuously. As the tandem axle of the test truck crossed reference lines on the bridge, a feature of the data acquisition system was used to specially mark the strain data for use in the analysis. The reference lines were: the centerline of the west abutment, the 1/4 span, the midspan, the 3/4 span, and the centerline of the east abutment.

The instrumentation plan used in testing BCB2 is illustrated in Figure 3.2. To verify transverse symmetry, the LFC and the bottom flanges of the six primary girders of the bridge were instrumented with strain transducers and deflection transducers at midspan, Detail C in Figure 3.2a. The deflection transducers were only attached to the bottom flange of each of the six primary girders, not the LFC. The placement of the strain transducers across the midspan is shown in Figure 3.2d; the strain transducers used to verify transverse bridge behavior are transducers 10 through 16. Photographs of a strain transducer and a deflection transducer on the bottom flange of an exterior girder are shown in Figures 3.3a and 3.3b, respectively. In addition to the bottom flanges, the top flanges of the three primary girders of the north RRFC were also instrumented with strain transducers, identified as transducers 17 through 19 in Figure 3.2d. The top and bottom flanges of the three primary girders on the north RRFC were instrumented with transducers 14 through 19 in order to determine the neutral axis of each girder.

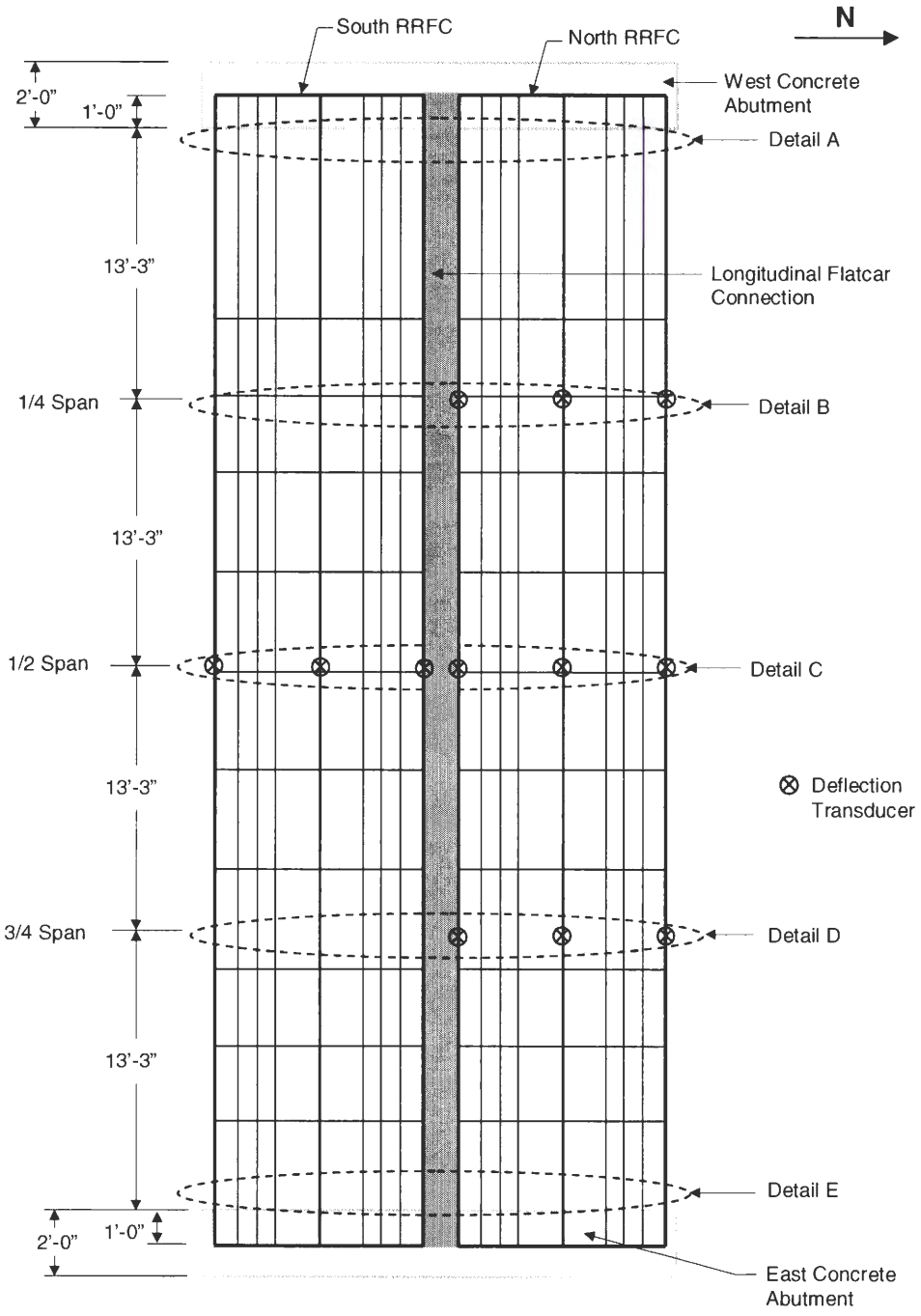

a. Plan View

Figure 3.2. Location of instrumentation in BCB2 tests.

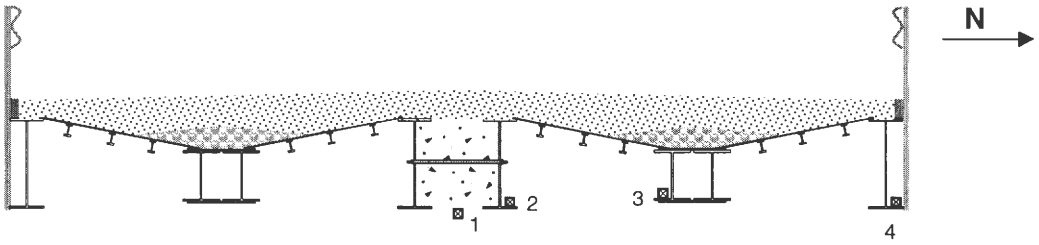

b. Details A and E

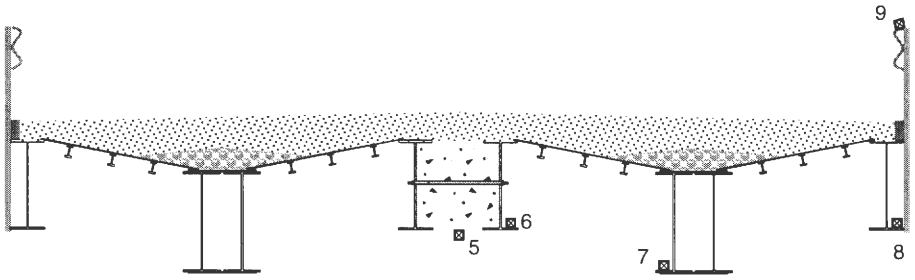

c. Details B and D

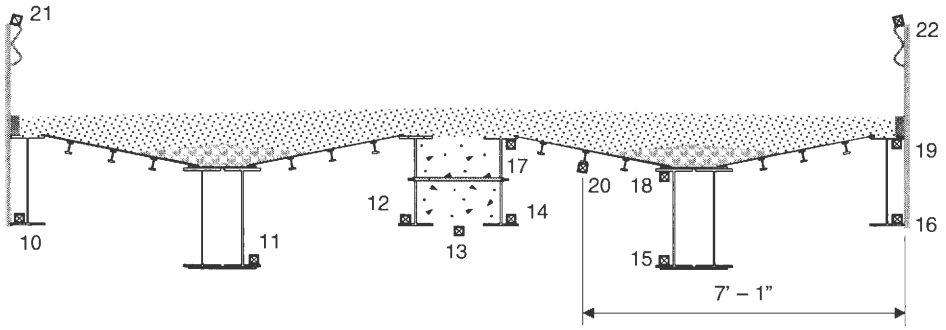

d. Detail C

Notes:

- Strain Transducers 1, 2, and 4 are in Detail E only.
- Strain Transducer 3 is in Details A and E.

Figure 3.2. Continued.

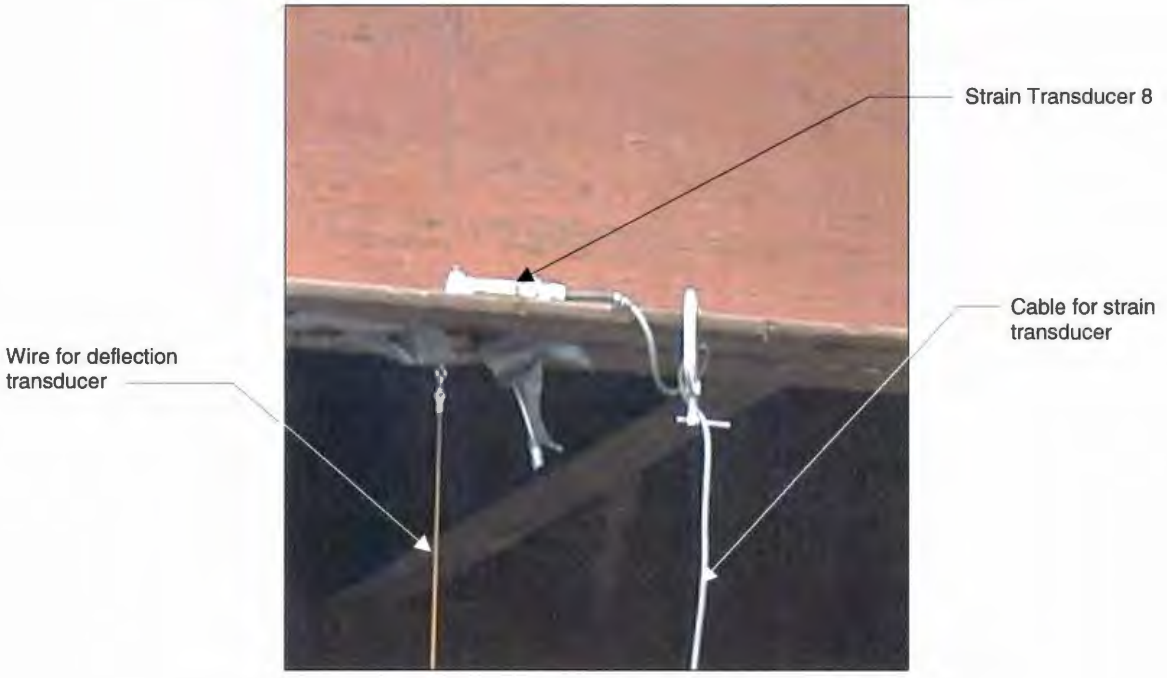

a. Strain transducer 8 on the bottom flange of the exterior girder

b. Deflection transducer for the exterior girder at the 1/4 span

Figure 3.3. Instrumentation used on BCB2.

In order to verify longitudinal symmetry, the interior girder of the north RRFC was instrumented with strain transducers along the length of the BCB2. One strain transducer was positioned at each of the following locations: 18 in. from the face of the west abutment, the 1/4 span, the midspan, the 3/4 span, and 18 in. from the face of the east abutment. As presented in Figure 3.2, the locations correspond with Details A through E, respectively; the strain transducers used to determine the longitudinal bridge behavior are identified as transducers 3, 7, and 15.

At the quarter spans, the bottom flanges of the primary girders of the north RRFC and the LFC were instrumented with strain transducers and deflection transducers to determine the strains and deflections at these locations. In Figure 3.2, the 1/4 span and the 3/4 span are identified as Details B and D, respectively. The strain transducers located at the quarter spans are labeled as transducers 5 through 8 in Figure 3.2c. Also, to determine the behavior of the bridge at the abutments, the LFC and the bottom flanges of the primary girders of the north RRFC were instrumented with strain transducers at the east abutment. Because mounting the strain transducers at the centerline of the abutment was not feasible, the transducers were mounted 18 in. from the face of the east abutment, Detail E in Figure 3.2. The strain transducers located at the east abutment are labeled as transducers 1 through 4 in Figure 3.2b.

In addition to the primary girders, a secondary member was instrumented with one strain transducer to determine the strains in the secondary members. The secondary member that was instrumented was located 7 ft – 1 in. from the north edge of the BCB2. As seen in Figure 3.2d, the strain transducer, identified as transducer 20, was mounted on the secondary member at midspan of the bridge. Finally, to determine the strains in the guardrail, the guardrail on the north edge of the BCB2 was instrumented with strain transducers at the midspan, the 1/4 span, and the 3/4 span and the guardrail on the south

edge of the BCB2 was instrumented with a strain transducer at the midspan. The placement of the strain transducers is shown in Figure 3.2; the strain transducers on the guardrail are labeled 9, 21, and 22. A photograph of a strain transducer on the south guardrail is shown in Figure 3.4a.

As discussed in Section 2.1.2, the formwork for the LFC was left in place; thus, the plywood had to be cut so that the strain transducers mentioned in this section could be mounted on the concrete. A photograph showing the plywood removed from the LFC and a strain transducer mounted to the concrete LFC is presented in Figure 3.4b.

3.1.2 BCB2 Testing

The BCB2 was divided into three lanes as shown in Figure 3.5 to determine the behavior of the bridge under different load conditions. As may be seen in Figures 3.5a and 3.5c, when in Lanes 1 or 3, the truck was positioned with the edge of the double tires 2 ft from the north or south edge of the bridge, respectively. With the truck positioned on the edge of the bridge, an eccentric load condition is created. The results from the test with the truck positioned in Lane 1 can be compared to the results from the test with the truck positioned in Lane 3 in order to verify transverse symmetry in the BCB2. The results from the tests with an eccentric load condition can also be used to determine the effectiveness of the LFC. A photograph of the test truck positioned in Lane 3 is shown in Figure 3.6a. As may be seen in Figure 3.5b, the truck was centered transversely on the bridge when in Lane 2. The results from the test with a centered load condition can be used to verify transverse symmetry. A photograph of the test truck positioned in Lane 2 is shown in Figure 3.6b.

For the field load tests, the truck, shown in Figure 3.6c, was driven slowly across the bridge in each of the three lanes while the data acquisition system recorded the strains and deflections measured by the strain and deflection transducers. The tests on the BCB2 were

a. Strain transducer at midspan on the south guardrail

b. Strain transducer on the concrete LFC

Figure 3.4. Strain transducers used on BCB2.

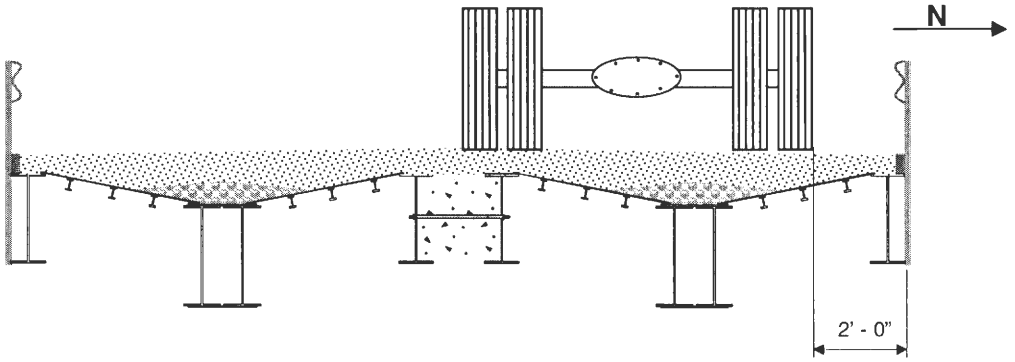

a. Lane 1

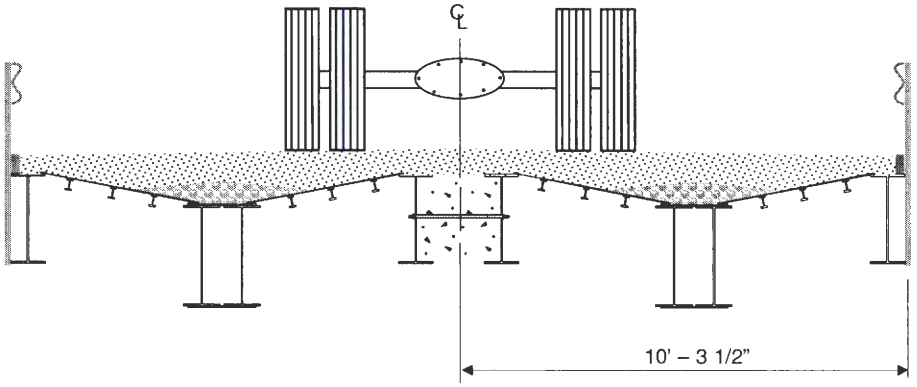

b. Lane 2

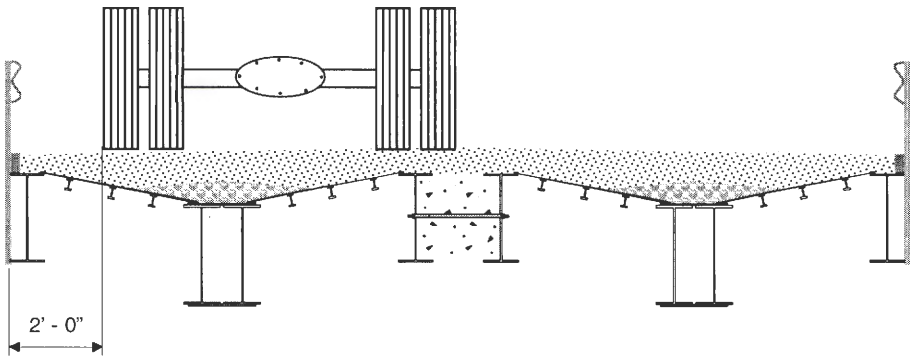

c. Lane 3

Figure 3.5. Transverse locations of truck in the BCB2 tests.

a. Loading BCB2 with truck on south RRFC (Lane 3)

b. Truck centered on BCB2 (Lane 2)

c. Photograph of BCB2 test truck

Figure 3.6. Photographs of the truck used in the BCB2 tests.

essentially static load tests because when traveling slowly, the truck did not produce a dynamic amplification on the girder strains and deflections.

3.2 DCB Field Testing

Unlike the BCB2, both static and dynamic field load tests were conducted on the DCB. The following sections will describe the instrumentation and testing methods used for the static and dynamic tests.

3.2.1 DCB Instrumentation for Static Tests

As with the BCB2 field load test, to determine the structural strength and behavior of the bridge, girder strains in the DCB were measured and recorded during the static field load tests using strain transducers and a data acquisition system, respectively. For additional bridge behavior data and to determine the load distribution to the primary girders, girder deflections were measured during the tests using deflection transducers. Throughout each test, deflections and strains were measured and recorded continuously. As the tandem axle of the test truck crossed reference lines on the bridge, a feature of the data acquisition system was used to specially mark the strain data for use in the analysis. The reference lines were the centerline of the west abutment, the 1/4 span, the midspan, the 3/4 span, and the centerline of the east abutment.

The instrumentation plan used in testing the DCB, illustrated in Figure 3.7, is similar to the plan used in testing the BCB2. To verify transverse symmetry, the bottom flanges of the six primary girders of the bridge were instrumented with strain transducers and deflection transducers at midspan, Detail E in Figure 3.7a. The deflection transducers were attached to the bottom flange of each of the six primary girders. A photograph of the deflection transducers for the LFC and interior girder of the south RRFC is presented as Figure 3.8. The placement of the strain transducers across the midspan is shown in Figure 3.7f. The strain transducers used to verify transverse bridge behavior are transducers 14

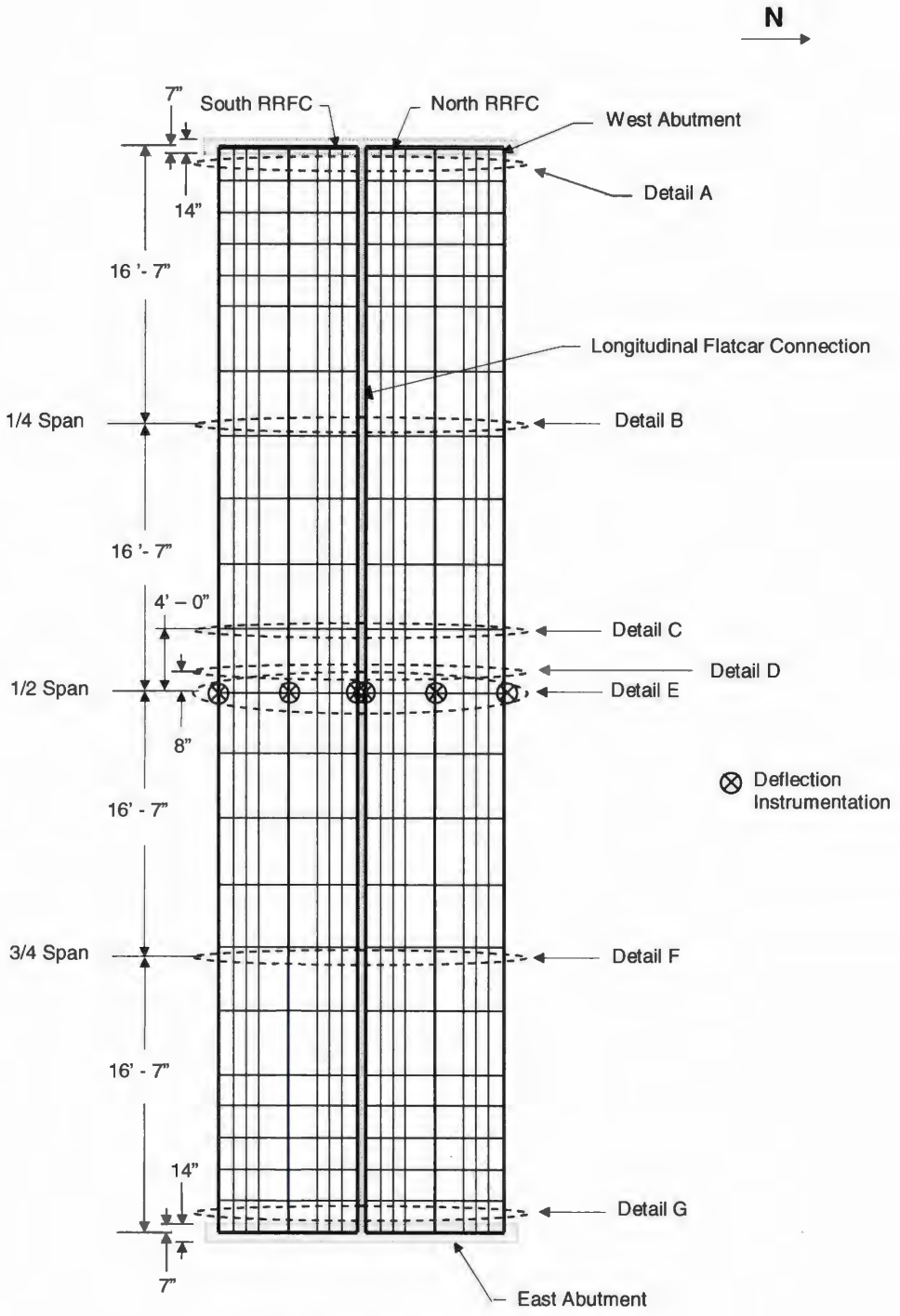

a. Plan View

Figure 3.7. Location of instrumentation in DCB tests.

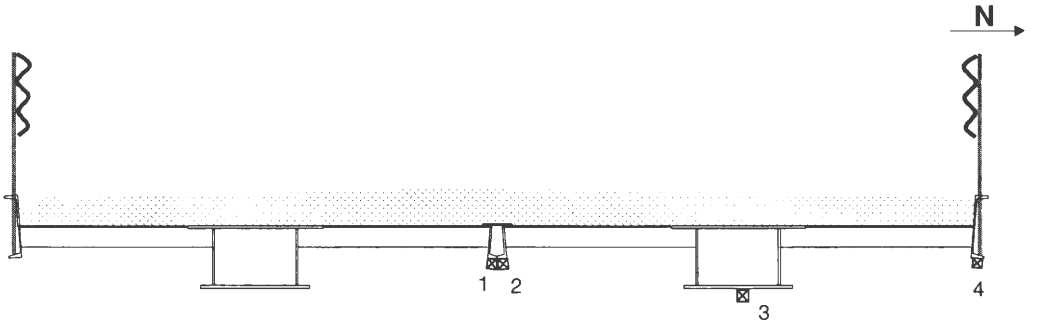

b. Details A and G

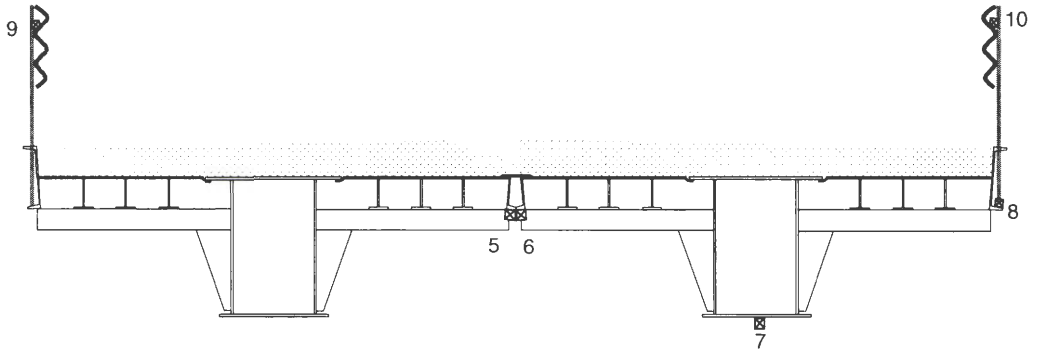

c. Details B and F

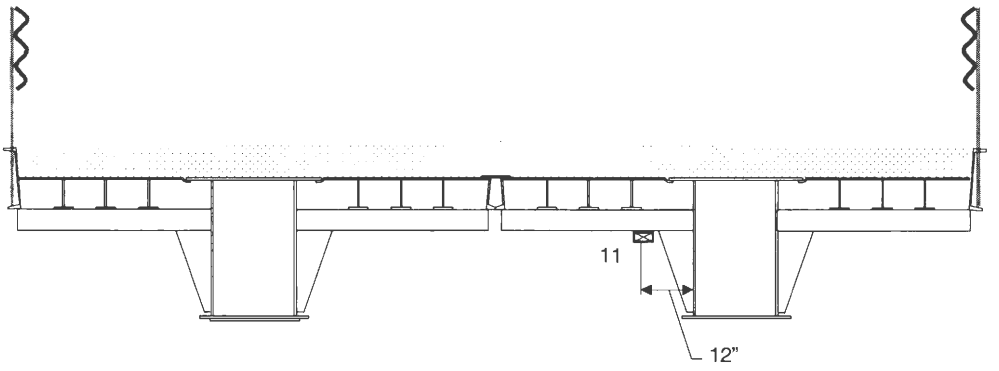

d. Detail C

Figure 3.7. Continued.

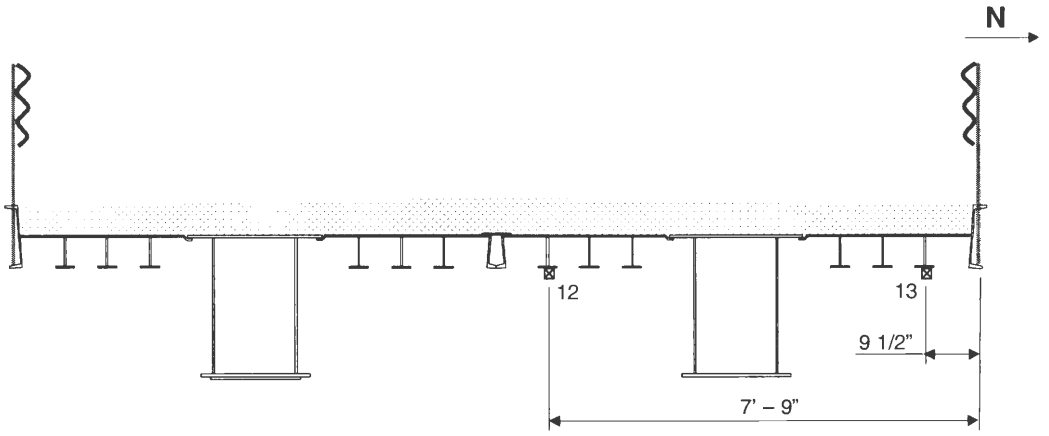

e. Detail D

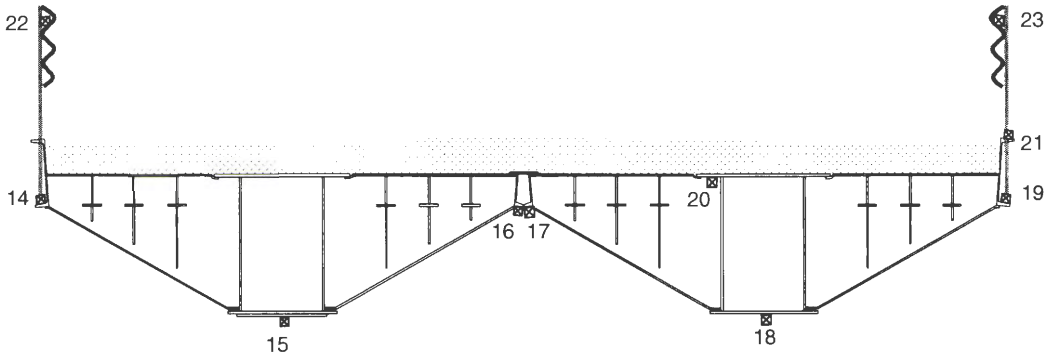

f. Detail E

Notes:

- Strain Transducers 1, 2, and 4 are in Detail G only.
- Strain Transducers 5, 6, and 10 are in Detail F only.

Figure 3.7. Continued.

Figure 3.8. Deflection transducers used on DCB.

through 19. Photographs of strain transducers 16 and 17 at the midspan of the two girders at the LFC and strain transducer 7 on the interior girder are shown in Figure 3.9. In addition to the bottom flanges, the top flanges of the interior girder of the north RRFC and the exterior girder on the north edge of the DCB were instrumented with strain transducers, identified as transducers 20 and 21 in Figure 3.7f. The top and bottom flanges of the interior girder of the north RRFC and the exterior girder on the north edge of the bridge were instrumented with transducers 18 through 21 to determine the neutral axis of each girder.

In order to verify longitudinal symmetry, the interior girder of the north RRFC was instrumented with strain transducers along the length of the DCB. One strain transducer was positioned at each of the following locations: 12 in. from the face of the west abutment, the 1/4 span, the midspan, the 3/4 span, and 12 in. from the face of the east abutment. As presented in Figure 3.7, the locations correspond with Details A, B, E, F, and G, respectively; the strain transducers used to determine the longitudinal bridge behavior are identified as transducers 3, 8, and 18.

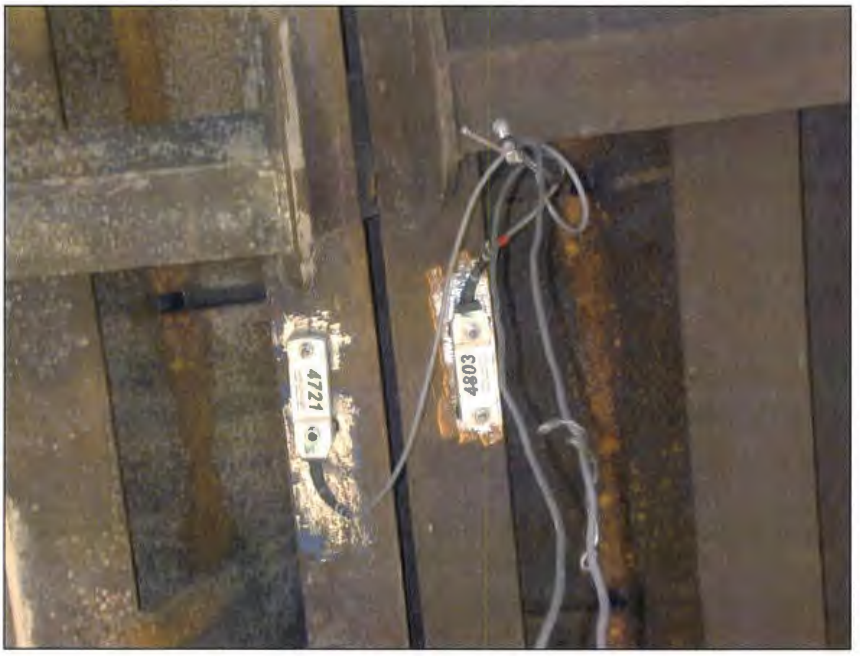

a. Strain transducers 16 and 17 on bottom flanges of girders at LFC

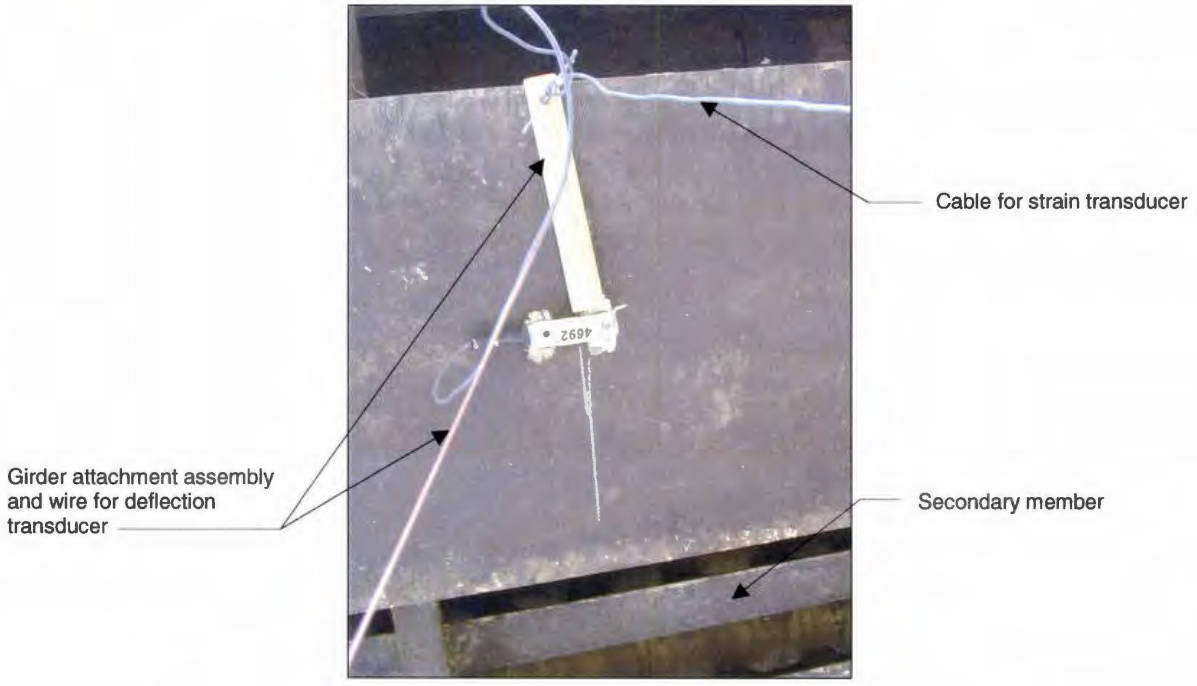

b. Strain transducer 7 on bottom flange of interior girder

Figure 3.9. Strain transducers on the DCB LFC.

At the quarter spans, the bottom flanges of the primary girders of the north RRFC were instrumented with strain transducers to determine the strains and deflections at these locations. At the 3/4 span, both girders at the LFC were instrumented with strain transducers. In Figure 3.7, the 1/4 span and the 3/4 span are identified as Details B and F, respectively, and the strain transducers located at the quarter spans are labeled as transducers 5 through 8 in Figure 3.7c. Also, to determine the behavior of the bridge at the abutments, the bottom flanges of the primary girders of the north RRFC were instrumented with strain transducers at the east abutment. Because mounting the strain transducers at the centerline of the abutment was not feasible, the transducers were mounted 12 in. from the face of the east abutment, Detail G in Figure 3.7. The strain transducers located at the east abutment are labeled as transducers 1 through 4 in Figure 3.7b.

In addition to the primary girders, two secondary members and one S-shaped transverse member were instrumented with strain transducers to determine the strains in the secondary and S-shaped transverse members. As seen in Figure 3.7e, strain transducers 12 and 13 were mounted on the secondary members that were located 7 ft – 9 in. and 9 1/2 in. from the north edge of the DCB, respectively. The longitudinal position of the strain transducers, identified as Detail D in Figure 3.7a, is 8 in. west of the midspan. A photograph of strain transducer 13 on the secondary member is shown in Figure 3.10a. The transverse member that was instrumented is identified as Detail C in Figure 3.7a and was approximately 4 ft west of the midspan. As shown in Figure 3.7d, the strain transducer on the transverse member, transducer 11, is mounted 12 in. south of the web of the interior girder of the north RRFC. In Figure 3.10b, a photograph of strain transducer 11 on the S-shaped transverse member is shown.

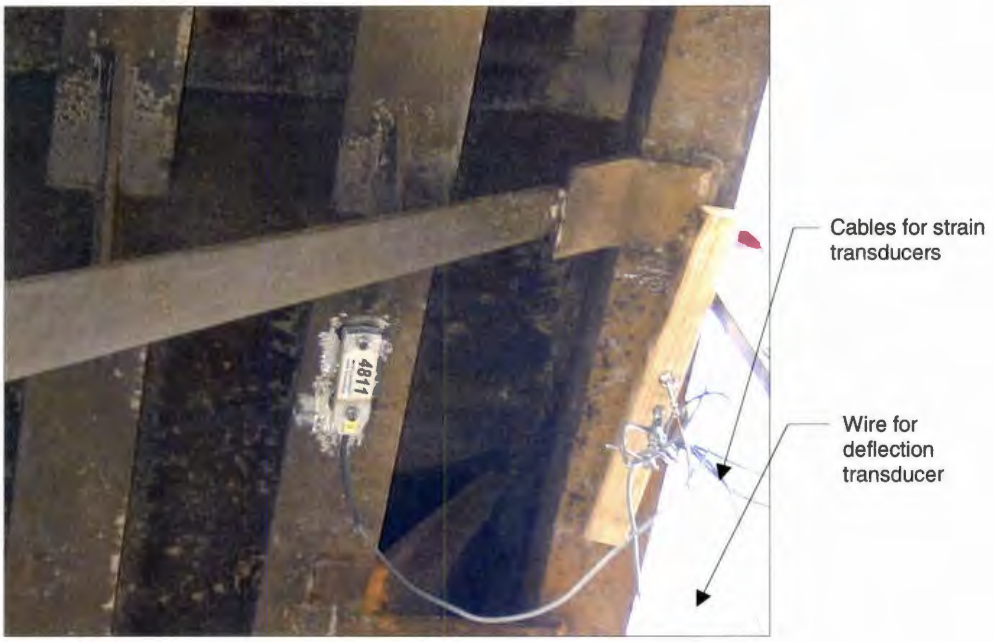

a. Strain transducer 13 on a secondary member

b. Strain transducer 11 on an S-shaped transverse member

Figure 3.10. Photographs of strain transducers used on DCB.

Finally, to determine the strains in the guardrail, both the north and south guardrails of the DCB were instrumented with strain transducers at the midspan and the 3/4 span. The placement of the strain transducers is shown in Figure 3.7; the strain transducers on the guardrail are labeled 9, 10, 22, and 23.

3.2.2 DCB Static Testing

As with the BCB2, the DCB was divided into the three lanes shown in Figure 3.11 to determine the behavior of the bridge under different load conditions. As may be seen in Figures 3.11a and 3.11c, when in Lanes 1 or 3, the truck was positioned with the center of one set of the double tires 2 ft from the south or north edge of the bridge, respectively. With the truck positioned in Lane 1 or 3, an eccentric load condition is created. The results from test with the truck positioned in Lane 1 can be compared to the results from the test with the truck in Lane 3 in order to verify transverse symmetry in the DCB. The effectiveness of the LFC can also be determined with the results from the tests with an eccentric load condition. As may be seen in Figure 3.11b, the test truck was centered transversely on the DCB when in Lane 2, creating a centered load condition. The results from the test with a centered load condition can be used to verify transverse symmetry. Photographs of the test truck positioned in Lanes 2 and 3 are shown in Figures 3.12a and b, respectively.

For the static field load tests, the truck, shown in Figure 3.12c, was driven slowly across the bridge in each of the three lanes while the data acquisition system recorded the strains and deflections measured by the strain and deflection transducers. The tests were considered static because when traveling at a slow speed, the truck did not cause significant dynamic effects to occur in the bridge.

3.2.3 DCB Instrumentation for Dynamic Tests

To determine the dynamic behavior of the bridge, girder strains in the DCB were measured and recorded during the dynamic field load tests using strain transducers and a

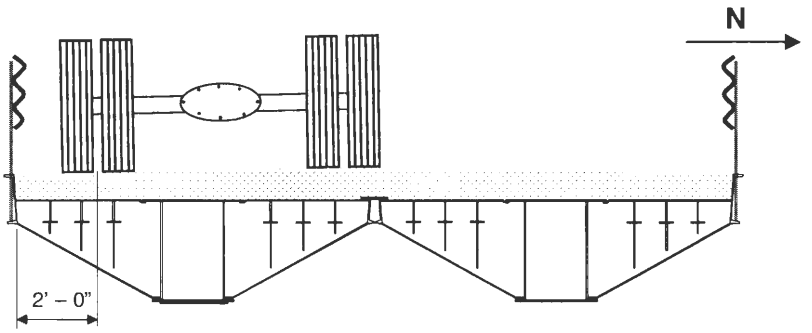

a. Lane 1

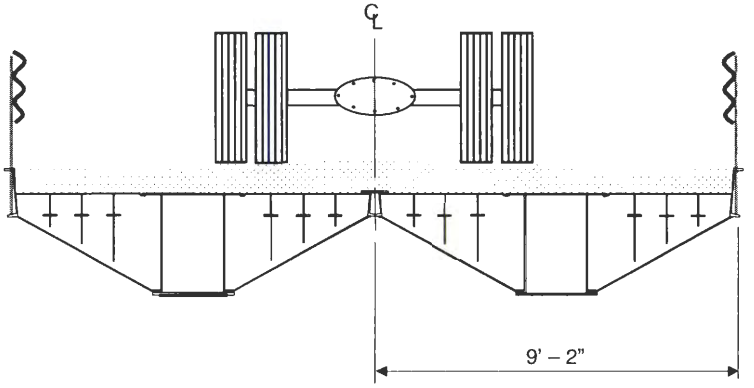

b. Lane 2

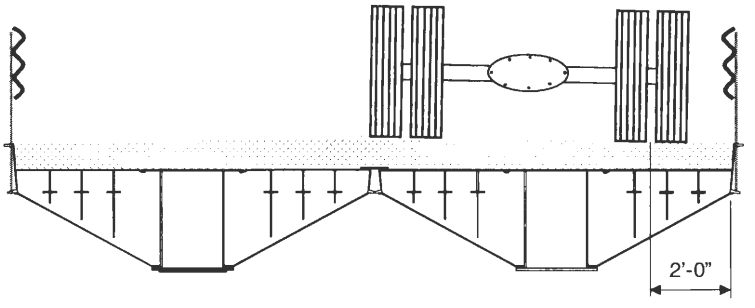

c. Lane 3

Figure 3.11. Transverse locations of truck in DCB tests.

a. Truck centered on DCB (Lane 2)

b. Loading DCB with truck on north RRFC (Lane 3)

c. Photograph of DCB test truck

Figure 3.12. Photographs of the truck used in the DCB tests.

data acquisition system, respectively. For additional bridge behavior data, girder deflections were measured during the tests using deflection transducers. Throughout each test, deflections and strains were measured and recorded continuously. As the front axle of the test truck crossed the centerline of the west abutment of the bridge, a feature of the data acquisition system was used to specially mark the strain data for use in the analysis.

The instrumentation plan for the dynamic field load tests of the DCB is identical to the instrumentation plan for the static field load tests which was described in Section 3.2.1 and shown in Figure 3.7. The strains and deflections measured with the strain and deflection transducers shown in Figure 3.7 during the dynamic load tests can be used to determine the behavior of the bridge under dynamic loads. Also, the data collected during the dynamic load tests can be compared with the data from the static load tests in order to determine the dynamic amplification factors for the girder strains and deflections due to the test truck traveling at faster speeds.

3.2.4 DCB Dynamic Tests

Because the DCB is only 18 ft – 4 in. wide and is on a low-volume road, the daily traffic on the bridge is most likely to cross the DCB while centered on the bridge. Thus, for the dynamic field load tests, the truck was driven across the bridge while centered on the bridge. This position of the test truck corresponds to Lane 2 of the static tests which was shown in Figure 3.11b.

Two dynamic load tests were run on the DCB. In the first dynamic test, the test truck was driven across the DCB while traveling at 10 mph. For the second dynamic test, the test truck was driven across the DCB at 15 mph. At these speeds, the girder strains and deflections of the DCB will be amplified due to the dynamic effects of the test truck. Thus, the tests can be considered to be dynamic.

4. RESULTS AND ANALYSIS

As discussed in Sections 3.1 and 3.2, deflections and strains were measured in longitudinal girders and secondary and transverse members of the BCB2 and DCB. In the following sections, the deflection and strain results from the field load tests will be presented and analyzed in order to determine the structural behavior of the BCB2 and DCB and thus satisfy objective 1 of this project.

In order to determine the stresses in the girders from the strains measured during the field load tests, the elastic modulus of the steel in the RRFCs must be known. To determine the acceptability of these stresses, the strength of the steel must be known. In the demonstration project, TR-444, tensile tests were performed on steel coupons from a 56-ft V-deck RRFC and an 89-ft RRFC. The results of the tensile tests showed that the modulus of elasticity and the yield strength of both types of RRFCs were 29,000 ksi and 40 ksi, respectively [4]. As stated in the 2003 *AASHTO Standard Specifications for Highway Bridges,* the allowable flexural stress for compact steel members not subjected to lateral-torsional buckling is 55 percent of the yield strength [6]. The girders in both types of RRFCs used in this study are compact and not subjected to lateral-torsional buckling; therefore, the allowable flexural stress in the steel members of the RRFCs used in the BCB2 and DCB was 22 ksi, 55 percent of 40 ksi.

4.1 BCB2 Results and Analysis

4.1.1 Dead Load Analysis

The total stress in the BCB2 is the stress caused by the test truck during the field load test plus the stress due to the dead load on the bridge. To determine the total stresses in the primary girders of the BCB2, a dead load analysis was performed. To simplify this analysis, several assumptions were made. First, it was assumed that each primary girder supported its self-weight along with the weight of the secondary girders and transverse

members within the tributary width of the primary girder. Since the 56-ft V-deck RRFC has three primary girders, the RRFC width was divided into quarters as shown in Figure 4.1. Thus, the tributary width of an exterior girder was about 2 ft – 4 in. and the tributary width of the interior girder was about 4 ft – 8 in. Following conventional methods for bridge design, the connected RRFCs were assumed to form a rigid cross-section such that any additional dead load could be considered uniform on the bridge. Thus, the total weight of the pea gravel and the gravel driving surface was assumed to be uniform on the bridge even though the pea gravel was only located in the V-deck above the interior girders as described in Section 2.1.2. Based on quantities and weights from the demonstration project, the total weight of the pea gravel and the gravel driving surface was assumed to be 98 lb/ft^2 and the weight of the RRFC was taken as its delivery weight, 35,000 lbs [4]. Finally, the BCB2 was assumed to be simply supported.

In order to determine the dead load stresses in the interior and exterior girders of one RRFC, two analyses were completed, one for an interior girder and one for an exterior

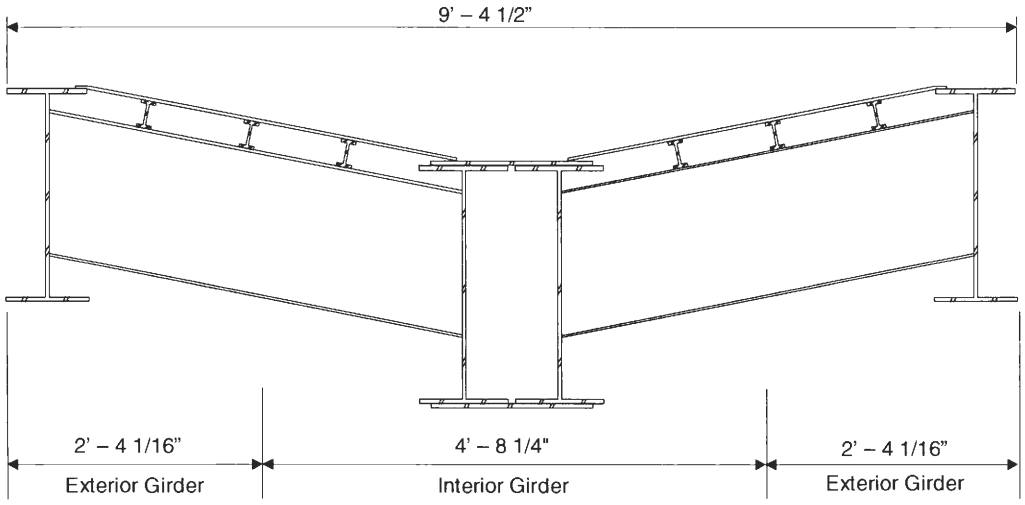

Figure 4.1. Tributary width of RRFC girders for dead load analysis.

girder. The dead loads in the tributary width of the girder were used to determine the moment at the midspan of the simply-supported girder. With the midspan moment and the section modulus of the girder, the dead load stress at the midspan of the girder was determined using Equation 4.1.

$$\sigma_{DL} = \frac{M}{S} \tag{4.1}$$

where:

σ_{DL} = The dead load stress at the midspan of the girder

M = The midspan dead load moment

S = The section modulus of the girder

Using this procedure, the tensile dead load stresses in the bottom flanges of the interior and exterior girders of the BCB2 were determined to be 5.9 ksi and 11.0 ksi, respectively.

4.1.2 Field Load Test Results

The BCB2 instrumentation plan described in Section 3.1.1 included measuring the strain in one secondary member and the interior girders at the abutments (18 in. from the face of the abutments). The maximum strains at the abutments occurred in the bottom flanges of the interior girders. At the east abutment, the maximum strain was 33 MII (1.0 ksi), and at the west abutment, the maximum strain was 24 MII (0.7 ksi). The presence of strain in the sections close to the abutments indicates that end restraint is present in the BCB2 even though it was designed to be simply supported. However, the maximum strain in the girders at the abutments was considerably less than the maximum strains experienced in the interior and exterior primary girders at the midspan of the bridge; the maximum stresses in the interior girders at the abutments were also significantly less than 22 ksi, the allowable stress of the steel. Although end restraint reduces the midspan strains,

the effect is minimal because the strains at the abutments were significantly less than the strains at midspan. Thus, the abutment strains will not be discussed further.

As shown previously in Figure 3.2, the secondary member that was instrumented with Strain Transducer 20 was located 7 ft – 1 in. from the north edge of the bridge, or approximately half way between the interior girder of the north RRFC and the LFC. The maximum strain experienced in this member was 57 MII (1.6 ksi) and occurred when the truck was positioned in Lane 2, with the truck tires located directly above the transducer. Since the maximum strain in the secondary member was significantly less than the maximum strains experienced in the interior and exterior primary girders, the secondary members were determined to not be critical and will be excluded from the following discussion.

The maximum midspan deflections and strains that were measured when the truck was in Lanes 1 – 3 on the bridge are presented in Figures 4.2 – 4.4, respectively. As described in Section 3.1.1, the midspan of BCB2 was instrumented with six deflection transducers and seven strain transducers. The deflections and strains measured with these transducers are represented in Figures 4.2 – 4.4 by small diamonds. The dashed lines represent a trend that may occur between the measured deflections and strains and thus, do not represent measured deflections or strains. The measured deflections and strains shown in Figures 4.2 – 4.4 occurred when the center of the tandem axle of the truck was at the midspan of the bridge. As can be seen in Figures 4.2 and 4.4, the maximum deflection of the BCB2 was 0.37 in. and 0.35 in. when the truck was in Lane 1 or 3, respectively, and occurred at the exterior girder on the north or south edge of the bridge, respectively. When the truck was positioned in Lane 2, the maximum deflection as seen in Figure 4.3 was 0.24 in. and occurred at the LFC.

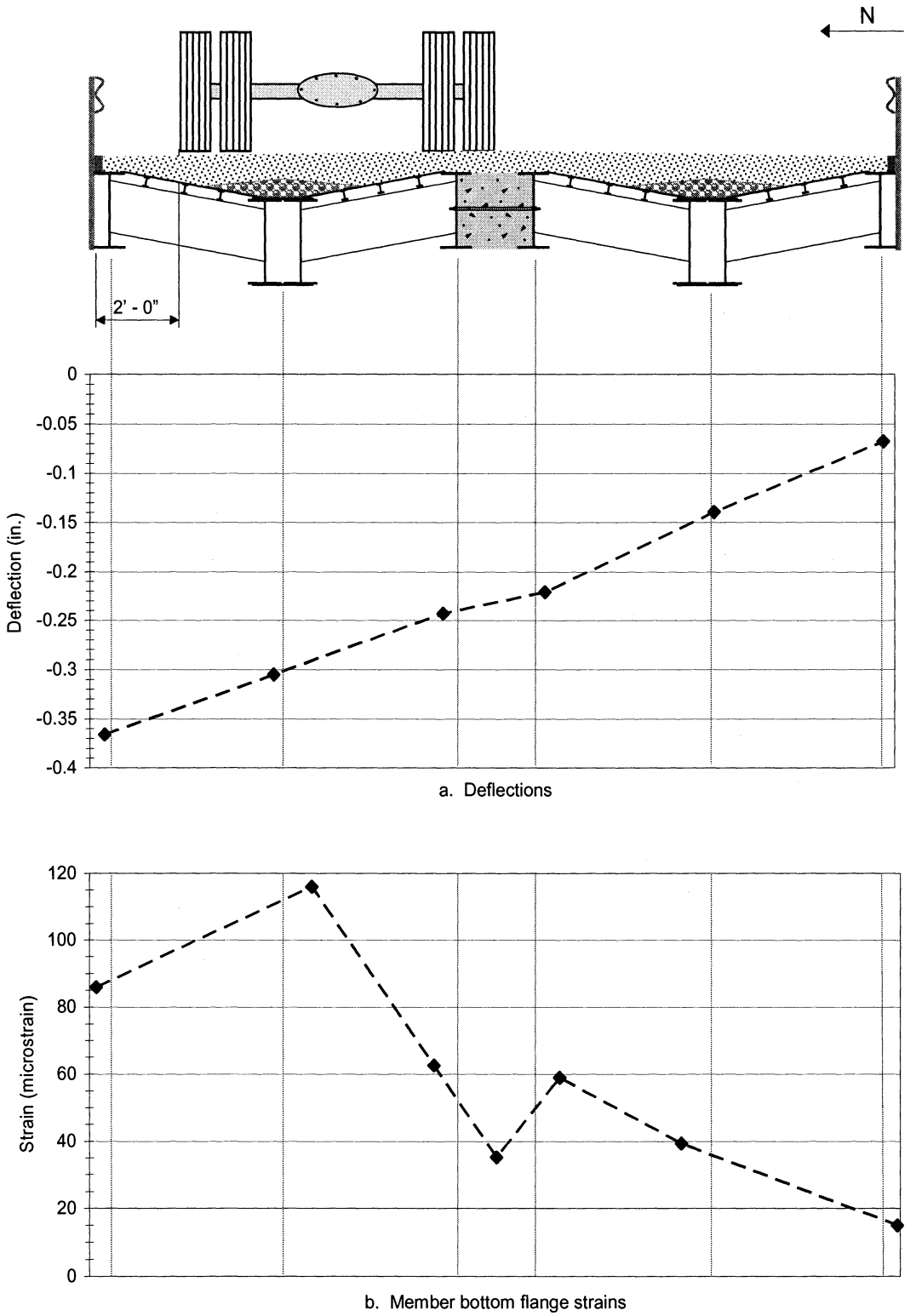

Figure 4.2. BCB2 Lane 1 midspan deflections and strains.

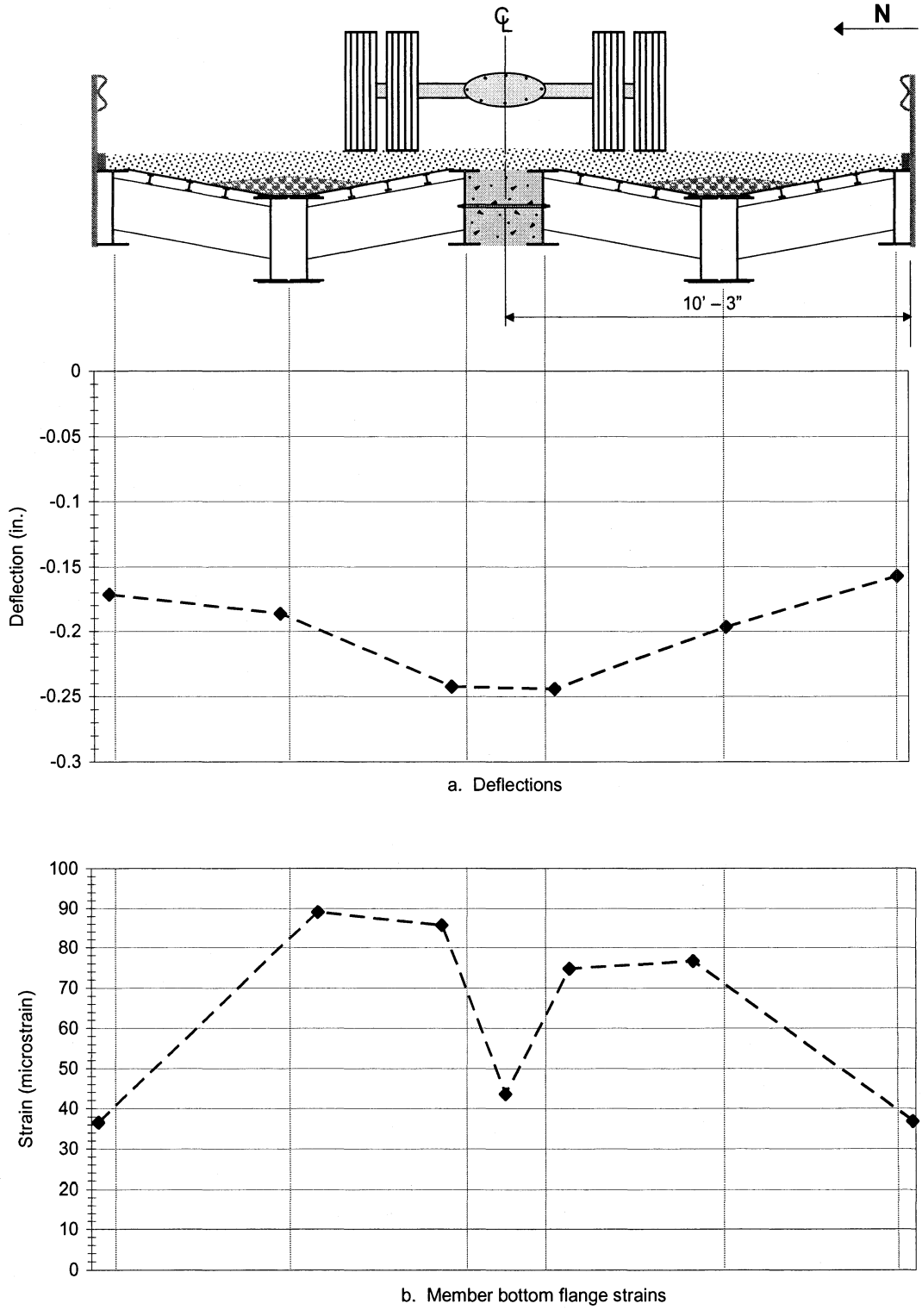

Figure 4.3. BCB2 Lane 2 midspan deflections and strains.

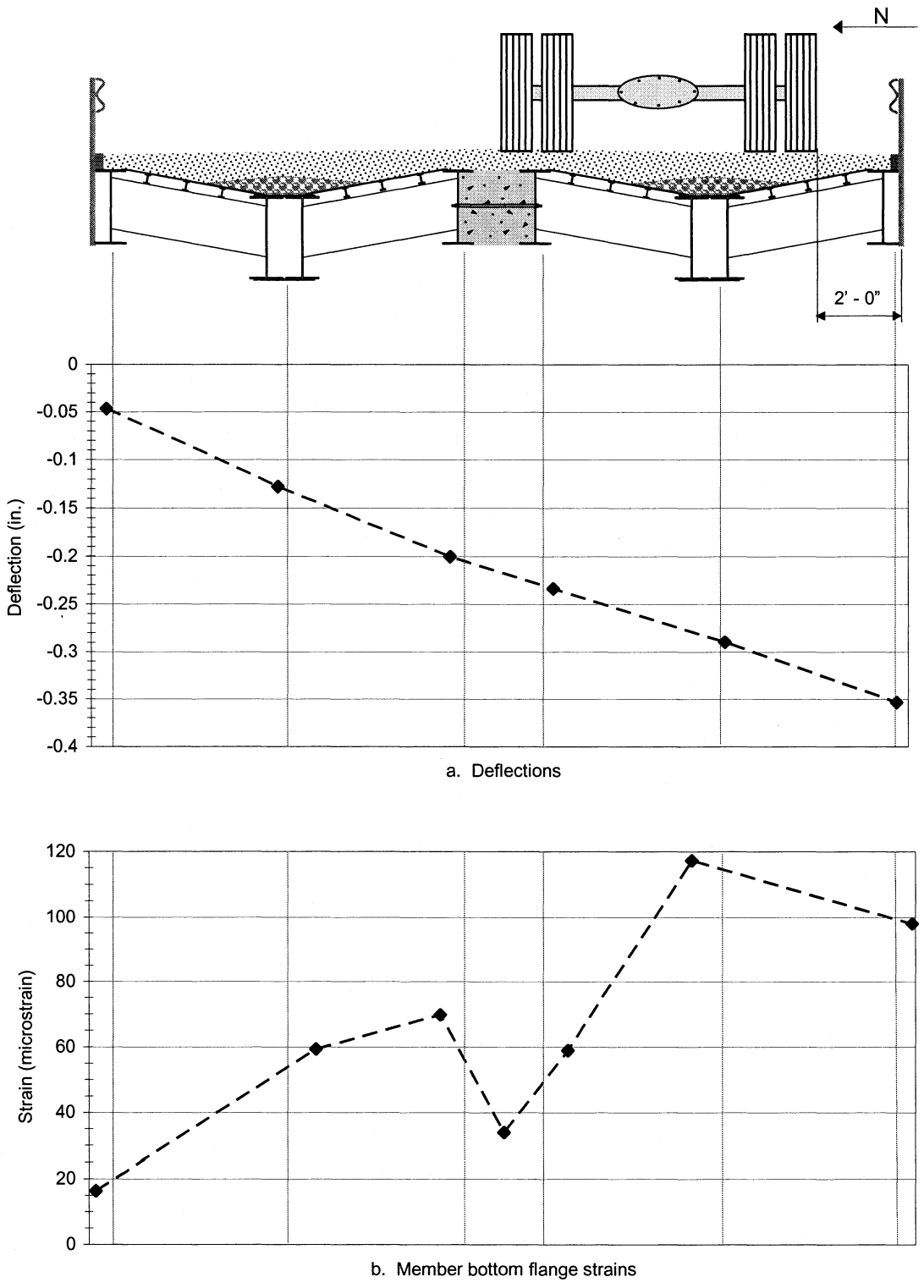

Figure 4.4. BCB2 Lane 3 midspan deflections and strains.

According to the 2003 AASHTO *Standard Specifications for Highway Bridges*, an optional limit for the deflection of a bridge is 1/800 of the span length [6]. This optional limit is not a strict requirement for legal bridges but rather a guideline. For a 54 ft – 0 in. span, the optional limit is 0.81 in. However, the load of the test truck was not the maximum load that may cross the BCB2 and cannot be compared to the deflection limit. The maximum load is most likely that of an AASHTO HS-20 truck. In order to determine the maximum deflection of the BCB2, the deflections recorded during the field tests were multiplied by a load adjustment factor. To determine the load adjustment factor for the BCB2, the maximum moments at the midspan of a simply-supported beam due to point loads representing the BCB2 test truck axle loads and due to point loads representing an HS-20 truck were calculated. The load adjustment factor was then determined using Equation 4.2.

$$\beta = \frac{M_{HS-20}}{M_{TT}} \tag{4.2}$$

where:

β = The load adjustment factor

M_{HS-20} = The maximum midspan moment of a simply-supported beam due to an HS-20 truck

M_{TT} = The maximum midspan moment of a simply-supported beam due to the test truck

Using Equation 4.2, the load adjustment factor for the BCB2 was determined to be 1.26. Therefore, the adjusted maximum deflection of the BCB2 was 0.46 in. which is below the optional AASHTO deflection limit of 0.81 in.

In each test, the maximum strain in the bridge occurred in the interior girder beneath the test truck. When the test truck was in Lane 1 or 3, the maximum exterior girder strain occurred in the exterior girder on the north or south edge of the bridge, as seen in Figures 4.2 and 4.4. With the truck positioned in Lane 2, the maximum exterior girder strain

Table 4.1. BCB2 midspan strains recorded during field load tests.

Girder	Position of Test Truck		
	Lane 1	Lane 2	Lane 3
Interior	115 MII (3.3 ksi)	89 MII (2.6 ksi)	116 MII (3.4 ksi)
Exterior at Bridge Edge	86 MII (2.5 ksi)	36 MII (1.0 ksi)	97 MII (2.8 ksi)
Exterior at LFC	62 MII (1.8 ksi)	86 MII (2.5 ksi)	70 MII (2.0 ksi)

occurred at the LFC. As presented in Figures 4.2 – 4.4 and summarized in Table 4.1, the maximum interior and exterior girder strains recorded during the field tests were 116 MII (3.4 ksi) in tension and 97 MII (2.8 ksi) in tension, respectively, and occurred in the north interior girder when the truck was in Lane 1. When the dead load stresses were combined with the live load stresses determined from the field test results, the maximum total stresses in the longitudinal interior and exterior girders were both tensile stresses, 9.3 ksi and 13.8 ksi, respectively.

As mentioned previously, the test truck was not an AASHTO HS-20 truck which is likely the maximum load that will cross the BCB2. Therefore, the maximum strains measured in the field tests were adjusted using the previously described adjustment factor of 1.26. The adjusted maximum strains in the interior and exterior girders were 146 MII (4.2 ksi) in tension and 122 MII (3.5 ksi) in tension, respectively. The adjusted maximum stresses were then added to the dead load stresses; the adjusted maximum total stresses in the interior and exterior girders were 10.1 ksi and 14.5 ksi, respectively, which are below 22 ksi, the allowable flexural stress.

As seen in Figures 4.2 – 4.4, the strain in the R/C beam LFC was less than the strains in the two adjacent RRFC girders. If the R/C beam was composite with the RRFC girders, the strain in the R/C beam would be about the same as the strain in the girders. Because the strains shown in Figures 4.2 – 4.4 could have been anomalies, the strain-time

histories of the three strain transducers at the LFC for each of the three lanes were plotted and are presented in Figure A.1 in Appendix A. The strain-time histories revealed that the strains shown in Figures 4.2 – 4.4 are not anomalies; the strain in the R/C beam was less than the strain in the two RRFC girders consistently throughout each test. Thus, the R/C beam is not behaving compositely with the RRFC girders since there is insufficient connection between the two materials.

As expected, the maximum deflections and strains for each test occurred in the girders directly below the axle loads of the test truck. One would expect an effective lateral load distribution to be demonstrated with linearly varying strain and deflection patterns across the cross-section of the bridge. This behavior is demonstrated in the girder deflections and strain patterns shown in Figures 4.2 – 4.4. Thus, the BCB2 effectively distributes load through the LFC. In Figure 4.3, the deflections and strain patterns reveal symmetrical bridge behavior, and in Figures 4.2 and 4.4, transverse symmetry is demonstrated by the mirrored deflection and strain patterns.

4.1.3 Comparison of BCB2 with BCB

As mentioned in Section 2.1.1, the BCB2 design was based on the BCB designed, constructed, and tested for the demonstration project, TR-444 [4]. Because the BCB is composed of three RRFCs, more tests were run, including tests with two trucks. However, load tests were run with one test truck traveling down the center of the bridge and 2 ft off either side of the bridge. These tests can be compared with the load tests on BCB2 with the truck positioned in Lanes 1 – 3 because the positions of the trucks and the loads carried by the trucks were approximately the same.

The final report for the demonstration project, TR-444, noted that the north edge of the BCB deflected upward when the test truck crossed the bridge 2 ft from the south edge of the bridge. Likewise, the south edge of the BCB deflected upward when the test truck

crossed the bridge 2 ft from the north edge of the bridge [4]. Although the same behavior does not occur in the BCB2, the deflection patterns of the two bridges are similar. For the comparison of the behavior of the two bridges, the north edge of the bridges were aligned as shown in Figures 4.5a and 4.5b. Because the BCB consists of three RRFCs while the BCB2 has two RRFCs and the width of the LFCs used in the two bridges is different, the south exterior girder of the BCB2 most closely corresponds to the south girder in the south LFC of the BCB. In both bridges, the maximum deflection occurred at the exterior girder at the north edge of the bridge on which the truck was positioned. As shown in Figure 4.5, the maximum deflection of the both the BCB and BCB2 was 0.37 in. Although the deflections of the BCB2 are not identical to the deflections of the BCB, the deflection patterns are both nearly linear. Thus, the BCB and BCB2 exhibit similar deflection behavior when the deflections (which are very small) in the third RRFC of the BCB are neglected; the third RRFC was the exterior RRFC on which the truck was not positioned.

Similar stress patterns should also be expected in the two bridges because in the BCB, the live load strain in the third RRFC was nearly zero. As seen in Figure 4.6c, the strain patterns of the BCB and BCB2 are similar, but they have two major differences. In the BCB, the maximum live load strain occurred in the exterior girder along the edge of the bridge beneath the test truck rather than in the interior girder beneath the test truck as the in BCB2. The difference in the location of the maximum strain is due to the position of the test truck along the edge of each bridge. As shown in Figures 4.6a and 4.6b, for the BCB field tests, the center of the tandem axle double tires was positioned 2 ft from the edge of the bridge, but in the BCB2 field tests, the edge of the tandem axle double tires was positioned 2 ft from the edge of the bridge. Thus, the center of the double tires at the tandem axle was positioned 3 ft from the edge of the bridge. By shifting the truck this 1 ft farther from the edge of the bridge, it was positioned partially on the LFC. Also, because in the BCB2 test,

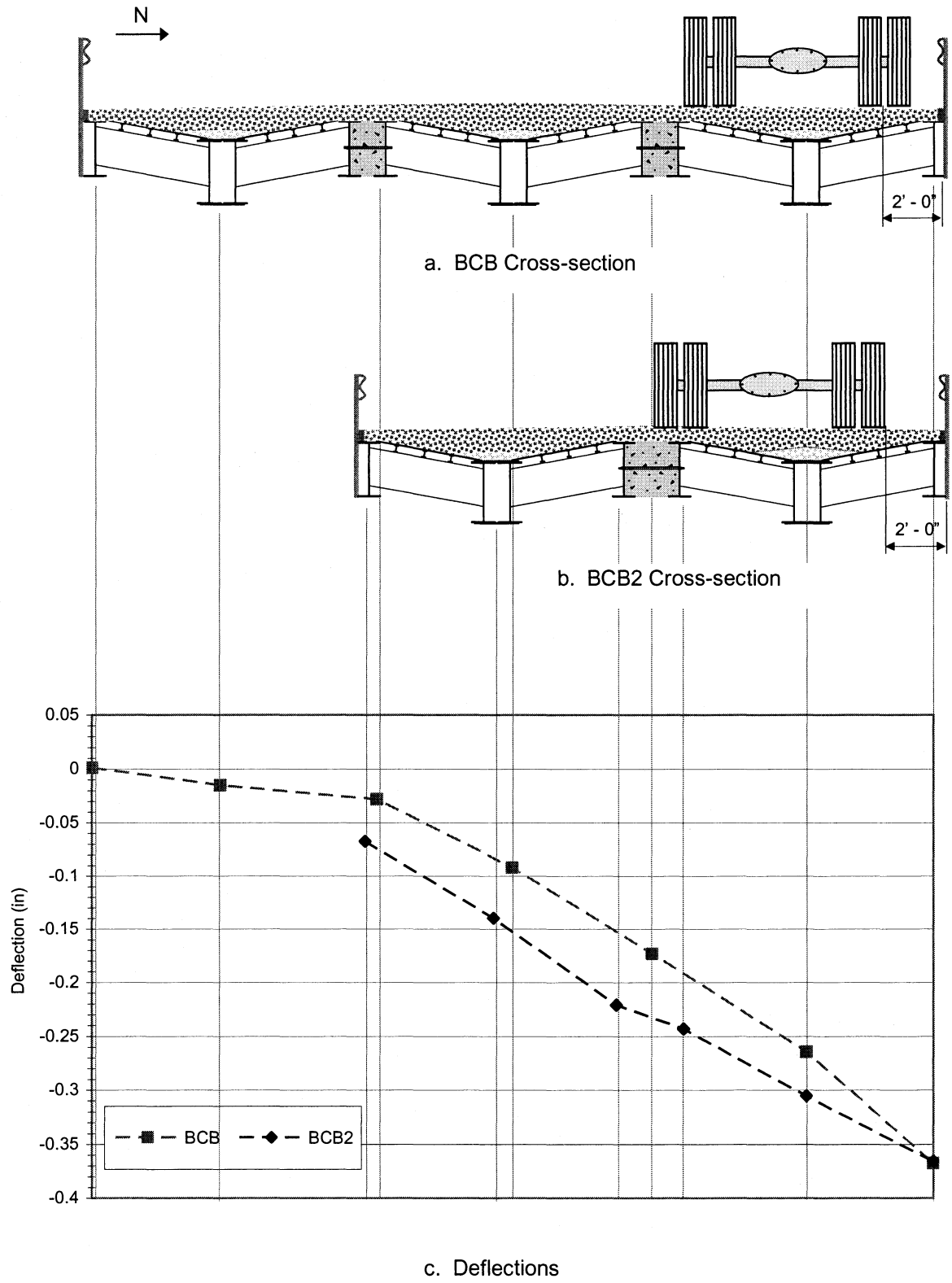

Figure 4.5. BCB and BCB2 deflection comparison.

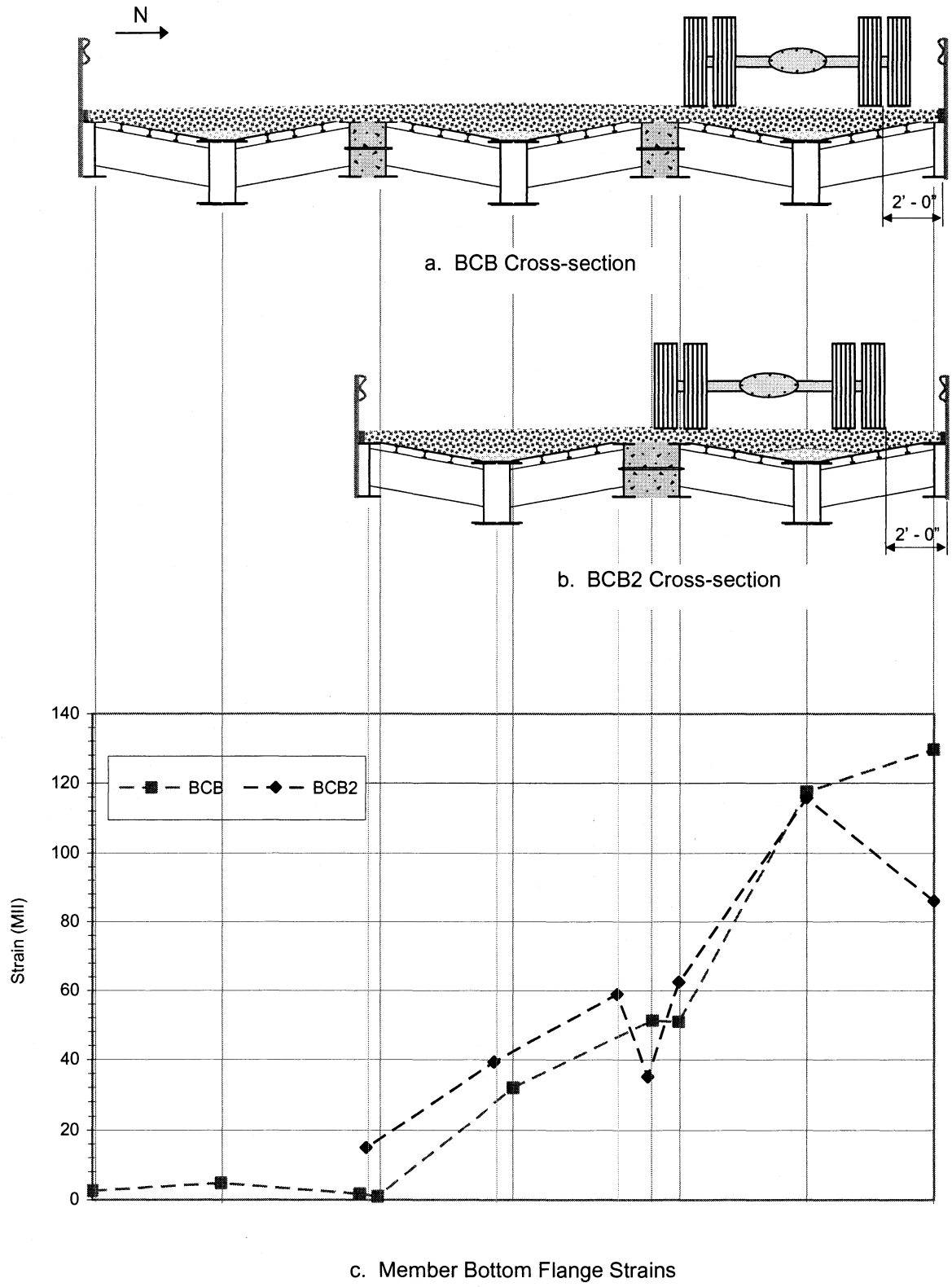

Figure 4.6. BCB and BCB2 strain comparison.

the truck was farther away from the edge, less strain occurred in the exterior girder at the edge of the bridge than in the interior girder. Although the location of the maximum live load strain was different in the BCB and BCB2, the maximum total stress in both bridges occurred in the exterior girder at the north edge of the bridge while the truck was positioned along that edge of the bridge. The maximum stresses due to the combined dead and live loads on the BCB and BCB2 were 12.7 ksi and 13.8 ksi, respectively. The difference in stresses is due to the difference in the amount of dead load on each bridge as well as the difference in truck position.

By reviewing the strains in the R/C beams in the two bridges in Figure 4.6c, one observers the better composite action in the BCB connection. The lack of composite action in the BCB2 connection has been previously noted.

The strain and deflection patterns from the tests with the truck positioned in the center of the bridge reveal symmetrical bridge behavior in both the BCB and BCB2. In tests with the truck positioned along the edge of the bridge (with the center of the tandem axle double tires positioned 2 ft from the edge of the bridge in the BCB and with the edge of the tandem axle double tires positioned 2 ft from the edge of the bridge in the BCB2), the strain and deflection patterns were mirrored. Thus, transverse symmetry is displayed in the behavior of both bridges. This similarity indicates that the wider R/C beam acting as the BCB2 LFC is as effective as the narrower R/C beam acting as the BCB LFC. The comparison of the BCB and BCB2 field test results reveals that the modifications in the BCB design did not significantly alter the structural strength or bridge behavior of the BCB2.

4.2 DCB Results and Analysis

4.2.1 Dead Load Analysis

The total stress in the DCB is the stress caused by the test truck in the field load test plus the stress due to the dead load on the bridge. To determine the total stresses in the

primary girders of the flatcar, a dead load analysis was performed. As with the BCB2 dead load analysis, several assumptions were made to simplify the analysis. Because the geometry of the 89-ft RRFCs is different from that of the 56-ft V-deck RRFCs, slightly different assumptions were made for the DCB dead load analysis. Due to the geometry, the exterior girders were assumed to be incapable of resisting the weight of the steel deck, secondary members, and transverse members and the driving surface. This assumption is based on the results of a grillage analysis in the demonstration project, TR-444, which determined that 99.9% of the bending moment was resisted by the interior girder [4]. Thus, for the dead load analysis of the DCB, the entire dead load was assumed to be resisted by the interior girders. As with the BCB2, the connected flatcars were assumed to form a rigid cross-section following conventional methods of bridge design. This allows any additional dead load to be considered uniform on the bridge. The driving surface of the DCB consists of a layer of 120-pcf gravel which is 10 in. deep at the centerline of the bridge and 7 in. at the edges of the bridge. Based on a weight of 42,000 lbs for one 89-ft RRFC [4], the DCB was assumed to weigh 944 lb/ft. Finally, the DCB was assumed to be simply supported.

In order to determine the dead load stresses present in the interior girder of one RRFC, half of the dead load on the DCB was applied as a distributed load to a simply-supported model of the girder. The moment at the midspan of the girder was then calculated. With the midspan moment and the section modulus of the interior girder, the dead load stress in the interior girder at midspan was calculated using Equation 4.1, as in the BCB2 analysis. Using this procedure, the maximum dead load stress in the bottom flange of the interior girders at the midspan was determined to be 16.1 ksi in tension.

4.2.2 Static Field Load Test Results

Besides instrumenting the primary girders at midspan, the DCB instrumentation plan described in Section 3.2.1 included measuring the strain in two secondary members, one

transverse member, and one interior girder at both abutments (12 in. from the face of the abutments). The maximum strains at the abutments occurred in the bottom flanges of the interior girders. The maximum strain at the east abutment was 43 MII (1.2 ksi), and at the west abutment, the maximum strain was 55 MII (1.6 ksi). The presence of strain in the girders close to the abutments indicates that end restraint is present in the DCB, even though the bridge was designed to be simply-supported. However, the maximum strains in the interior girder at the abutments were considerably less than the maximum strains experienced in the interior and exterior primary girders at the midspan of the bridge. Also, the maximum stresses in the interior girder at the abutments were well below the allowable stress limit. Although end restraint reduces the midspan strains, the effect is minimal because the maximum strain at the abutments was significantly less than the maximum strain at midspan. Thus, the strains in the girders close to the abutments will not be discussed further.

As shown previously in Figure 3.7, the secondary members that were instrumented with Strain Transducers 12 and 13 were both located on the north RRFC, as was the S-shaped transverse member that was instrumented with Strain Transducer 11. The maximum strains that occurred in the two instrumented secondary members were 77 MII (2.2 ksi) and 34 MII (1.0 ksi) and occurred when the truck was positioned in Lane 3 on the north RRFC. The maximum strain that occurred in the transverse member was 47 MII (1.4 ksi) and occurred when the truck was positioned in Lane 2, with the truck tires directly above the transducer. The maximum strains in the secondary and S-shaped transverse member were significantly less than the maximum strains experienced in the interior primary girders, and the maximum stresses were well below the allowable stress limit. Thus, the secondary and S-shaped transverse members were determined to not be critical members and will be excluded from further discussion.

The maximum midspan deflections and strains in the primary girders that were measured when the truck was in Lanes 1 – 3 on the DCB are presented in Figures 4.7 – 4.9, respectively. As described in Section 3.2.1, the midspan of DCB was instrumented with six deflection transducers and six strain transducers. The deflections and strains measured with these transducers are represented in Figures 4.7 – 4.9 by small diamonds. The dashed lines represent a trend that may occur between the measured deflections and strains and thus, do not represent actual measured deflections or strains. The deflections and strains shown in Figures 4.7 – 4.9 occurred when the center of the tandem axle of the truck was at the midspan of the bridge. As can be seen in Figures 4.7 and 4.9, the maximum deflection of the DCB was 0.69 in. and 0.84 in. when the truck was in Lane 1 or 3, respectively, and occurred at the exterior girder on the south or north edge of the bridge, respectively. When the truck was positioned in Lane 2, the maximum deflection as seen in Figure 4.8 was 0.6 in. and occurred at the LFC.

As previously noted, the 2003 AASHTO *Standard Specifications for Highway Bridges* states that an optional limit for the deflection of a bridge is 1/800 of the span length [9]. For a 66 ft – 4 in. span, this optional limit is 1.0 in. As with the BCB2 field tests, the test truck used in the DCB field tests was not an AASHTO HS-20 truck, which is one of the design loads used in bridge design. Using Equation 4.2, the load adjustment factor for the DCB was determined to be 1.37. By multiplying the measured deflections by the load adjustment factor, the adjusted maximum deflection of the DCB was determined to be 1.15 in., which is 15 percent over than the optional AASHTO deflection limit of 1.0 in. However, as stated in Section 4.1.2, the optional AASHTO deflection limit is a guideline, not a strict requirement for legal bridges. Because the DCB is a rural bridge on a low-volume road, exceeding the optional deflection limit was decided to be acceptable. If the deflections of the DCB were

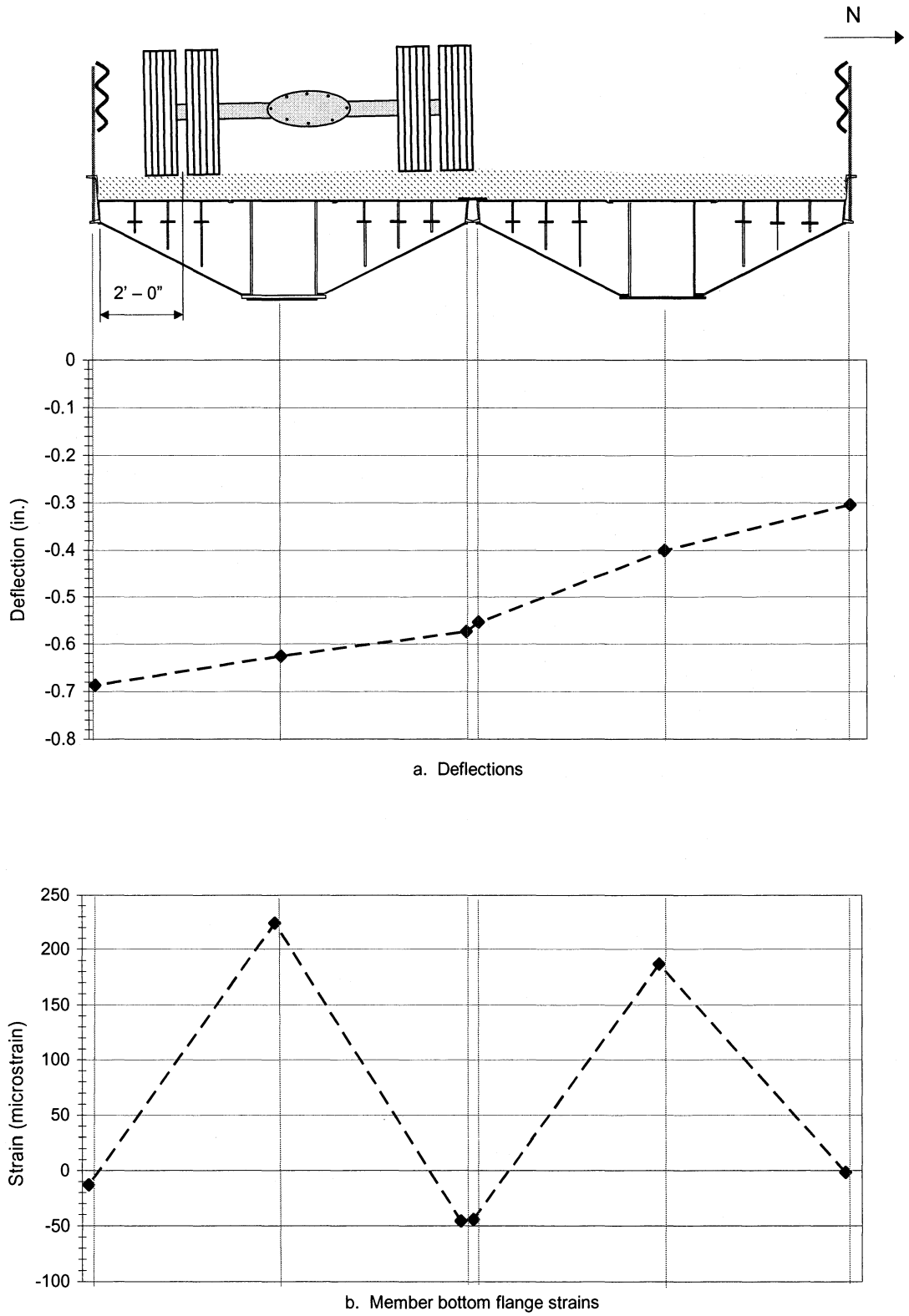

Figure 4.7. DCB Lane 1 midspan deflections and strains.

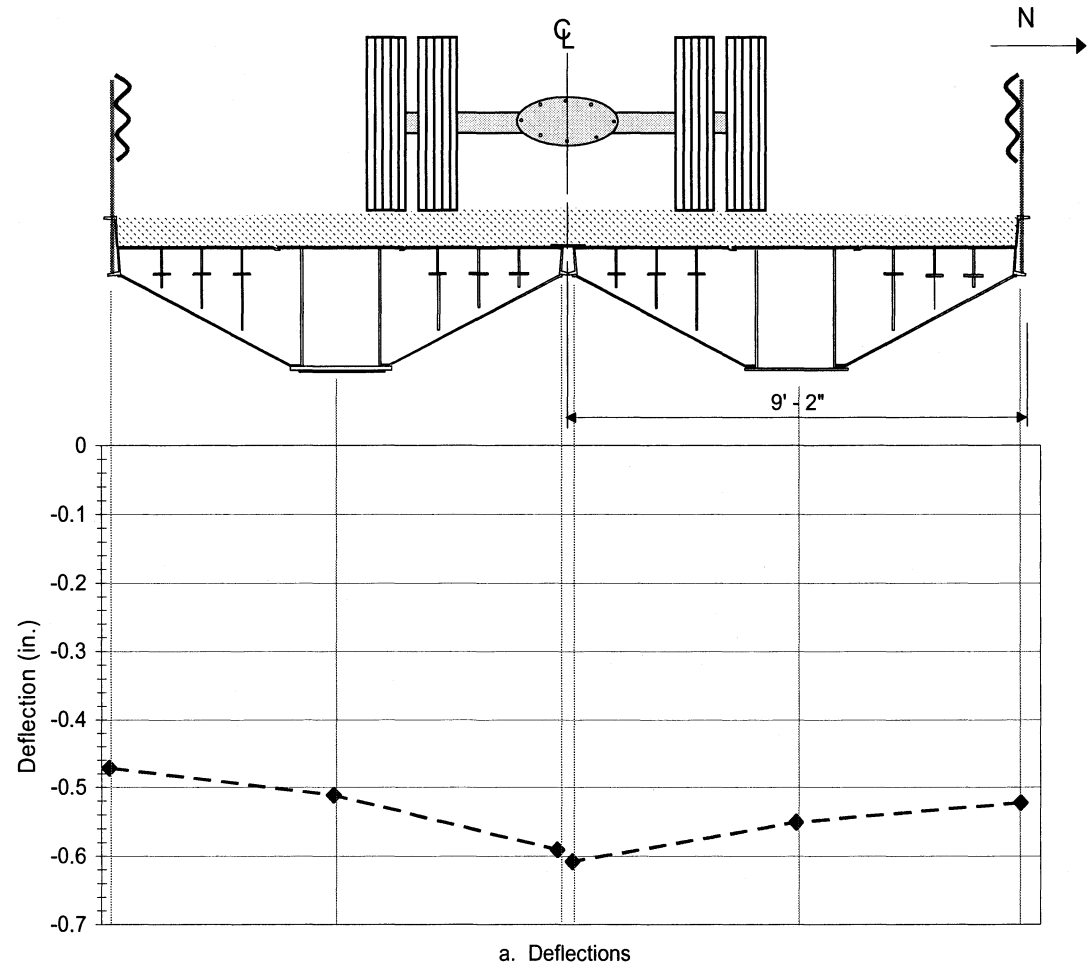

a. Deflections

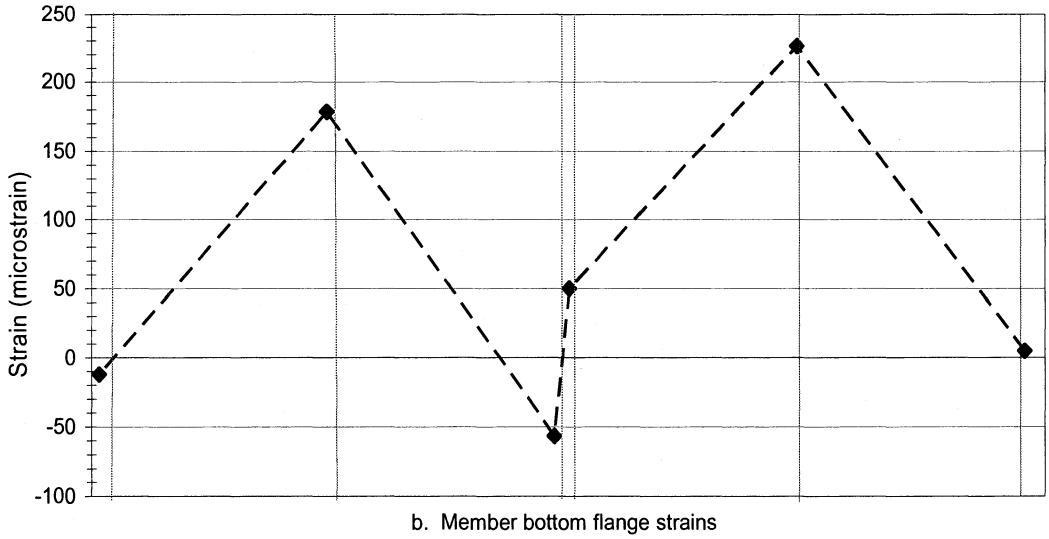

b. Member bottom flange strains

Figure 4.8. DCB Lane 2 midspan deflections and strains.

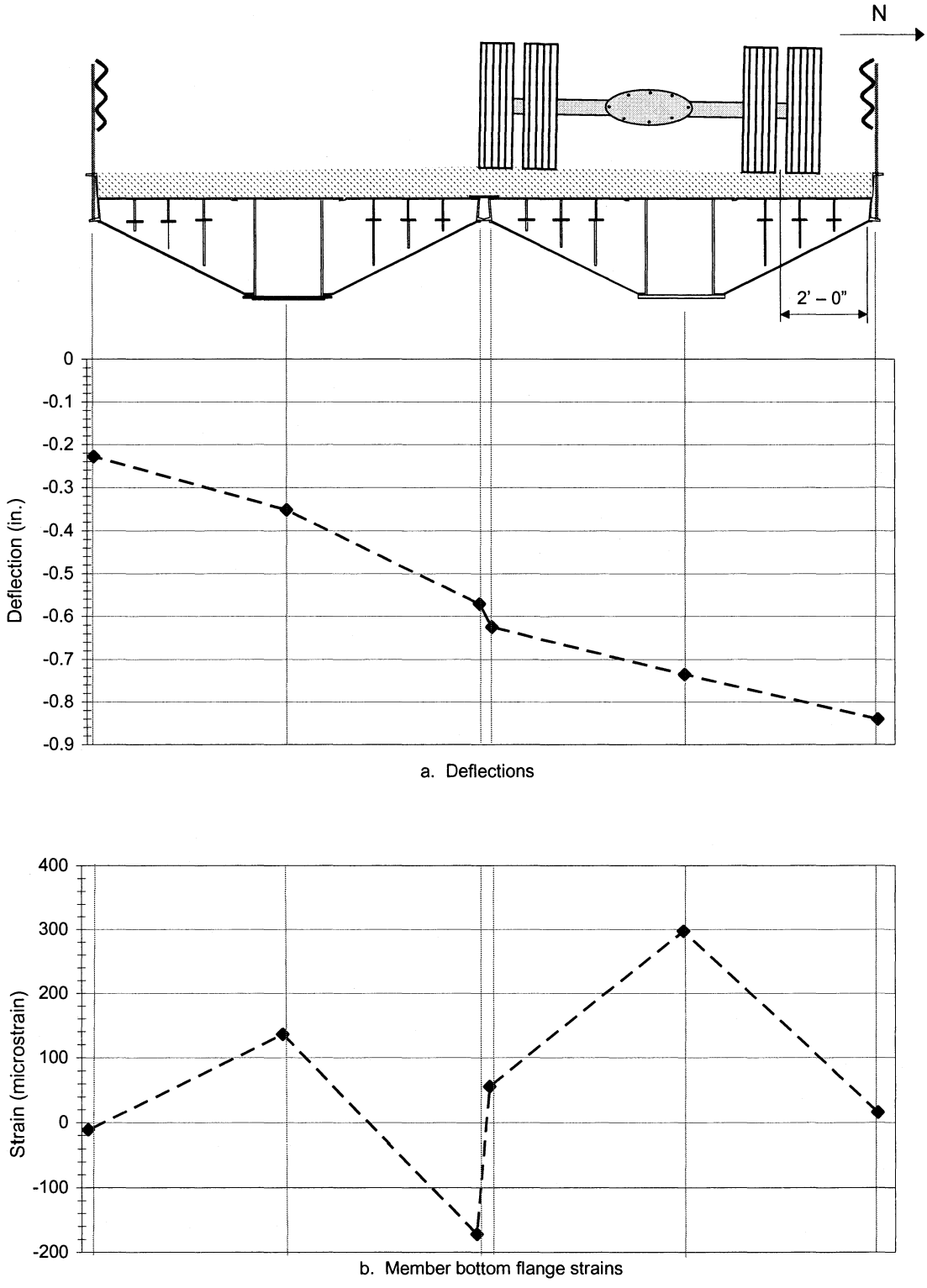

Figure 4.9. DCB Lane 3 midspan deflections and strains.

to be required to meet the AASHTO limit, the load of a truck with HS-20 axle spacings would have to be reduced to 30 tons.

In each test, the maximum strain in the DCB occurred in the interior girder beneath the test truck. Maximum strains occurred in the exterior girders at the LFC. As seen in Figure 4.9, the maximum strains measured in the interior and exterior girders due to the live loads were 297 MII (8.6 ksi) in tension and 172 MII (5.0 ksi) in compression, respectively. When the dead load stresses were combined with the live load stresses determined from the field test results, the maximum total stresses in the longitudinal interior and exterior girders were 24.7 ksi in tension and 5.0 ksi in compression, respectively. Thus, the maximum total stress in the DCB exceeds the allowable stress of 22 ksi by 12 percent.

As mentioned previously, the test truck was not an AASHTO HS-20 truck which is likely the maximum load that will cross the DCB. Therefore, the maximum strains measured in the field tests were adjusted using the load adjustment factor of 1.37 previously mentioned for the adjustment of the maximum deflections. The adjusted maximum strain in the interior girders was 408 MII (11.8 ksi) in tension. The adjusted maximum total stress in the interior girders was 27.9 ksi (27 percent greater than the allowable stress for flexure). In order to keep the maximum total stress below the allowable stress limit, the thickness of the gravel driving surface should be limited to 3 in. Decreasing the thickness of the gravel layer will reduce the dead load stress in the interior girder to 9.9 ksi which in turn will reduce the total stress in the interior girder to 21.7 ksi, which is less than the allowable flexural stress.

As expected, the midspan maximum strains and deflections for each test occurred in the girders directly below the test truck axle loads. As seen in Figures 4.7 and 4.9, the north edge of the bridge deflected downward when the truck was positioned in Lane 1, and the south edge of the bridge deflected downward when the truck was positioned in Lane 3. This

behavior demonstrates effective lateral load distribution through the longitudinal flatcar connection.

Symmetrical bridge behavior is shown in the deflection patterns in Figure 4.8 and the mirrored deflection and strain patterns in Figures 4.7 and 4.9. Although the strain patterns in these figures are mostly symmetric, the strains in the exterior girders at the LFC are not symmetric. In Figures 4.8 and 4.9, the strain in the bottom flange of the south girder is compressive while the strain in the bottom flange of the north girder is tensile. As can be seen in Figures 4.8 and 4.9, the deflections of the two girders at the LFC are not equal; thus, the two RRFCs do not act as a rigid structure. The strain difference is likely due to the relationship of the bottom flange of the girder with the different neutral axes for the two RRFCs. The neutral axes of the two RRFCs are not equal because, as noted in Section 2.2.1, the south RRFC has an additional 1-in. plate welded to the bottom flange of the interior girder. On the north RRFC, the bottom flange of the LFC girder is below the neutral axis so the flange is in tension. However, on the south RRFC, the bottom flange of the LFC girder is above the neutral axis so the flange is in compression.

Another asymmetrical aspect of the DCB behavior is that the magnitudes of the strains and deflections in the girders of the south RRFC are less than the corresponding strains and deflections in the girders of the north RRFC. This difference is due to the additional 1-in. plate welded to the bottom flange of the interior girder of the south RRFC. The plate increases the stiffness of the interior girder, and thus, the south RRFC will experience smaller strains and deflections than the north RRFC.

4.2.3 Dynamic Load Test Results

As described in Sections 3.2.3 and 3.2.4, dynamic load tests were run on the DCB with the test truck traveling across the bridge in Lane 2 at 10 mph and 15 mph. The maximum strain measured in the primary girders due to the test truck traveling at 10 mph

was 235 MII (6.8 ksi) in an interior girder. When the test truck was driven at 15 mph across the bridge, the maximum interior girder strain in the DCB increased to 240 MII (7.0 ksi). As with the static load tests, the stresses measured during the dynamic load tests must be adjusted to represent the stresses due to an HS-20 truck using the 1.37 load adjustment factor from Section 4.2.2; the maximum adjusted strain during the dynamic tests was 329 MII (9.5 ksi) for the test with the truck traveling at 15 mph. When combined with the stresses due to the dead load of the bridge to accurately determine the total stresses in the DCB due to the dynamic load tests, the maximum adjusted total stress was 25.6 ksi (16 percent greater than the allowable stress for flexure), which is less than the maximum adjusted total stress determined in the static load tests. By decreasing the amount of gravel on the DCB as suggested in Section 4.2.2, the maximum adjusted total stress for the dynamic load test decreases to 19.9 ksi, which is less than the allowable stress limit.

The maximum deflections measured in the DCB when the test truck was driven across the bridge at 10 mph and 15 mph were 0.61 in. and 0.63 in., respectively. Again, these deflections were adjusted to represent the maximum deflection due to an HS-20 truck. The adjusted maximum deflections of the DCB during the dynamic load tests were 0.84 in. and 0.86 in. when the truck was traveling at 10 mph and 15 mph, respectively. These deflections are below the optional AASHTO limit of 1.0 in.

With the results from the both the static and dynamic load tests, the girder strains and deflections were compared to determine the dynamic amplification factors due to the faster speed of the test truck. In order to accurately determine the dynamic amplification factors, the deflections and strains of the dynamic load tests were compared with the maximum strain and deflection from Figure 4.6, the static load test with the truck positioned in Lane 2. Thus, for the purpose of determining the dynamic amplification factors for the

girder strains and deflections, the maximum strain in the DCB was 226 MII (6.6 ksi) in an interior girder and the maximum deflection was 0.60 in.

The dynamic amplification factors, DAF, were determined as shown with Equation 4.3 by calculating the percent difference between the static and dynamic load test results.

$$DAF = \frac{\text{Dynamic Result - Static Result}}{\text{Static Result}} * 100\% \qquad (4.3)$$

Because the strains and deflections were larger in the load test with the truck traveling across the bridge at 15 mph, this load test was used to determine the dynamic amplification factors. The dynamic amplification factors for the girder strains and deflections were 6.2 percent and 5.0 percent, respectively.

In addition to the dynamic amplification factors for the DCB, the results from the dynamic load tests were used to analyze the dynamic deflection behavior of the DCB. For both dynamic load tests, the maximum deflections due to the test truck were located at midspan of the north girder in the LFC. Since the load test with the truck traveling at 15 mph resulted in larger deflections, the deflection behavior from this load test was used in the analysis. In Figure 4.10, the deflection behavior of the DCB is presented. The deflection of the exterior girder of the north RRFC at the LFC during the load test is shown in Figure 4.10a. The large spike in Figure 4.10a represents the deflection of the DCB as the test truck crosses the bridge. As expected, the maximum deflection of the bridge occurs when the truck is approximately at midspan, shown graphically in Figure 4.10a as the spike occurs halfway through the test. The free vibration of the DCB measured at the midspan of the bridge in the north RRFC in the exterior girder at the LFC, shown in Figure 4.10b, was recorded for approximately 11 seconds after the test truck crossed the bridge. As seen in Figure 4.10b, the DCB completed 11 cycles of vibration during the first 4 seconds of free

vibration. Finally, using Equations 4.4 and 4.5, the period, T_D, and the damped frequency, f_D, of the DCB were determined to be 0.36 seconds and 2.75 Hz, respectively.

$$T_D = \frac{t}{n} \tag{4.4}$$

where:

t = time required to complete n cycles of free vibration

n = number of cycles of free vibration

$$f_D = \frac{1}{T_D} \tag{4.5}$$

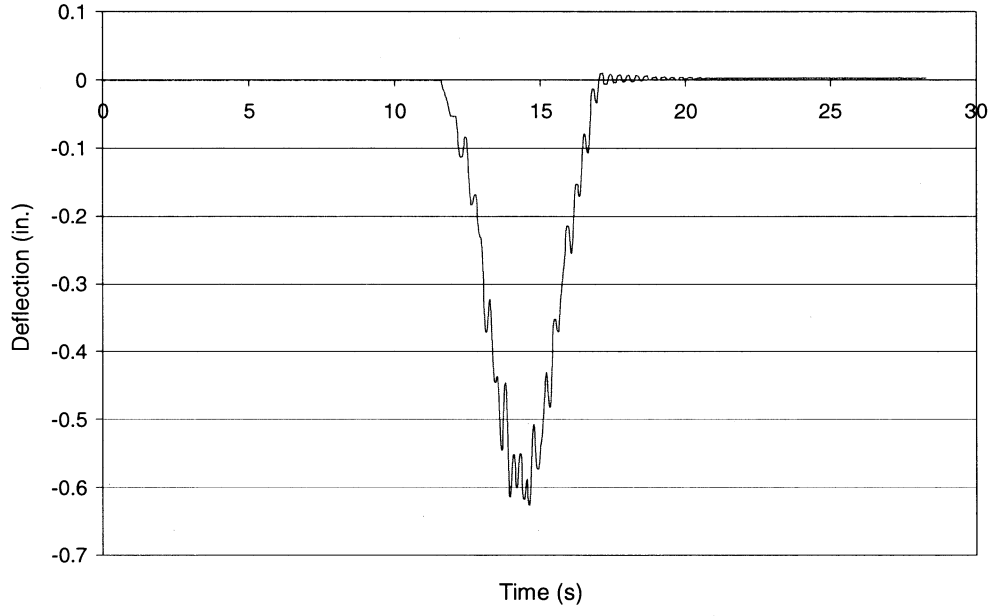

a. Deflection response during dynamic load test

Figure 4.10. Deflection results of DCB 15 mph dynamic load test.

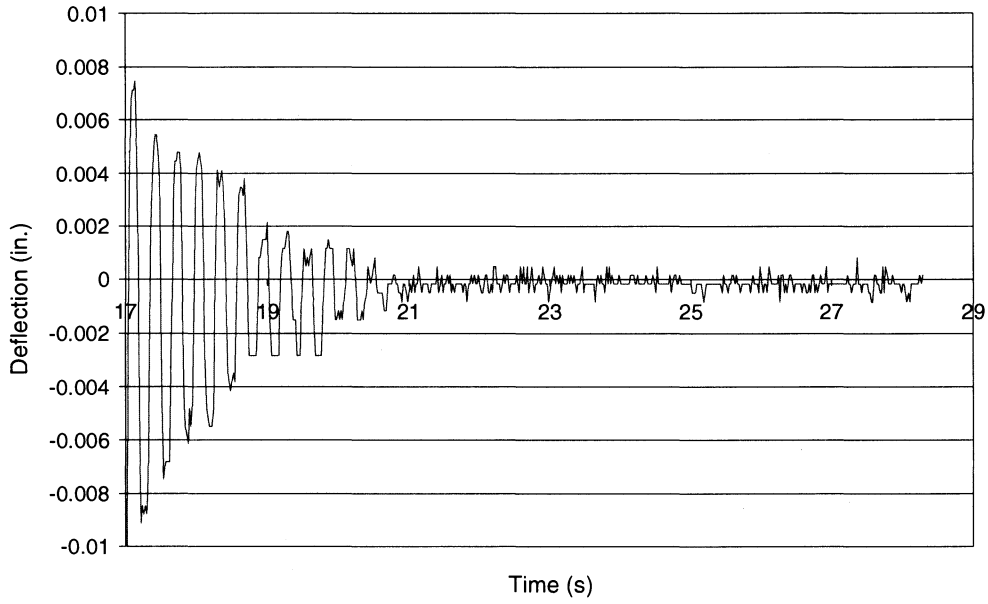

b. Free vibration of DCB after dynamic load test (50 samples per second)

Figure 4.10. Continued.

5. DESIGN AND ANALYSIS OF THE RRFC BRIDGES

5.1 Recommendations for Live Load Distribution

In the demonstration project, equations for the live load moments were presented; these equations were developed for the bridges and LFCs described in the report [4]. The BCB is a single-span simply-supported bridge composed of three 56-ft V-deck RRFCs, and the WCB is a three-span bridge composed of 89-ft RRFCs. Since the BCB2 and DCB are both single-span bridges composed of two RRFCs, the live load moment equations were modified to more accurately determine the live load moments in the interior and exterior girders in such bridges.

As determined in the results in Sections 4.1 and 4.2, the maximum stresses were recorded in the three primary girders of the RRFC. The live load moments in each girder can be determined with the following equation:

$$M_{LL} = \frac{2}{3} \psi \, \omega \, M_{SD} \tag{5.1}$$

where:

M_{LL} = The actual, maximum midspan live load moment in the girder being investigated

M_{SD} = The maximum, midspan live load moment in the statically determinate RRFC bridge based on the live load

$$\omega = \text{Inertia ratio} = \frac{I_D}{\Sigma I_{RRFC}} \tag{5.2}$$

I_D = Strong-axis moment of inertia for the girder being investigated

ΣI_{RRFC} = Sum of the girders' strong-axis moments of inertia in one RRFC
$= (2)(I_{EXT})+I_{INT}$ (5.3)

I_{EXT} = Strong-axis moment of inertia for the exterior girder

I_{INT} = Strong-axis moment of inertia for the interior girder

ψ = Adjustment factor to correct for the simplified analysis [4]

For interior girders in RRFC bridges like the BCB2,

$\psi = 0.8$

For exterior girders in RRFC bridges like the BCB2,

$\psi = 0.75$

For interior girders without extra plates in RRFC bridges like the DCB,

$\psi = 0.9$

For exterior girders in RRFC bridges like the DCB,

$\psi = 0.4$

The preceding adjustment factors were determined as described in Appendix B so that the maximum live load moment at midspan calculated with Equation 5.1 would adequately approximate the actual live load moment measured during the field load test. Grillage models of the BCB and WCB were created for the demonstration project, so a variety of inertia ratios were examined for the two different LFCs used in the two bridges [4]. Thus, the adjustment factors that were provided for the BCB and WCB are equations based on the inertia ratio of the girder being investigated.

Summarized in Table 5.1 are the adjustment factors for the BCB and WCB interior and exterior girders determined using the equations in the demonstration project and the adjustment factors for the BCB2 and DCB interior and exterior girders determined as described in Appendix B. The adjustment factors for the interior girders of the BCB (ψ = 0.809) and BCB2 (ψ = 0.8) are nearly identical, as are the adjustment factors for the interior girders of the WCB (ψ = 0.871) and DCB (ψ = 0.9). However, the adjustment factors for the exterior girders of the BCB (ψ = 1.107) and BCB2 (ψ = 0.75) are significantly different, as are the adjustment factors for the exterior girders of the WCB (ψ = 0.855) and DCB (ψ = 0.4). These comparisons indicate, as one would expect, that the LFC has significantly

Table 5.1. Summary of the live load distribution adjustment factors (ψ).

Bridge Design	Adjustment Factor (ψ)	
	Interior Girder	Exterior Girder
BCB	0.809	1.107
BCB2	0.8	0.75
WCB	0.871	0.855
DCB	0.9	0.4

more influence on the exterior girder adjustment factors than it does on the interior girder adjustment factors .

The moment fraction equal to 2/3 in Equation 5.1 represents the fraction of the total area under the deflection curve for one railroad car when the truck is positioned on that car. This value was first determined in the demonstration project for bridges with three RRFCs, though the actual fraction was 0.69 for the BCB and 0.62 for the WCB [7]. The same method described in Appendix D of the *Demonstration Project Using Railroad Flatcars for Low-Volume Road Bridges* [7] was used to determine the moment fraction for the bridges with two RRFCs. For the BCB2, the fraction was 0.65 while for the DCB, the fraction was 0.66. Appendix C of this thesis presents the calculations used to determine these moment fractions. The similar fractions developed for the three-RRFC bridges in the demonstration project and for the two-RRFC bridges investigated in this thesis are due to the minimal load carried by the exterior RRFC when the truck is positioned over the other exterior RRFC in a three-RRFC bridge, (i.e. the BCB and WCB) [7]. Since the BCB2 and DCB moment fractions are also approximately 2/3, the moment fraction in the live load distribution factor was determined to be 2/3 for bridges with two RRFCs as or three RRFCs. Because of this, Equation 5.1 (with the appropriate values of ψ an ω included) is valid for bridges composed of two or three RRFCs.

5.2 Rating Procedure for RRFC Bridges

The rating procedure for RRFC bridges follows the allowable stress method for rating bridges. Following the allowable stress method for rating bridges in the AASHTO *Manual for Condition Evaluation of Bridges* (Rating Manual) [8], the equation used to determine the rating of each member in a typical highway bridge is as follows:

$$RF = \frac{C - A_1 D}{A_2 L (1+I)} \tag{5.4}$$

where:

RF = The rating factor for the live-load carrying capacity

C = The allowable stress capacity of the member

D = The dead load effect on the member

L = The live load effect on the member

I = The impact factor to be used with the live load effect = 0.33

A_1 = Factor for dead loads = 1.0 for the allowable stress method

A_2 = Factor for live load = 1.0 for the allowable stress method.

The allowable stress capacity of the member, C, is determined using the properties in tables provided in the Rating Manual; for bridge materials or construction that is unknown, the engineer should determine the allowable stresses based on field investigations and/or material testing [8]. The dead load effect on the member, D, is calculated using standard bridge analysis methods and is based on the existing conditions of the bridge. Appendices are provided in the Rating Manual for determining the live load effect on girders and stringers in typical highway bridges. However, RRFC bridges are not composed of uniform girders at equal spacing like standard slab on girder bridges; thus, a different method must be used to determine the live load effect. For RRFC bridges, the effect of the live load on a member, L, should be determined by multiplying the maximum live load moment by a

distribution factor. The distribution factor to be used is the fraction of the live load transferred to the member. The distribution factors for the RRFCs used in the bridges tested for this thesis were presented in Section 5.1 as part of Equation 5.1 and now explicitly as Equation 5.5.

$$DF = \frac{2}{3} \psi \omega \tag{5.5}$$

The variables in Equation 5.5 are the same as in Equation 5.1.

The majority of the RRFCs have three primary girders and several secondary and transverse members. As assumed in Sections 4.1 and 4.3, primary girders carry nearly all the load on the bridge. Because of this, the primary girders are assumed to carry the entire load of the bridge for the distribution of the live load. Thus, no distribution factors are presented for the secondary members, and only the primary girders are given a numerical rating. On a bridge composed of 89-ft RRFCs, the transverse members may be part of the critical load path of the bridge; however, more data must be collected and analyzed to accurately include the transverse members in the numerical load rating. For all RRFC bridges, all members of the bridge, including the secondary members and the transverse members, should be visually inspected for damage as described in the Rating Manual [8].

To determine the rating of each bridge member, the Rating Factor, RF, from Equation 5.4 should be multiplied by the weight of the truck used in determining the live load effect, L. This will result in the bridge member rating in tons, and the actual bridge rating will be controlled by the bridge member with the lowest rating [8]. An example RRFC bridge rating is provided as Appendix D.

6. SUMMARY AND CONCLUSIONS

6.1 Summary

In this investigation, the behavior of RRFC bridges composed of two flatcars was examined. The first objective was to obtain more data on the behavior of RRFC bridges. This objective was accomplished through the field testing of two RRFC bridges located in Buchanan and Delaware Counties in Iowa. The data collected during the field load tests on the BCB2 and DCB were also used to refine the design methodology and to develop a rating procedure for RRFC bridges, the second and third project objectives.

The BCB2 is composed of two 56-ft V-deck RRFCs sitting on concrete abutments and a LFC between the RRFCs consisting of a 30.5-in. R/C beam and transverse threaded rods. The BCB2 has a width of 20 ft – 7 in. and spans 54 ft -0 in. The design of the BCB2 was based on the BCB, which was designed and constructed as part of the demonstration project, TR-444 [4]. The DCB is composed of two 89-ft RRFCs; however, 10 ft – 9 in. were removed from each end of the RRFCs so that a symmetric 67 ft – 6 in. portion of the RRFC remained. The DCB has a width of 18 ft – 4 in. and spans 66 ft – 4 in. The LFC for the DCB consists of a 14-in. by 1/2-in. plate welded over the trimmed exterior girders of the adjacent RRFCs along the entire length of the connection.

In order to determine the structural strength and behavior of the two bridges, strain transducers and deflection transducers were mounted on the primary girders at the midspan, the 1/4 span, and the 3/4 span. The interior girder of one RRFC in each bridge was also instrumented with strain transducers near the abutment to determine the presence of end restraint at the abutments. In addition to the primary girders, secondary members in both bridges and a transverse member in the DCB were instrumented with strain transducers to determine the strains in those members. Strain transducers were also mounted on the R/C beam in the BCB2. During the field load tests on both bridges, strains

and deflections were continuously measured by the transducers and recorded with a data acquisition system. With the data acquisition system, it was possible to specially mark the data as desired during the tests. The specially marked data were then used as reference points in the analysis of the results. For the static load tests, the strain data were specially marked as the tandem axle of the test truck crossed the centerline of the west abutment, the 1/4 span, the midspan, the 3/4 span, and the centerline of the east abutment.

In the static load tests, both the BCB2 and DCB were divided into three lanes in which the test truck would be positioned. When in Lane 1 or 3 on the BCB2, the edge of the double tires at the rear axle of the test truck was positioned 2 ft from the edge of the bridge. When in Lane 1 or 3 on the DCB, the center of the double tires at the rear axle of the truck was positioned 2 ft from the edge of the bridge. On both bridges, the truck was centered on the bridge when in Lane 2. In the dynamic load tests of the DCB, the test truck was driven across the bridge in Lane 2 at 10 mph and at 15 mph to produce a dynamic amplification in the girder strains and deflections. Because the DCB is only 18 ft – 4 in. wide and on a low-volume road, the majority of the daily traffic crossing the bridge will be centered on the bridge. Thus, the truck was only positioned in Lane 2 for the dynamic load tests.

In the demonstration project, tensile tests on coupons from a 56-ft V-deck RRFC and an 89-ft RRFC determined that the modulus of elasticity and yield strength of the steel used in both RRFCs was 29,000 ksi and 40 ksi, respectively [4]. This information was required so that the stresses in the girders from the strains recorded during the field tests could be calculated and then compared to the allowable stress of the steel used in the RRFCs. Following the 2003 AASHTO *Standard Specifications for Highway Bridges* as a guideline, the allowable stress of the steel used in the BCB2 and DCB was determined to be 22 ksi, 55 percent of the yield strength [6]. The *Standard Specifications for Highway Bridges* was also used as a guideline for determining the optional deflection limit, 1/800 of the bridge span [6].

In order to determine the total stresses that occurred in the BCB2 and DCB during the field load tests, a dead load analysis was performed for both bridges. Because the exterior girders in the BCB2 are of a substantial size, both the interior and exterior girders were assumed to carry the dead load of the BCB2. This was not the case in the DCB where the exterior girders are much smaller than the interior girder, thus, only the interior girders were assumed to carry the dead load of the DCB.

As expected, the maximum strains and deflections measured during the static load tests on both bridges occurred in the girders directly below the axle loads of the test truck when the center of the tandem axle of the test truck was at the midspan of the bridge. The weights of the test trucks used in the load tests on the BCB2 and DCB were not the legal load that may cross either bridge. Thus, the maximum strains and deflections recorded during the load tests were multiplied by a load adjustment factor to determine an approximation of the maximum strains and deflections caused by an HS-20 truck, the maximum load likely to cross either bridge. The load adjustment factor was the ratio of the midspan moment of a simply-supported beam due to the load of an HS-20 truck to the midspan moment of a simply-supported beam due to the loaded test truck.

In the BCB2, the maximum total stress occurred in an exterior girder at the edge of the bridge and was 14.5 ksi, which is less than the allowable flexural stress, 22 ksi. The maximum deflection of the bridge occurred in an exterior girder at the edge of the bridge and was 0.46 in., which is less than 0.81 in., the AASHTO optional limit of 1/800 of a 54 ft – 0 in. span. In the DCB, the maximum total stress occurred in an interior girder and was 27.9 ksi, which exceeds the allowable stress limit by 27 percent. In order to keep the maximum total stress below the allowable stress, the gravel driving surface on the DCB should be limited to 3 in. The maximum deflection of the DCB was 1.15 in., which slightly exceeds 1.0 in., the optional AASHTO limit of 1/800 of a 66 ft – 4 in. span. However, the optional limit is a

guideline, not a requirement, and because the DCB is a rural bridge on a low-volume road, slightly exceeding the optional limit is acceptable. If the deflection of the DCB were to be required to meet the optional limit, the weight of a truck with HS-20 spacings would have to be limited to 30 tons.

The results of the static load tests revealed that both the BCB2 and DCB displayed effective lateral load distribution through the LFC. Also, the strain and deflection patterns at midspan of both bridges exhibited symmetrical bridge behavior when the truck was in Lane 2 and transverse symmetry when the truck was in Lanes 1 and 3

In the dynamic load tests of the DCB, the adjusted maximum total stress and the adjusted maximum deflection were 25.3 ksi and 0.83 in., respectively, and occurred when the test truck was traveling at 15 mph. Although the maximum deflection is less than the optional limit of 1.0 in., the maximum total stress exceeds the allowable stress limit. However, the maximum total stress in the static load test was greater than that in the dynamic load test; thus, by changing the thickness of the driving surface as suggested for the static load tests, the adjusted maximum total stress in the dynamic load test decreases to 19.6 ksi, which is below the allowable stress limit. The results of the dynamic load tests of the DCB were also compared to the results of the static load tests in order to determine the dynamic amplification factor for the girder strains and deflections. Through this comparison, it was determined that the dynamic amplification factor for the girder strains was 6 percent and the dynamic amplification factor for the girder deflections was 5 percent. Finally, the dynamic deflection behavior of the DCB revealed that the damped period and damped frequency of the bridge were 0.36 seconds and 2.75 Hz, respectively.

The second and third objectives of this study were met using the results from the field load tests. To satisfy the second objective, the refinement of the design methodology first presented in the demonstration project [4, load distribution factors were determined for

the interior and exterior members of the RRFCs. As part of the determination of the load distribution factors, it was determined that a moment fraction equal to 2/3 is valid for RRFC bridges composed of two RRFCs and three RRFCs. Thus, with the appropriate adjustment factors, the equation for the live load distribution factor developed for the demonstration project [4] is valid for bridges with two or three RRFCs.

After the determination of the distribution factors, a procedure for rating RRFC bridges was developed. In this procedure, all members of the bridge should be visually inspected, but only the interior and exterior primary girders are assigned a numerical rating. This rating should be found following the AASHTO *Manual for Condition Evaluation of Bridges* [8]. However, due to the variation of the size of girders and girder spacing, the live load effect of a member cannot be determined with the tables provided in the Rating Manual. Instead, the live load effect should be determined using the load distribution factors developed either for this thesis or for the demonstration project [4].

6.2 Conclusions

The following conclusions can be drawn from the information and analysis obtained in this investigation on the use of RRFCs in LVR bridges:

- The maximum girder stresses in RRFC bridges designed like the BCB2 are less than the allowable stress of the steel used in the 56-ft V-deck RRFCs.
- The maximum deflection due to an HS-20 truck on RRFC bridges designed like the BCB2 is less than the optional limit suggested in the AASHTO *Standard Specifications for Highway Bridges* [6].
- The maximum girder stresses in bridges designed like the DCB, which has an 8.5-in. driving surface, exceed the allowable stress of the steel used in the 89-ft RRFCs. However, if the gravel driving surface is reduced to 3 in., the maximum girder stresses will be less than the allowable stress.
- The maximum deflection of the DCB exceeds the optional limit suggested in the *AASHTO Standard Specifications for Highway Bridges* [6]. However, the optional limit is a guideline, not a requirement, and because the DCB is a rural bridge on a low-volume road, the maximum deflection of the DCB is acceptable.

- Using the load distribution factors presented in this thesis, the live load moments developed in the primary girders of bridges designed like the BCB2 and DCB can be determined.

- RRFC bridges can be rated by following the AASHTO *Manual for Condition Evaluation of Bridges* [8] and using the load distribution factors presented in this thesis to determine the live load effects.

- The LFC consisting of a 22-in. wide R/C beam (BCB2 LFC) effectively transfers load between RRFCs.

- The LFC formed by connecting the RRFCs by welding a 1/2-in. plate to the decks of the RRFCs at the connection (DCB LFC) effectively transfers load between RRFCs.

- RRFC bridges composed of two RRFCs are efficient and economical options for LVR bridges.

- Although deflections slightly exceed the optional AASHTO limit, RRFC bridges composed of symmetric 67 ft – 6 in. portions of 89-ft RRFCs are efficient options for LVR bridges if the gravel driving surface is limited to 3 in.

7. ACKNOWLEDGMENTS

The Bridge Engineering Center at Iowa State University conducted the investigation presented in this report. The Iowa Department of Transportation, Highway Division, and the Iowa Highway Research Board sponsored the research as a phase of Research Project TR-498.

The author wishes to thank Brian Keierleber, Buchanan County Engineer, and Mark Nahra, Delaware County Engineer, for their cooperation with this project. Thanks are also given to Doug Wood, ISU Research Laboratory Manager, for his assistance with the field tests. Thanks to the following ISU graduate and undergraduate students who helped with the instrumentation and field testing of the bridges: Holly Boomsma, Elizabeth Kash, Jon Greenlee, Travis Konda, and Ben Woline. Finally, the author thanks the Program of Study committee: Dr. Wayne Klaiber, Dr. Terry Wipf, and Dr. Loren Zachary.

8. REFERENCES

1. National Bridge Inventory Study Foundation. *NBI Report 2004.* http://www.nationalbridgeinventory.com/nbi_report_200414.htm. Accessed February 1, 2005.

2. US Census Bureau. *State Rankings—Statistical Abstract of the United States—Resident Population.* http://www.census.gov/statab/ranks/rank01.html. Accessed September 7, 2004.

3. Wipf, T. J., F. W. Klaiber, and T. L. Threadgold. *Use of Railroad Flat Cars for Low-Volume Road Bridges.* Iowa DOT Project TR-421. Iowa Department of Transportation. August, 1999. 141 pp.

4. Wipf, T. J., F. W. Klaiber, J. D. Witt, and J. D. Doornink. *Demonstration Project Using Railroad Flatcars for Low-Volume Road Bridges.* Iowa DOT Project TR-444. Iowa Department of Transportation. February 2003. 193 pp.

5. Mapquest.com, Inc. *Mapquest.* http://www.mapquest.com. Accessed July 7, 2004.

6. American Association of State Highway and Transportation Officials (AASHTO). *Standard Specifications for Highway Bridges, 17th Edition.* Washington, D.C. 2003.

7. Doornink, J. D. Demonstration Project Using Railroad Flatcars for Low-Volume Road Bridges. M.S. Thesis, Iowa State University, 2003.

8. American Association of State Highway and Transportation Officials (AASHTO). *Manual for Condition Evaluation of Bridges.* Washington, D.C. 1994.

9. American Association of State Highway and Transportation Officials (AASHTO). *AASHTO LRFD Bridge Design Specifications, First Edition, Customary US Units.* Washington, D.C. 1994.

APPENDIX A. BCB2 LFC STRAIN-TIME HISTORIES

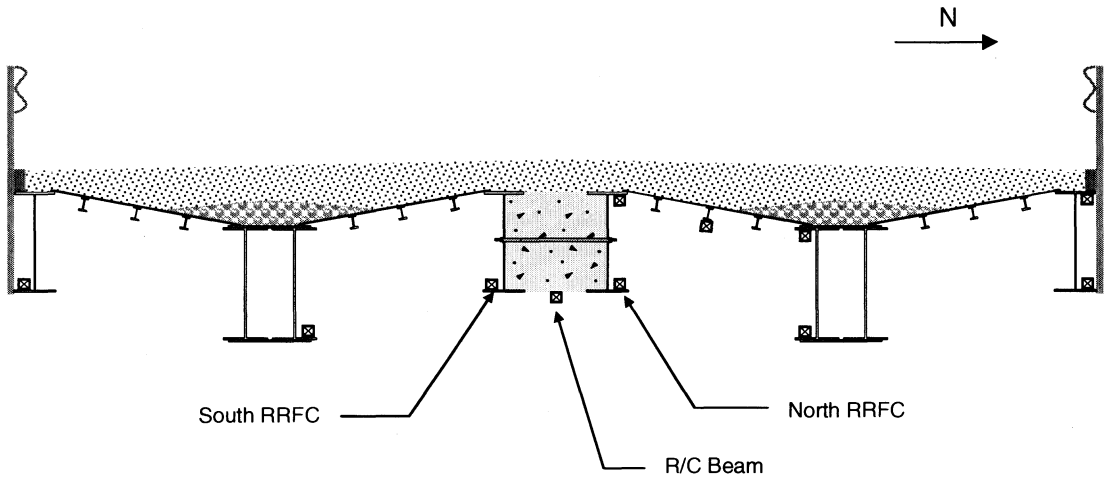

a. BCB2 cross-section at midspan

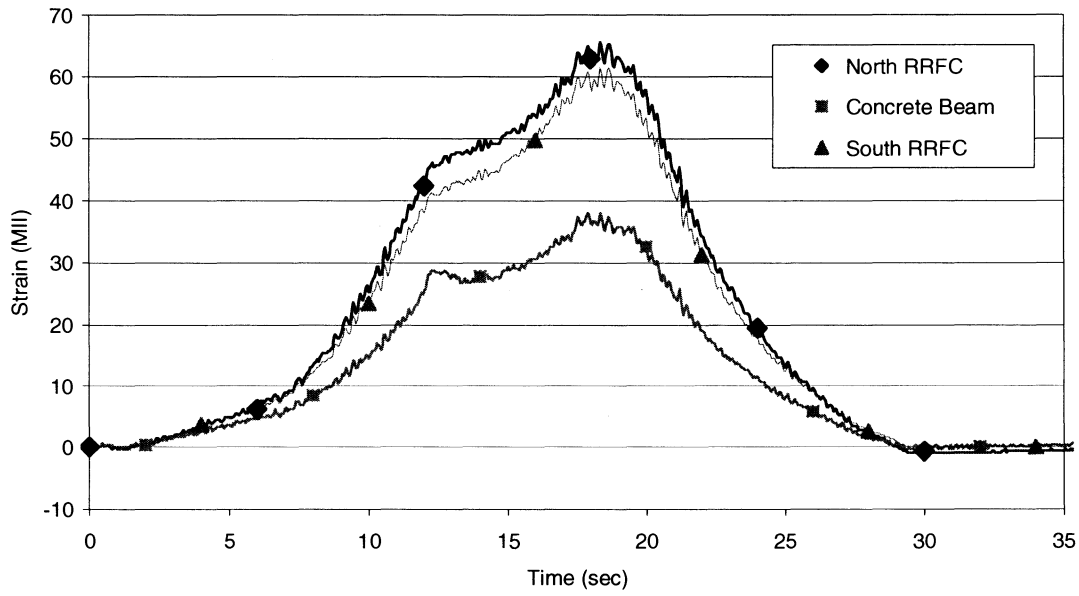

b. Lane 1 strain-time history

Figure A1. BCB2 LFC strain-time history.

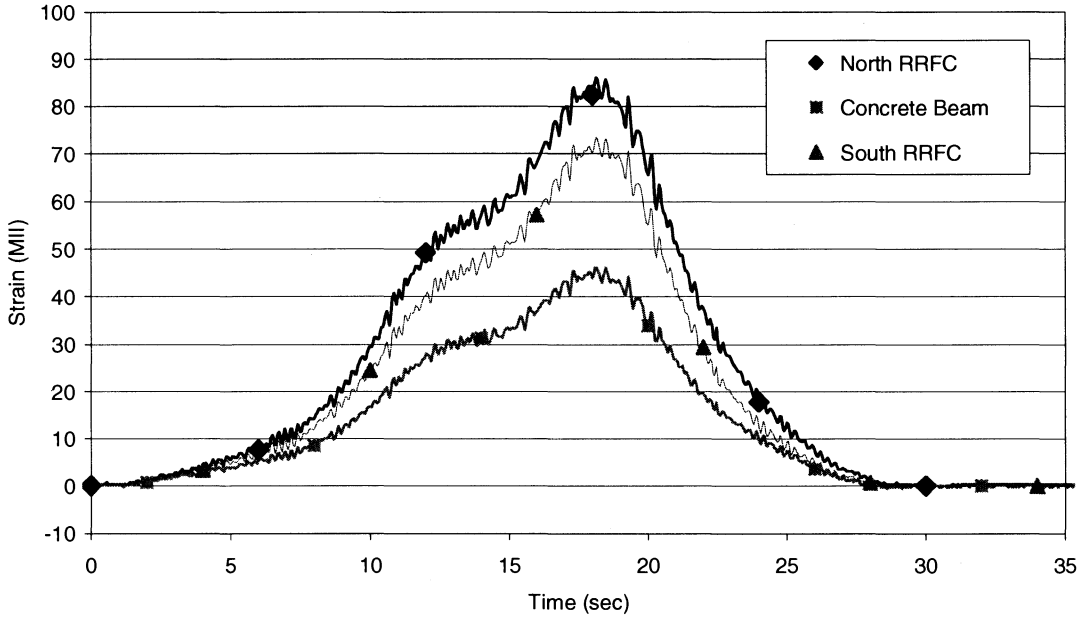

c. Lane 2 strain-time history

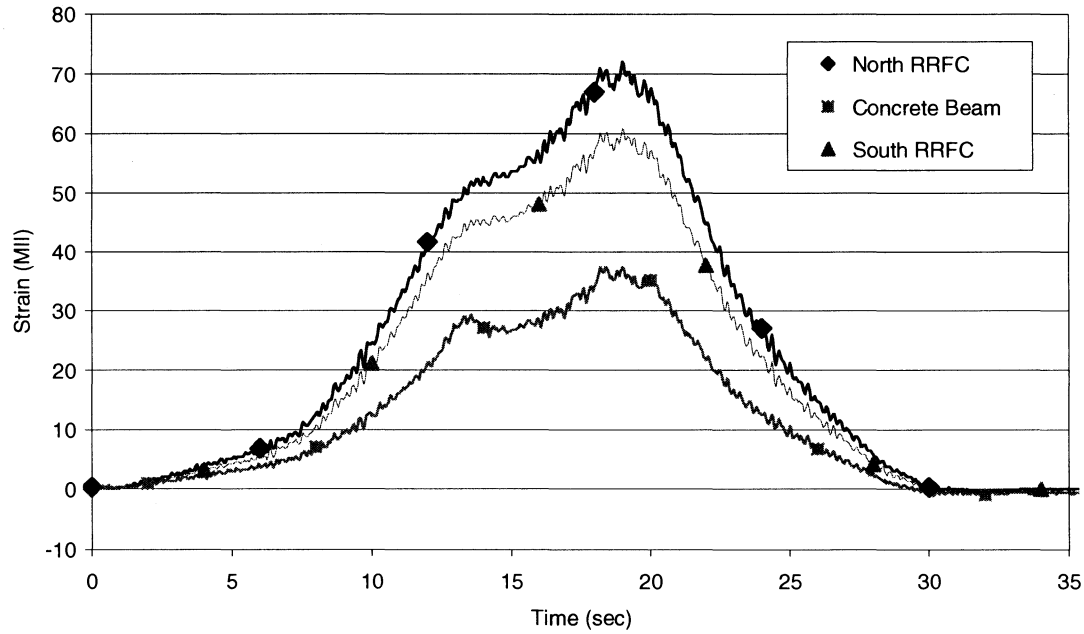

d. Lane 3 strain-time history

Figure A1. Continued.

APPENDIX B. DETERMINATION OF THE ADJUSTMENT FACTOR

In order to determine the adjustment factor, ψ, required for the live load distribution factor of Equation 5.5, a trial-and-error process was used. As reported in Section 5.1, separate adjustment factors were determined for the interior and exterior girders of both the BCB2 and the DCB. The trial-and-error process will be described using the equations presented in Section 5.1 and the calculation for the BCB2 interior girder live load distribution factor.

First, develop a statically determinate structure for the BCB2. Center the tandem axle loads of the test truck used in the field load tests over the center of the span and analyze the BCB2 as a simply-supported structure:

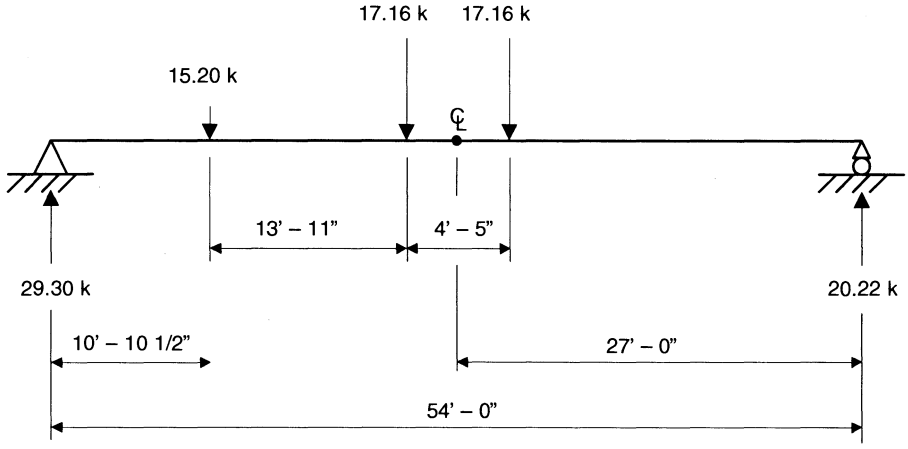

Determine the maximum live load moment, M_{SD}, at midspan of the BCB2 with the center of the tandem axles at midspan:

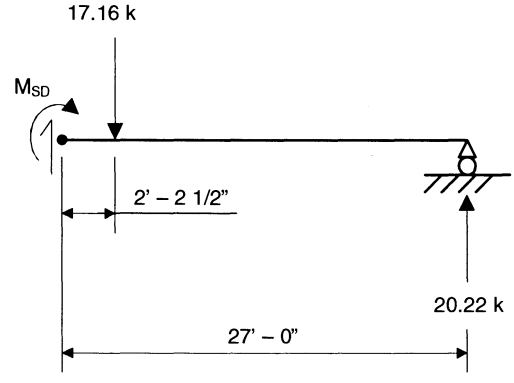

M_{SD} = (20.22 k)(27.00 ft) – (17.16 k)(2.208 ft) = 508.1 k-ft

Next, determine the section properties of the primary girders and the inertia ratio, ω, for the interior girder of one RRFC:

c_{INT} = 13.7 in.

I_{INT} = 8,322 $in.^4$

I_{EXT} = 1,964 $in.^4$

I_D = 8,322 $in.^4$

$\Sigma I_{RRFC} = (2)(I_{EXT}) + I_{INT} = (2)(1{,}964) + 8{,}322 =$ 12,250 $in.^4$

$$\omega = \frac{I_D}{\Sigma I_{RRFC}} = \frac{8{,}322\,in.^4}{12{,}250\,in.^4} = 0.679$$

Assume the adjustment factor, ψ, is equal to 1.0, and calculate the theoretical live load moment, M_{LL}, in the interior girder at midspan of the bridge:

$$M_{LL} = \frac{2}{3}\psi\,\omega\,M_{SD} = (\frac{2}{3})(1.0)(0.679)(508.1) = 230.0\text{ k-ft}$$

Determine the theoretical strain in the interior girder at midspan:

$$\varepsilon_{theo} = \frac{M_{LL}}{S * E} = \frac{(230.0\,k\text{-}ft)(12\,in./ft)(13.7\,in.)}{(29{,}000\,ksi)(8{,}322\,in.^4)}(10^6) = 157\text{ MII}$$

Determine the relative error between the theoretical strain and the experimental strain measured during the field load test, ε_{exp} = 116 MII:

$$\text{Error} = \frac{\varepsilon_{exp} - \varepsilon_{theo}}{\varepsilon_{exp}} * 100\% = \frac{(116 - 157)}{116} * 100\% = -35.3\%$$

A relative error less than zero indicates that the experimental strain is less than the theoretical strain; thus, the theoretical strain is conservative. For the assumed adjustment factor to be acceptable, the relative error between the two strains must be negative and the absolute value of the relative error must be less than 10 percent. With a relative error less

than 10 percent, the theoretical live load moment can be assumed to adequately approximate the experimental live load moment. A sensitivity analysis on the effect of the relative error on the adjustment factor indicated that there is a minimal difference between adjustment factors determined with a maximum relative error of 10 percent and adjustment factors determined with a maximum relative error 1 percent. Because the relative error is 35.3 percent, which is more than 10 percent, assume a new value for the adjustment factor and recalculate the theoretical live load moment:

$$\psi = 0.8$$

$$M_{LL} = \frac{2}{3}\psi\,\omega\,M_{SD} = (\frac{2}{3})(0.8)(0.679)(508.1) = \underline{184.0\text{ k-ft}}$$

Determine the revised theoretical strain in the interior girder at midspan:

$$\varepsilon_{theo} = \frac{M_{LL}}{S * E} = \frac{(184.0\,\text{k - ft})(12\,\text{in./ft})(13.7\,\text{in.})}{(29{,}000\,\text{ksi})(8{,}322\,\text{in.}^4)}(10^6) = \underline{125\text{ MII}}$$

Determine the relative error between the revised theoretical strain and the experimental strain measured during the field load test, ε_{exp} = 116 MII:

$$\text{Error} = \frac{\varepsilon_{exp} - \varepsilon_{theo}}{\varepsilon_{exp}} * 100\% = \frac{(116 - 125)}{116} * 100\% = \underline{-7.2\%}$$

When the adjustment factor, ψ, is equal to 0.8, the relative error between the theoretical and experimental strains is negative and less than 10 percent. Thus, for the interior girder of the BCB2, the adjustment factor, ψ, is 0.8.

This procedure was followed to determine the adjustment factors for an exterior girder of the BCB2 and the interior and exterior girders of the DCB.

APPENDIX C. DETERMINATION OF THE MOMENT FRACTION

Equation 5.1, which is presented in Section 5.1 and used to determine the maximum live load moment at midspan of a bridge, includes a moment fraction of 2/3 as part of the live load distribution factor. The moment fraction is determined using the deflection curve that describes the maximum deflection of the bridge. The area beneath the deflection curve is the total energy of the system, and the moment fraction is the fraction of the system energy for one RRFC. The procedure for determining the moment fraction was first developed in the demonstration project for RRFC bridges consisting of three RRFCs [4]. To verify that the moment fraction is the same for bridges composed of two RRFCs, the procedure described in Appendix D of the *Demonstration Project Using Railroad Flatcars for Low-Volume Road Bridges* [7] is used in the following sections to determine the moment fractions for the BCB2 and DCB.

C.1 BCB2 Moment Fraction

To determine the moment fraction, one first plots the maximum deflections at midspan due to the test truck and fits a "best-fit" curve to the deflections; the "best-fit" curve for the BCB2 is shown in Figure C.1 using the deflections from the field load test with the truck in Lane 3. Using the equation of the "best-fit" curve, calculate the area under the "best-fit" curve for the unloaded RRFC (the system energy of the unloaded RRFC):

$$A_1 = \int_0^{134.5} (1.119)(10^{-6})(x^2) - (1.554)(10^{-3})(x) - (0.03976)dx = \underline{-19.01\ in^2}$$

Calculate the area under the "best-fit" curve beneath the RRFC on which the test truck is positioned (the system energy of the loaded RRFC):

$$A_2 = \int_{134.5}^{247} (1.119)(10^{-6})(x^2) - (1.554)(10^{-3})(x) - (0.03976)dx = \underline{-34.60\ in^2}$$

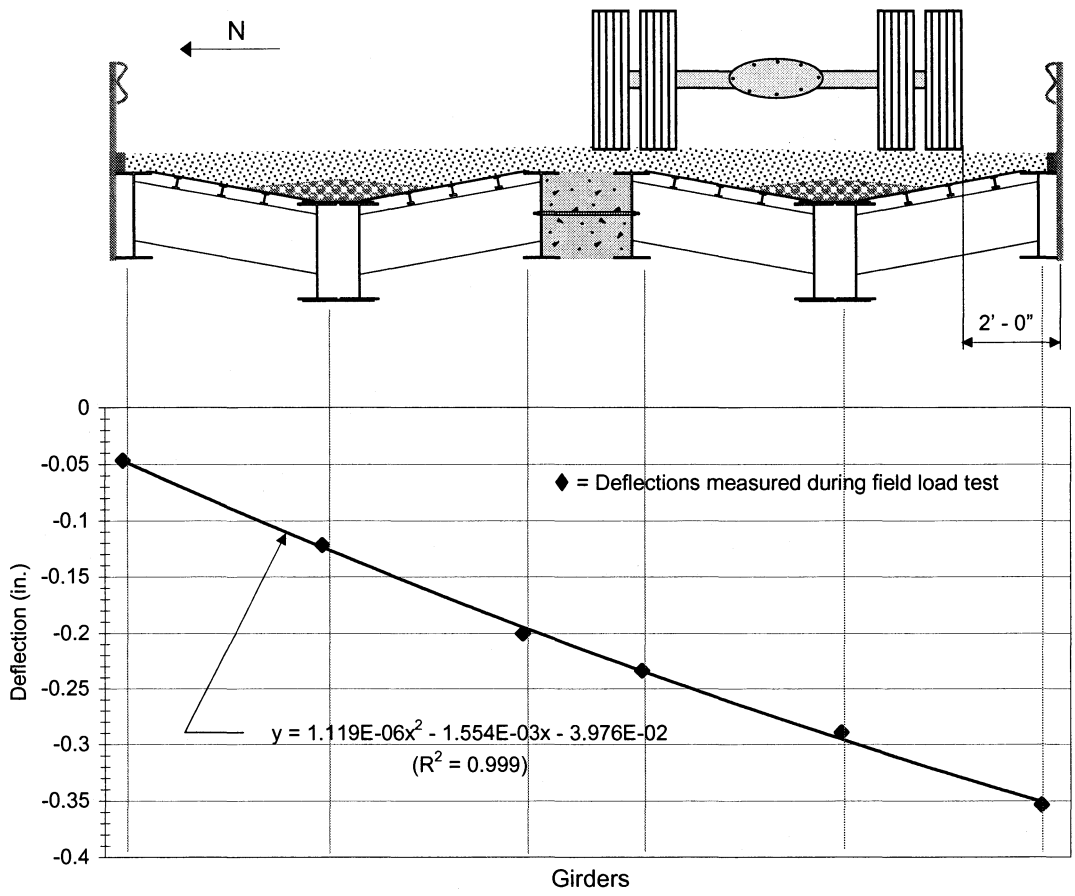

Figure C.1. BCB2 midspan deflection "best-fit" curve.

Determine the moment fraction for the BCB2 (the fraction of the system energy for the loaded RRFC):

$$MF_{BCB2} = \frac{A_2}{A_1 + A_2} = \frac{-34.60}{-19.01-34.60} = \underline{0.65}$$

C.2 DCB Moment Fraction

The "best-fit" curve for the DCB is shown in Figure C.2 using the deflections from the field load test with the truck in Lane 3. As with the BCB2, one calculates the area under the best-fit curve for the unloaded RRFC (the system energy of the unloaded RRFC):

$$A_1 = \int_0^{109.5} (7.880)(10^{-8})(x^3) - (2.113)(10^{-6})(x^2) - (1.905)(10^{-3})(x) - (0.2186)dx$$

$$= \underline{-41.89 \text{ in}^2}$$

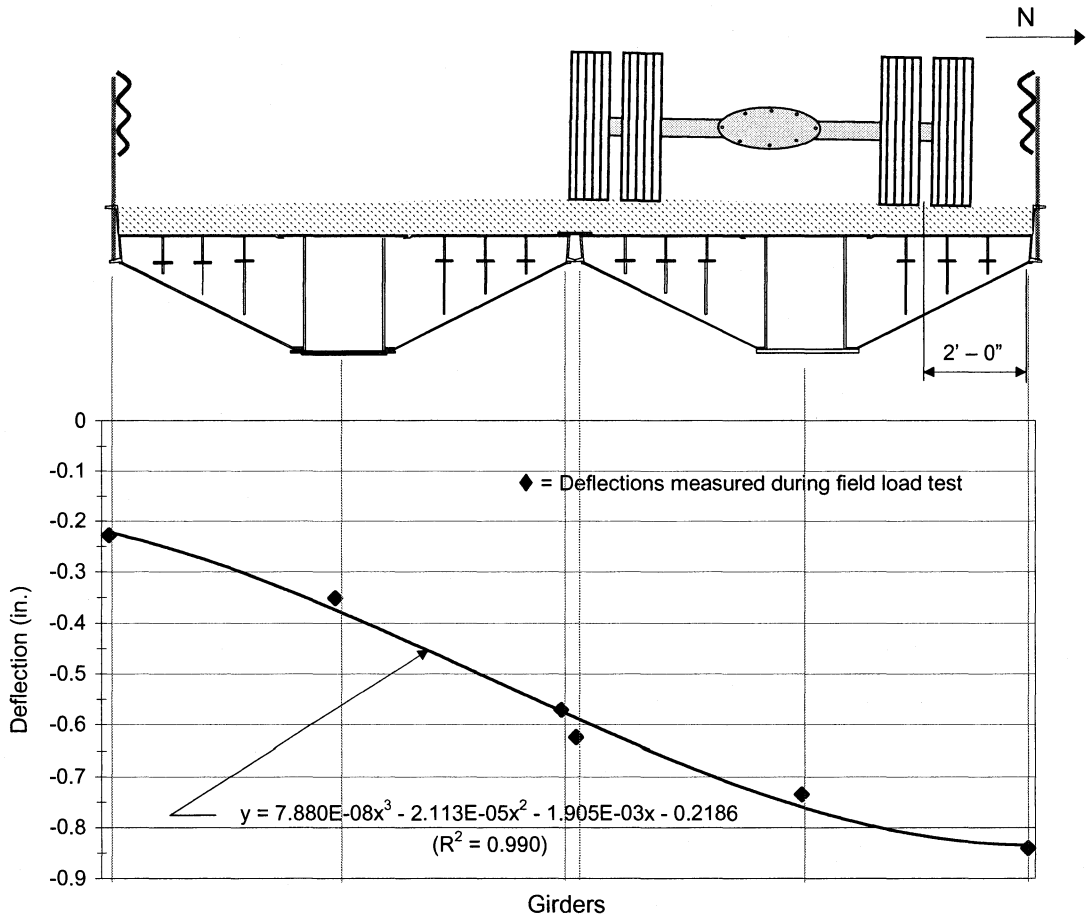

Figure C.2. DCB midspan deflection "best-fit" curve.

Then, calculate the area under the "best-fit" curve beneath the RRFC on which the test truck is positioned (the system energy of the loaded RRFC):

$$A_2 = \int_{109.5}^{219} (7.880)(10^{-8})(x^3) - (2.113)(10^{-6})(x^2) - (1.905)(10^{-3})(x) - (0.2186)dx$$

$$= \underline{-81.25 \text{ in}^2}$$

Determine the moment fraction for the DCB (the fraction of the system energy for the loaded RRFC):

$$MF_{DCB} = \frac{A_2}{A_1 + A_2} = \frac{-81.25}{-41.89 - 81.25} = \underline{0.66}$$

APPENDIX D. RRFC BRIDGE RATING EXAMPLE

Following the procedure of Section 5.2, the bridge inventory rating for the BCB2 will be determined as an example for rating RRFC bridges. First, determine the rating factor for an interior girder. To do so, determine the allowable stress capacity of the member, C, from the inventory rating table (Table 6.6.2.1-1) provided in the Rating Manual [8]:

$C = 0.55\ F_y = (0.55)(40\ \text{ksi}) = 22\ \text{ksi}$

Next, determine the dead load effect on the interior girder, D, using the assumptions and procedure described in Section 4.1.1. First, calculate the equivalent uniform dead load acting on the interior girder:

Gravel = 98 lb/ft^2

Guard Rail System = 100 lb/ft

RRFC = 35,000 lb

RRFC Length = 56 ft

Bridge Span = 54 ft

Bridge Width = 20.5 ft

Interior girder tributary width = 4.688 ft

$$w = \left(\frac{4.688\ \text{ft}}{20.5\ \text{ft}}\right)\left[(98\ \text{lb/ft}^2)(20.5\ \text{ft}) + (100\ \text{lb/ft}) + (2)\left(\frac{35{,}000\ \text{lb}}{56\ \text{ft}}\right)\right] = \underline{769\ \text{lb/ft}}$$

Develop a statically determinate structure for the girder, and analyze the girder with the uniform dead load:

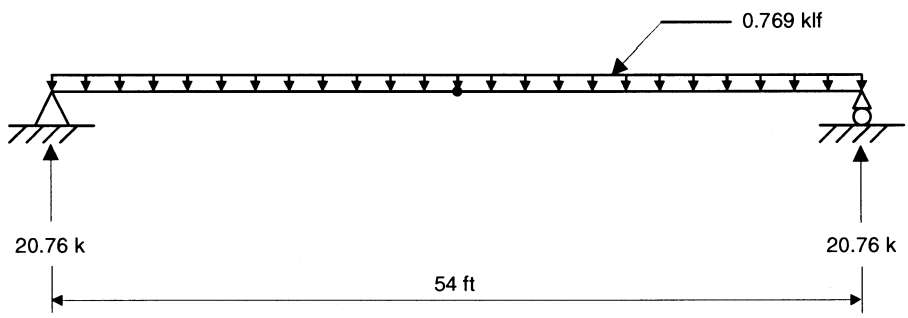

Determine the maximum dead load moment, M, at midspan of the bridge:

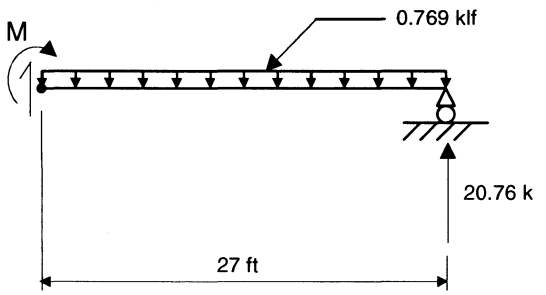

$M = (20.76\ k)(27\ ft) - (0.769\ klf)(27\ ft)(0.5)(27\ ft) = \underline{280\ k\text{-}ft}$

Determine the section modulus of the interior girder:

$I = 8{,}322\ in.^4$

$c = 13.73$ in. (to the bottom flange)

$$S = \frac{I}{c} = \frac{8{,}322\ in.^4}{13.73\ in.} = 606\ in.^3$$

Calculate the dead load effect, the stress in the bottom flange of the interior girder:

$$D = \sigma_{DL} = \frac{M}{S} = \frac{(280\ k\text{-}ft)(12\ in./ft)}{606\ in.^3} = \underline{5.6\ ksi}$$

In order to determine the live load effect on the interior girder of the BCB2, develop a statically determinate structure for the BCB2. Position the center of gravity of an HS-20 truck over the center of the span and analyze the bridge as simply supported over its clear span:

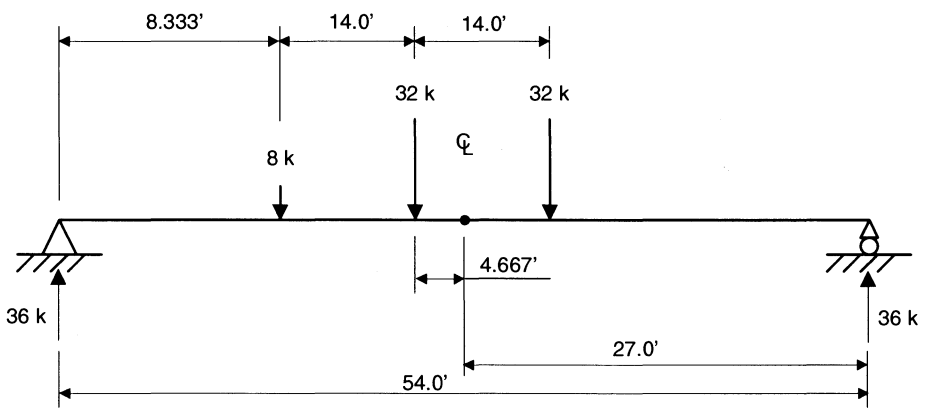

Determine the maximum midspan moment due to the HS-20 truck, M_{HS-20}:

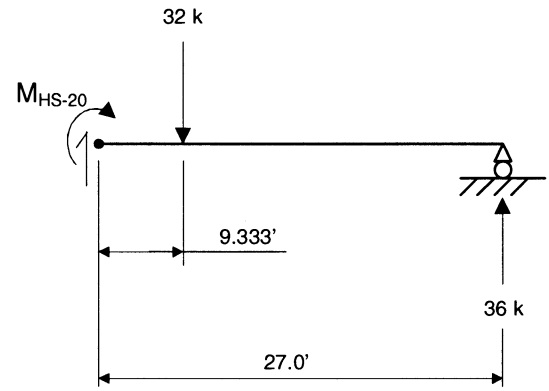

M_{HS-20} = (36 k)(27.0 ft) – (32 k)(9.333 ft) = 673 k-ft

Next, determine the section properties of the primary girders and the inertia ratio, ω, and adjustment factor, ψ, for the interior girder of one RRFC:

c_{INT} = 13.7 in.

I_{INT} = 8,322 $in.^4$

I_{EXT} = 1,964 $in.^4$

I_D = 8,322 $in.^4$

$\Sigma I_{RRFC} = (2)(I_{EXT}) + I_{INT} = (2)(1{,}964) + 8{,}322 = 12{,}250\ in.^4$

$$\omega = \frac{I_D}{\Sigma I_{RRFC}} = \frac{8{,}322\,in.^4}{12{,}250\,in.^4} = 0.679$$

ψ = 0.8 (from Section 5.1)

Calculate the distribution factor for the interior girder:

$$DF = \frac{2}{3}\psi\,\omega = \frac{2}{3}(0.8)(0.679) = 0.362$$

Determine the live load moment for the interior girder:

$M = (DF)(M_{HS-20}) = (0.362)(673\text{ k-ft}) = 244$ k-ft

Calculate the live load effect, L, the stress in the bottom flange of the interior girder:

$$L = \sigma_{LL} = \frac{M}{S} = \frac{(244\,k\text{ - }ft)(12\,in./ft)}{606\,in.^3} = \underline{4.83\ ksi}$$

The values for the impact factor, I, and the factors for dead and live loads, A_1 and A_2, are provided in Section 5.2. With these values, and the calculated values of the allowable stress capacity, C, the dead load effect, D, and the live load effect, L, determine the rating factor for the interior girder:

$$RF = \frac{C - A_1 D}{A_2 L (1+I)} = \frac{(22\,ksi) - (1.0)(5.6\,ksi)}{(1.0)(4.83\,ksi)(1+0.33)} = \underline{2.55}$$

Finally, determine the inventory rating of the interior girder of the BCB2:

Rating = (RF)(Weight of truck) = (2.55)(36 tons) = <u>91 tons</u>

To determine the actual bridge rating of the BCB2, this example should be repeated to find the rating for the exterior girders of the BCB2. If repeated using the properties of an exterior girder, the bridge rating is 80 tons. The BCB2 bridge rating is the lowest calculated rating; thus, the bridge rating for the BCB2 is 80 tons.

APPENDIX E. DETERMINATION OF THE LOAD ADJUSTMENT FACTOR

Equation 4.2, presented in Section 4.1, is used to determine the load adjustment factor, which modifies the strains and deflections measured in field load tests to reflect the strains and deflections caused by Iowa legal loads, an HS-20 truck. The load adjustment factor is the ratio of the midspan moment due to an HS-20 truck to the midspan moment do to the test truck. The load adjustment factors for the BCB2 and DCB are calculated in the following sections.

E.1 BCB2 Load Adjustment Factor

First, develop a statically determinate structure for the BCB2. Position the center of gravity of an HS-20 truck over the center of the span and analyze the bridge as simply supported over its clear span:

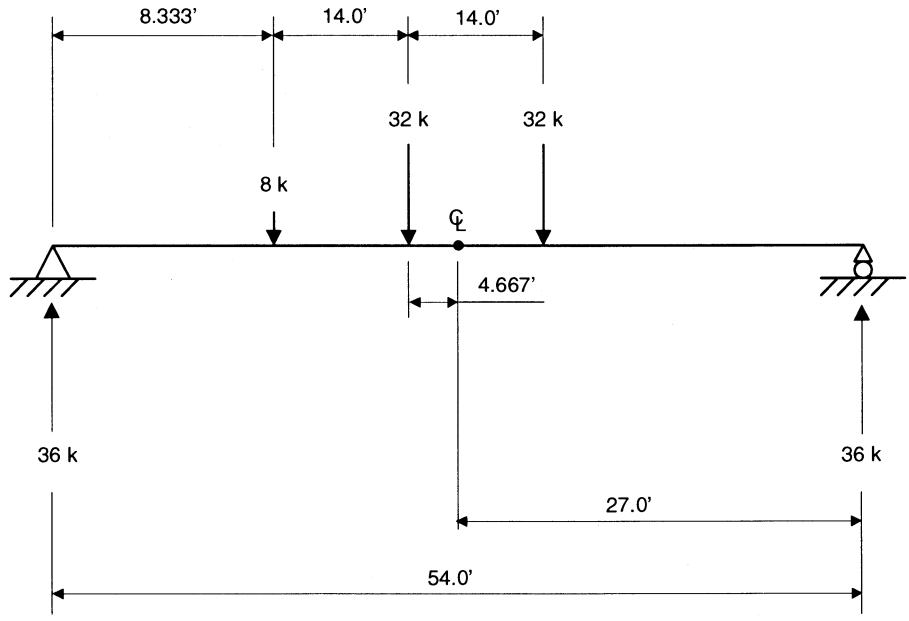

Determine the maximum midspan moment due to the HS-20 truck, M_{HS-20}:

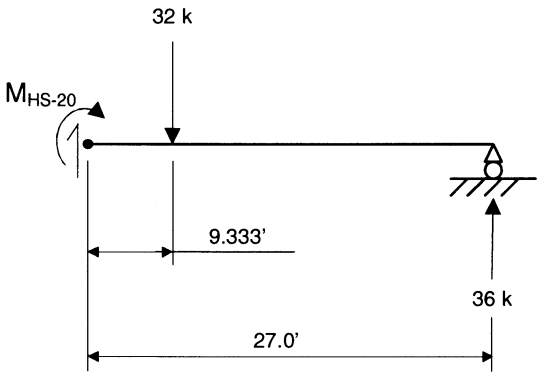

M_{HS-20} = (36 k)(27.0 ft) – (32 k)(9.333 ft) = <u>673 k-ft</u>

With the structurally determinate BCB2, position the center of gravity of the test truck over the center of the span and analyze the bridge as simply supported over its clear span:

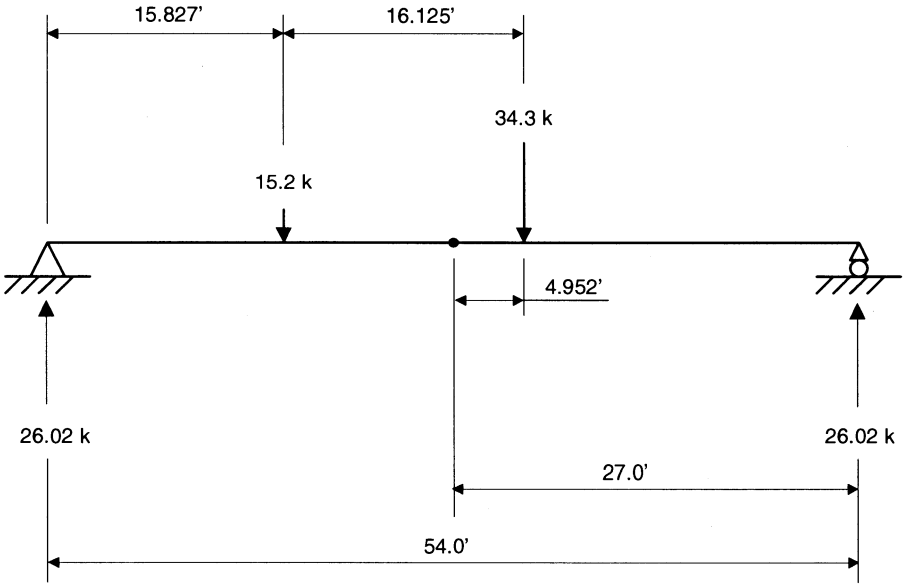

Determine the maximum midspan moment due to the test truck, M_{TT}:

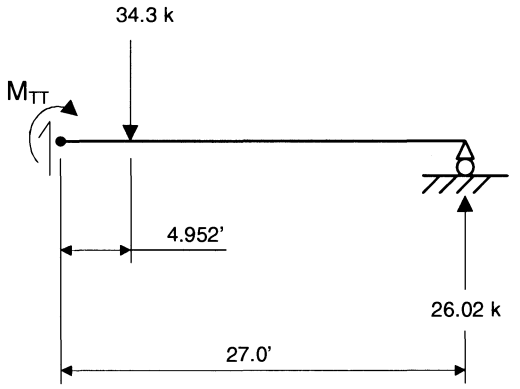

M_{TT} = (26.02 k)(27.0 ft) – (34.3 k)(4.952 ft) = 533 k-ft

Calculate the load adjustment factor for the BCB2:

$$\beta = \frac{M_{HS-20}}{M_{TT}} = \frac{673\,k\text{-}ft}{533\,k\text{-}ft} = 1.26$$

E.2 DCB Load Adjustment Factor

Develop a statically determinate structure for the DCB. Position the center of gravity of an HS-20 truck over the center of the span and analyze the bridge as simply supported over its clear span:

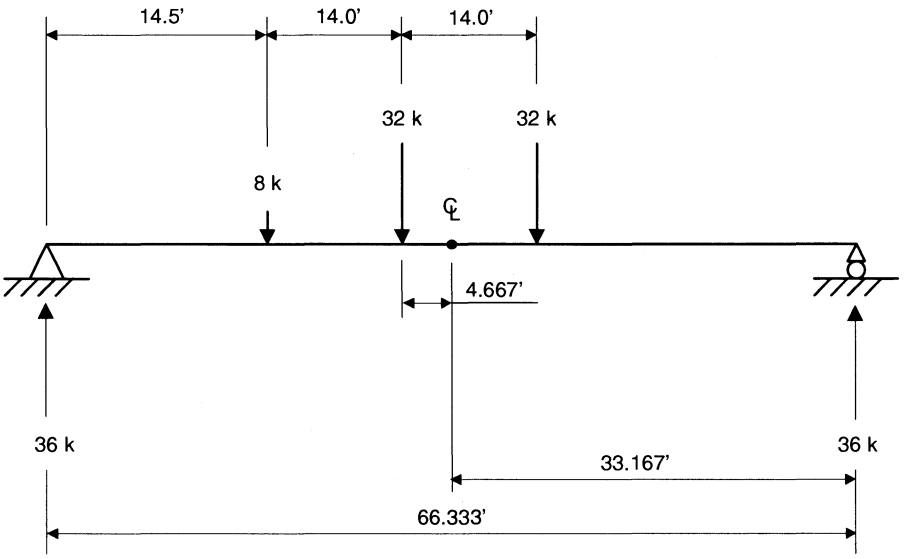

Determine the maximum midspan moment due to the HS-20 truck, M_{HS-20}:

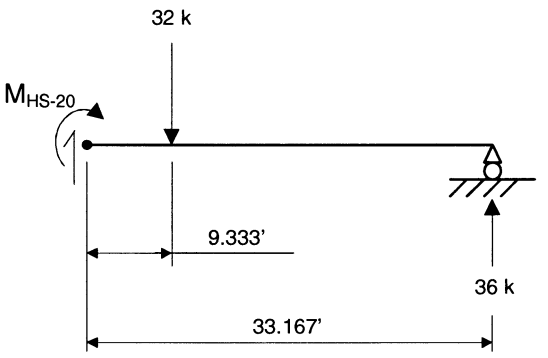

M_{HS-20} = (36 k)(33.167 ft) – (32 k)(9.333 ft) = <u>895 k-ft</u>

With the structurally determinate DCB, position the center of gravity of the test truck over the center of the span and analyze the bridge as simply supported over its clear span:

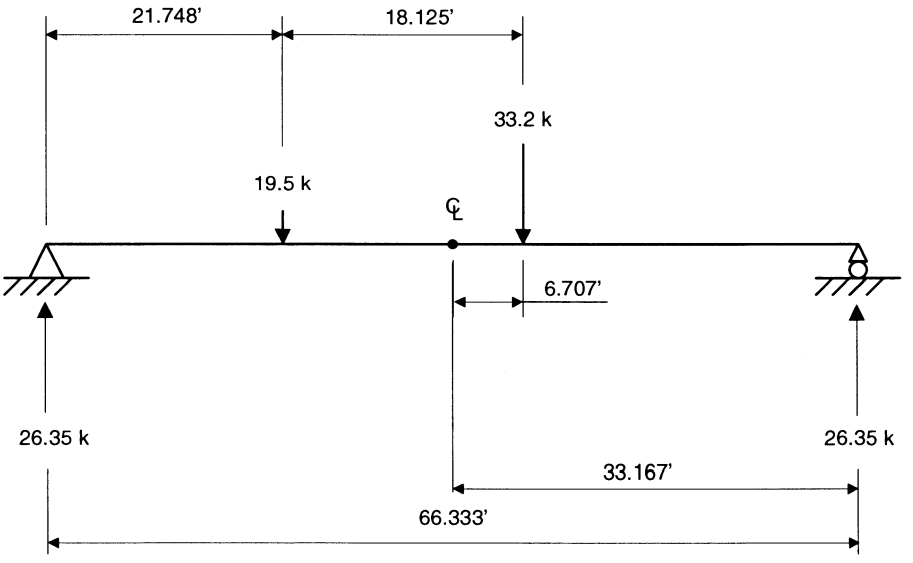

Determine the maximum midspan moment due to the test truck, M_{TT}:

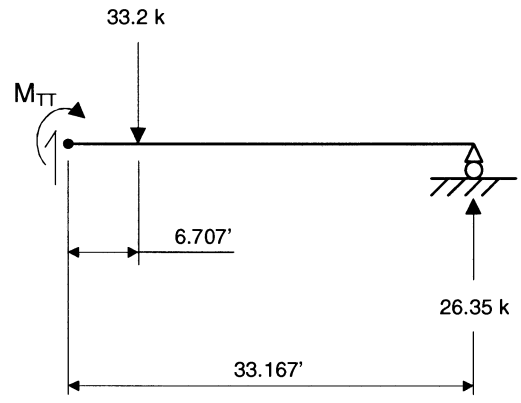

M_{TT} = (26.35 k)(33.167 ft) – (33.2 k)(6.707 ft) = <u>651 k-ft</u>

Calculate the load adjustment factor for the DCB:

$$\beta = \frac{M_{HS-20}}{M_{TT}} = \frac{895\,k\text{ - }ft}{651k\text{ - }ft} = \underline{1.37}$$

APPENDIX F. DETERMINATION OF THE MAXIMUM SPAN FOR 89-ft RRFCs

The sections that follow present the assumptions and equations used to determine the maximum clear span of 89-ft RRFCs without building up the cross-section at the midspan of the bridge and without a center pier. AASTHO LRFD equations and load factors are used for the calculations, and the maximum clear span is designed based on the effects of an HS-20 truck as specified in the *AASHTO LRFD Bridge Design Specifications* [9].

F.1 Assumptions

For the calculation in this appendix, the RRFCs are assumed to be symmetric about the midspan of the bridge, regardless of the clear span length. To theoretically determine the maximum stresses in the RRFC bridges, several other assumptions must be made. The assumptions made for the dead load on the bridge are:

1. One 89-ft RRFC weighs 42000 lbs
2. 3.5 in. thick wood planks cover the entire deck
3. The unit weight of the wood planks is 36.3 pcf
4. A 6 in. layer of gravel covers the wood planks
5. The unit weight of the gravel is 110 pcf
6. The guard rail system weighs 100 lb/ft

These loads are converted to pounds per unit length by assuming the bridge is composed of two RRFCs with a total width of 18 ft. Using these assumptions, the total weight of the components is 1040 lb/ft and the total weight of the wearing surface is 700 lb/ft.

F.2 Calculations

The maximum moment due to the uniform dead load occurs at midspan of a bridge. However, the maximum moment due to the concentrated live axle loads occurs beneath the load closest to the center of gravity of all the axle loads when the truck is positioned as described in the following section. Because the maximum moments due to the dead and live loads may not occur at the same point along the bridge, two cases must be considered. For Case 1, the dead and live load moments are determined at the midspan of the bridge; the maximum dead load moment and live load moment at midspan are combined. For Case

2, the dead and live load moments are determined at the point beneath one of the axle loads; the maximum live load moment is combined with the dead load moment at the same location.

F.2.1 Case 1 Calculations

First, develop a statically determinate model of the bridge. Position an HS-20 truck such that midspan of the bridge is half way between the center of gravity of the three axle loads and the nearest axle load, increase the axle loads by 33 percent to account for the impact load, and analyze the bridge as simply supported over its clear span:

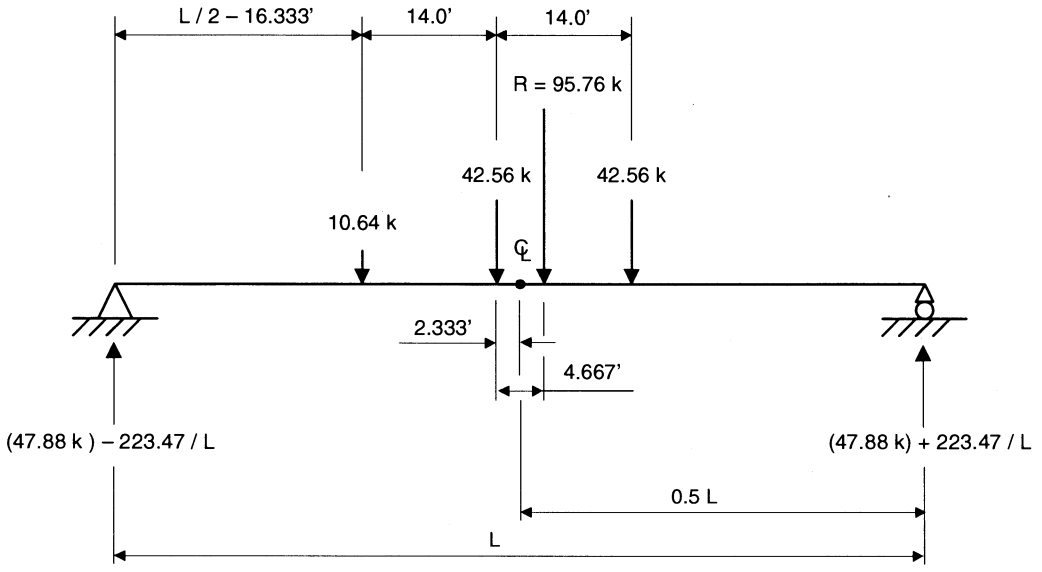

Determine the maximum live load moment, M_{SD}, at midspan of the bridge:

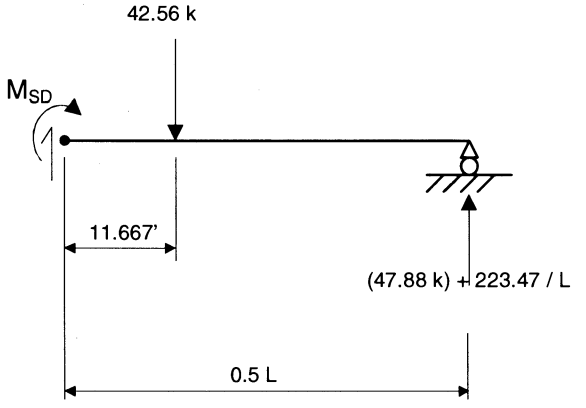

$$M_{SD} = (47.88 + \frac{223.47}{L})(0.5\ L) - (42.56)(11.667) = \underline{(23.94\ L - 384.8)\ k - ft}$$

Next, determine the section properties of the primary girders and the inertia ratio, ω, for the interior girder and one exterior girder of one 89-ft RRFC:

$I_{INT} = 8{,}999\ in.^4$

$I_{EXT} = 346\ in.^4$

$\Sigma I_{RRFC} = (2)(I_{EXT}) + I_{INT} = (2)(346) + 8{,}999 = \underline{9{,}691\ in.^4}$

$$\omega_{INT} = \frac{I_D}{\Sigma I_{RRFC}} = \frac{8{,}999\,in.^4}{9{,}961 in.^4} = \underline{0.929}$$

$$\omega_{EXT} = \frac{I_D}{\Sigma I_{RRFC}} = \frac{346\,in.^4}{9{,}961 in.^4} = \underline{0.036}$$

Because the inertia ratio for the interior girder is significantly larger than the inertia ratio for an exterior girder, assume that the capacity of the interior girder will control the maximum clear span. Assume the adjustment factor, ψ, is equal to 1.0, and calculate the live load moment, M_{LL}, in the interior girder at midspan of the bridge:

$$M_{LL} = \frac{2}{3}\psi\,\omega\,M_{SD} = (\frac{2}{3})(1.0)(0.929)(23.94\ L - 384.8) = \underline{(14.83\ L - 238.3)\ k - ft}$$

Next, analyze the bridge with the uniform dead load assumed in Section F.1, separating the dead load of the components (DC) from the dead load of the wearing surface (DW):

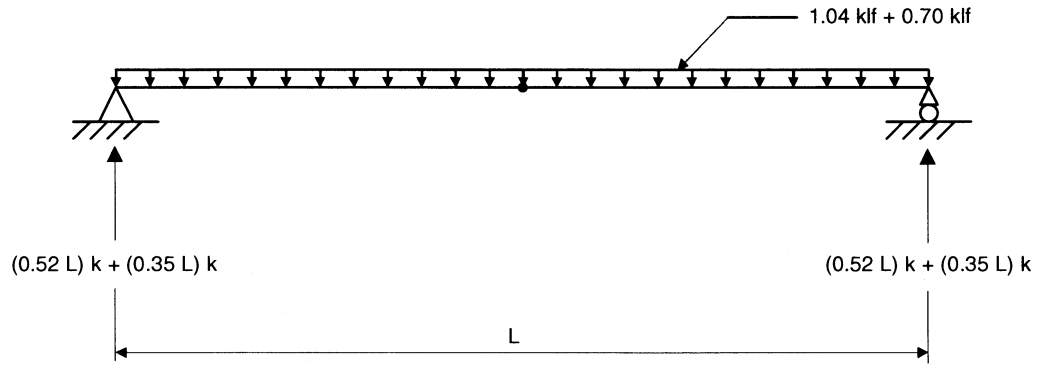

Determine the maximum dead load moment, M_{SD}, at midspan of the bridge:

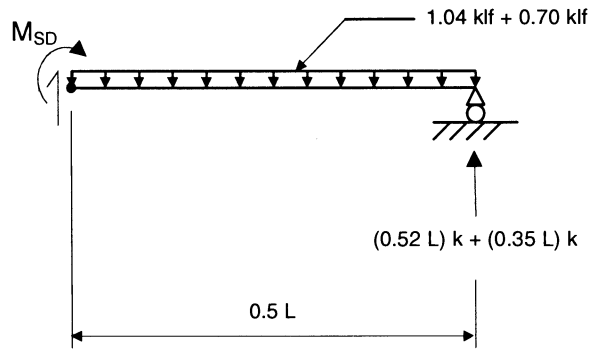

DC: $M_{SD} = (0.52\ L)(0.5\ L) - (1.04)(0.5\ L)(0.5)(0.5\ L) = \underline{(0.13\ L^2)\ k - ft}$

DW: $M_{SD} = (0.35\ L)(0.5\ L) - (0.70)(0.5\ L)(0.5)(0.5\ L) = \underline{(0.088\ L^2)\ k - ft}$

As with the live load analysis, the interior girders are assumed to carry the entire dead load on the bridge, thus, the maximum dead load moment in one interior girder at midspan of the bridge is:

$M_{DC} = (0.5)(M_{SD}) = (0.5)(0.13\ L^2) = \underline{(0.065\ L^2)\ k - ft}$

$M_{DW} = (0.5)(M_{SD}) = (0.5)(0.088\ L^2) = \underline{(0.044\ L^2)\ k - ft}$

Following the *AASHTO LRFD Bridge Design Specifications* [9], combine the maximum live load and dead load moments assuming the operational importance factor is 0.95 since RRFC bridges are used on low-volume roads:

$M_{MAX} = (0.95)(1.25 * M_{DC} + 1.5 * M_{DW} + 1.75 * M_{LL})$

$= (0.95)[(1.25)(0.065\ L^2) + (1.5)(0.044\ L^2) + (1.75)(14.83\ L - 238.3)]$

$= (0.14\ L^2 + 24.65\ L - 396.17)\ k - ft$

Determine the flexural capacity of an interior girder of an 89-ft RRFC following the procedure in the *AASHTO LRFD Bridge Design Specifications*:

$M_r = \underline{1{,}898\ k - ft}$

Calculate the maximum clear span, L, for which M_{MAX} is less than M_r:

$M_{MAX} = M_r$

$(0.14\ L^2 + 24.65\ L - 396.17) = 1{,}898$

$L = \underline{67.33\ ft}$

This is the maximum clear span for Case 1, using the maximum dead load and live load moments at the midspan of the bridge.

F.2.2 Case 2 Calculations

Using the statically-determinate structure developed for Case 1, determine the maximum live load moment, M_{SD}, at the point beneath the axle load closest to the center of gravity of the truck:

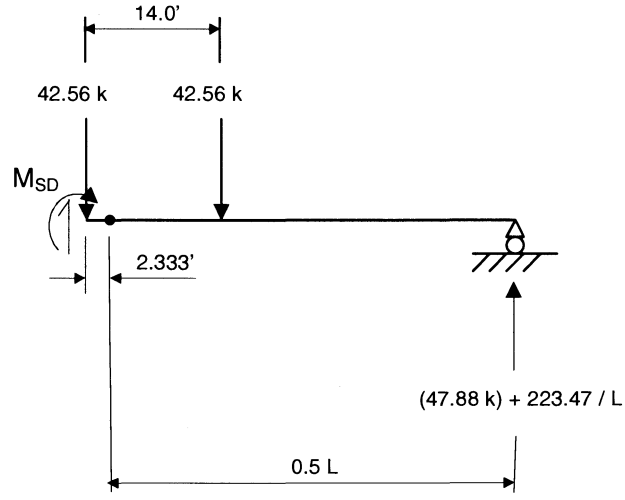

$$M_{SD} = (47.88 + \frac{223.47}{L})(0.5\ L + 2.333) - (42.56)(14.0)$$

$$= (23.94\ L + \frac{521.42}{L} - 372.40)\ k\text{-}ft$$

Use the section properties and inertia ratios used for the maximum dead load moment case, and again assume the adjustment factor, ψ, is equal to 1.0. Calculate the live load moment, M_{LL}, in the interior girder at midspan of the bridge:

$$M_{LL} = \frac{2}{3}\psi\,\omega\,M_{SD} = (\frac{2}{3})(1.0)(0.929)(\,23.94\,L + \frac{521.42}{L} - 372.40)$$

$$= \underline{(14.83\,L + \frac{322.93}{L} - 230.64)\ k\text{-}ft}$$

Next, determine the maximum dead load moment, M_{SD}, at the point 2 ft – 4 in. from the midspan of the bridge:

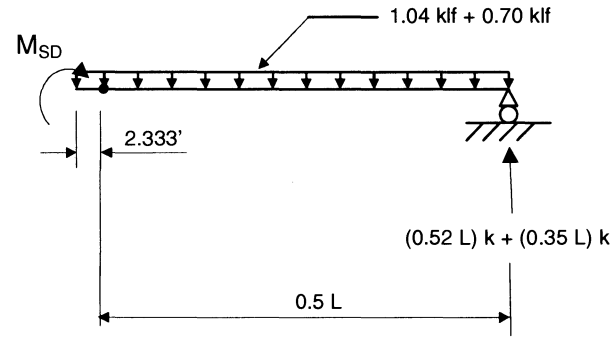

DC: $M_{SD} = (0.52\,L)(0.5\,L + 2.333) - (1.04)(0.5\,L + 2.333)(0.5)(0.5\,L + 2.333)$

$= \underline{(0.13\,L^2 - 2.83)\ k\text{-}ft}$

DW: $M_{SD} = (0.35\,L)(0.5\,L + 2.333) - (0.70)(0.5\,L + 2.333)(0.5)(0.5\,L + 2.333)$

$= \underline{(0.088\,L^2 - 1.91)\ k\text{-}ft}$

As with the live load analysis, the interior girders are assumed to carry the entire load on the bridge, thus, the maximum dead load moment in one interior girder at midspan of the bridge is:

$$M_{DC} = (0.5)(M_{SD}) = (0.5)(0.13\,L^2 - 2.83) = \underline{(0.065\,L^2 - 1.41)\ k\text{-}ft}$$

$M_{DW} = (0.5)(M_{SD}) = (0.5)(0.088\ L^2 - 1.91) = \underline{(0.044\ L^2 - 0.95)\ k\text{ - }ft}$

Following the AASHTO *LRFD Bridge Design Specifications* [9], combine the maximum live load and dead load moments assuming the operational importance factor is 0.95 since RRFC bridges are used on low-volume roads:

$$M_{MAX} = (0.95)(1.25{*}M_{DC} + 1.5{*}M_{DW} + 1.75{*}M_{LL})$$

$$= (0.95)[(1.25)(0.065\ L^2 - 1.41) + (1.5)(0.044\ L^2 - 0.95) + (1.75)(14.83\ L + \frac{322.93}{L} - 230.64)]$$

$$= \underline{(0.14\ L^2 + 24.65\ L + \frac{536.87}{L} - 386.47)\ k\text{ - }ft}$$

The flexural capacity of an interior girder of an 89-ft RRFC is the same as determined for Case 1:

$M_r = \underline{1{,}898\ k\text{ - }ft}$

Calculate the maximum clear span, L, for which M_{MAX} is less than M_r:

$$M_{MAX} = M_r$$

$$(0.14\ L^2 + 24.65\ L + \frac{536.87}{L} - 386.47) = 1{,}898$$

$L = \underline{66.93ft}$

This is the maximum clear span for Case 2, using the maximum live load moment. Because the shorter length controls the maximum clear span, Case 2 controls the maximum clear span. Thus, for a simply-supported bridge composed of two 89-ft RRFCs without a center pier or built-up girders, the maximum clear span is 66 ft – 11 in. As stated in Section F.1, this clear span assumes that the RRFC is symmetric about the midspan of the bridge; the portion of the 89-ft RRFC used for the maximum clear span is shown in Figure F.1

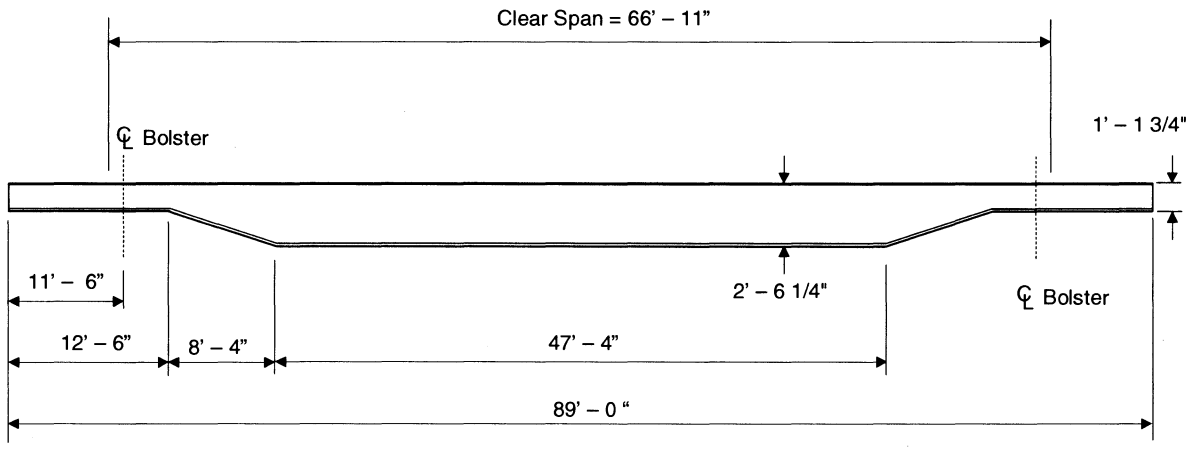

Figure F.1. Maximum clear span possible from a "cut" 89-ft RRFC.